User Authorization

In presenting this thesis in partial fulfillment of the requirements for an advanced degree at Idaho State University, I agree that the Library shall make it freely available for inspection. I further state that permission for extensive copying of my thesis for scholarly purposes may be granted by the Dean of the Graduate School, Dean of my academic division, or by the University Librarian. It is understood that any copying or publication of this thesis for financial gain shall not be allowed without my written permission.

Signature: _____ _____

Date: _____

Three-Phase Unbalanced Distribution System State Estimation (DSSE) Based on WLS (Using AMI) and Load Correction Method

By

Tazwar Muttaqi

A thesis

submitted in partial fulfillment

of the requirements for the degree of

Master of Science in the Department of Measurement and Control Engineering

Idaho State University

May 2019

Committee Approval

To the Graduate Faculty:

The members of the committee appointed to examine the thesis of **Tazwar Muttaqi** find it satisfactory and recommend that it be accepted.

_____

Dr. Steve C. Chiu,

Major Advisor

_____

Dr. Thomas Baldwin

Committee Member

_____

Dr. Alba Perez Gracia,

Graduate Faculty Representative (GFR)

Acknowledgment

First of all, I can't thank enough my major Advisor Dr. Thomas Baldwin for his guidance throughout my graduate study period. He always inspired and instructed me to the right direction to finish my thesis research. Every time I got stuck, he helped me to think the right way to reach the goal of my work. I am privileged to work under his articulated supervision.

I am very much honored to get Dr. Steve Chiu as my committee member and an instructor who always inspired to move forward. His support paved my way to pass this hurdle. I am also grateful to Dr. Alba Perez for being my GFR who supported my graduate study in many ways.

I also thank the almighty, my parents, my younger sister, all the professors I've taken class with, my friends for their tremendous support and love to succeed my thesis research.

Dedication

To,

My parents and younger sister.

Table of Contents

List of Tables

List of Figure

Abstract

Three-Phase Unbalanced Distribution System State Estimation (DSSE) Based on WLS (Using AMI) and Load Correction Method

Thesis Abstract- Idaho State University (2019)

Distribution System State Estimation (DSSE) is a significant component for reliable and optimal performance of a Distribution Management System (DMS). Many buses with limited available measurements and highly unbalanced loads that makes the estimation a very challenging task in DMS. Accuracy, observability, presentation and speed constraints still bring DSSE to a top research priority. This thesis research proposes two unbalanced distribution state estimation methods; one based on the Weighted Least Squares (WLS), and the other one is based on load calibration method that uses backward/forward algorithm to estimate the system with limited measurements. In addition, a universal line modeling database is built that asks for the data input to model the line parameter matrices which can be used for all distribution networks. Proposed methods are simulated for IEEE 13 and 37 bus feeder network systems in MATLAB platform.

Key Words: Distribution System State Estimation, Weighted Least Squares, Advanced Metering Infrastructure, Load Correction Method, Backward/Forward Sweep Power Flow.

Chapter 1: Introduction

1.1 Motivation and Objective

Traditionally, electric power distribution systems been designed and worked as passive system to meet customer's requirement. However, operational and reliability challenges have increased with the transformation of traditional grid to a smart grid. Many of the solution of these challenges in smart distribution grid is related to visualizing the perfect state of the network, which in essence relying on Distribution System State Estimation (DSSE). There are few techniques been implemented successfully for DSSE. Radial and weekly meshed distribution system contains many three-phase unbalanced branches with larger resistance/reactance (r/x) ratios and unbalanced loads set-apart by short distances. Adopting a transmission systems state estimation algorithm into a distribution system is preferable for modern smart distribution system. This research is based on a transmission system state estimation technique named Weighted Leas Square (WLS) and a Load correction technique for DSSE. The approach is to come up with WLS and Load Correction algorithms that are suitable for three-phase unbalanced distribution network. Advanced Metering Infrastructure (AMI) smart meters are widely used by utilities and near real time measurements are available. Load profile for each kind of customer is created relying on energy bill and few other monitored data from AMI which is found to be the best estimate. Due to voltage and current distortion, smart meters got errors in the measured values. These erroneous load data are used as input to state estimation process to estimate current state of the feeder network. Estimated voltage, current, active and reactive power for all three phases are compared with true case for each phase at any given time t. Simulation performance is demonstrated and analyzed for IEEE 13 Bus-Feeder

and IEEE 37 bus-feeder cases. Final goal of this research is to propose couple of reliable and accurate three-phase unbalanced DSSE technique that are applicable to all radial networks.

1.2 Modern Power Systems Structure

A modern power system network consists of several complex interconnected section such as generation, transmission, sub-transmission, distribution and loads. These subsystems are interconnected through transformers. It is necessary to analyze the whole system continuously for uninterrupted and reliable operation. Power system analysis is a complex process that combines few simulations into one that represent a clear state of the system. Each section of the power network is separated with protective devices for safety reasons; however, an interruption in any point of the network effects other operations both in upstream and downstream. Figure 1.1 illustrates a typical power system network and its components.

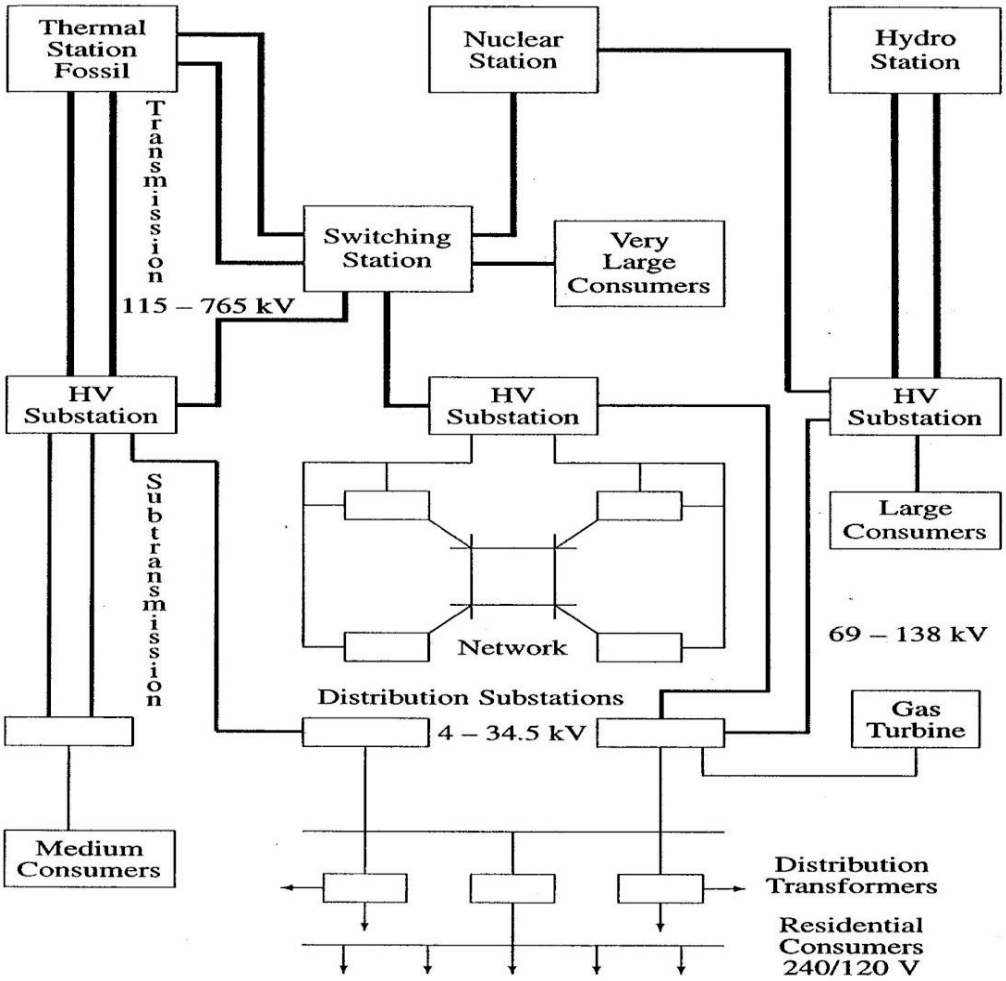

Figure 1. 1: Modern power system components (Image credit: Power systems analysis by Hadi Sadat, second edition)

1.3 Typical Distribution Operation

This research work is focused on the distribution part of the system. Usually, the transmission network is transposed and balanced that led the system modeling to a single-phase equivalent configuration. On the other hand, distribution feeder is inherently unbalanced due to many unequal single-phase loads that are served. Non-equilateral spacing of the three phase distribution lines add extra unbalanced components into the system. Distribution systems begins from a distribution substation which is fed by transmission line or sub-transmission line. In most cases, the distribution

feeders got unidirectional path for power flow from distribution substation to the customer. This is called radial distribution feeders. There are some advantages of radial distribution circuits over networked circuits such as easy fault current protection, low fault currents, flexible voltage control, easy prediction, easy control of the power flow, low cost etc. Primary distribution lines are ranged from 4kv to 34.4kv and serve the loads for a certain geographical land. Secondary distribution network further decreases the voltage for residential users. Customers are mostly served at the level of 240/120 v (single-phase three wire), 208Y/120 v (three-phase four wire), 480Y/277 v (three-phase four wire). Most number of primary lines are four wire multi-grounded (three phase conductors and a multi-grounded neutral conductor). Distribution systems may have one or more distribution substations that consist of one or more feeders. Distribution feeder analysis is always important to scrutinize the existing operating condition. It also estimates the future response of the network if anything changes to the feeder. Distribution feeder analysis is always challenging because of various electrical devices need to be modeled from number of data parameters available with feeder map. Additional data sets are necessary such as standard pole configuration, specific conductor data for each all lateral lines (Overhead or underground), three-phase transformer connections, voltage regulator specifications that are defined by IEEE PES. Every distribution network has suitable metering technology that provides measurement over a specific time period. Following are the components a distribution feeder might have-

- Three-phase primary feeder.
- Lateral branches (single-phase, two-phase or three-phase).
- In-line transformers.
- Shunt capacitor banks.
- Voltage regulators.

- Distribution transformer banks.
- Secondaries.
- Single-phase, two-phase or three-phase loads.
- Circuit breaker or recloser.
- Fuses.
- Metering device.

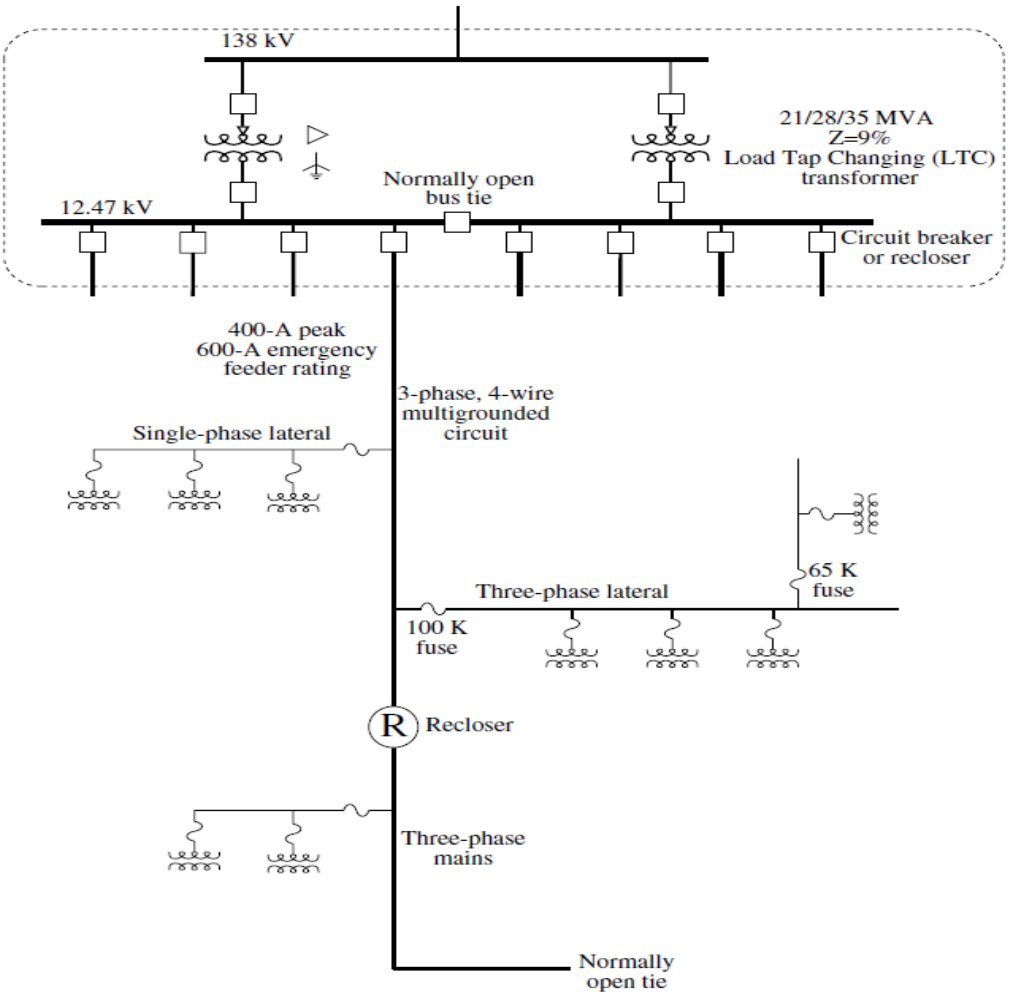

Figure 1. 2: Typical distribution substation with several feeders (Image credit: Electric Power Research Institute. 1000419. Engineering Guide for Integration of Distributed Generation and Storage into Power Distribution Systems)

1.5 Problem Statement

Power systems state estimation is a solidly implemented solution to address the metering errors at the transmission side and is typically solved using WLS method that is based on high quality measurement data from PMU. Transmission systems generally have a limited number of buses which is equipped with lot of measurement devices as it is always important to precisely monitor and control the system. However, distribution systems consist many nodes with limited measurements available with unbalanced loads. These fundamental differences and the need for efficient solutions refers to new state estimation approaches are needed for three-phase unbalanced distribution systems. In this thesis, a Weighted Least Squares (WLS) method and a load correction method are presented. Since the loads in the distribution system are highly distributed, it is very hard to determine the loads precisely. By observing same type of loads with resembling characteristic, a load profile is created for the DSSE measurement.

1.6 Transmission System SE against Distribution Systems SE

While in transmission systems state estimation is a routine task and a range of established methodologies exist, these cannot simply be duplicated in distribution systems due to distinctive planning, design and operational behaviors of the distribution network. The SE methodologies adopted in the transmission system started showing their limitations when exposed to specifics of the distribution network. The distribution network is typically characterized by the unbalanced system, smaller lines with high resistance/reactance (*r/x)* ratios connecting highly distributed loads. The consumer loads are not measured, and a large part of the distribution segment continues to operate in an unmonitored fashion. Usually voltage, current and power flows are measured in primary substations with virtually no monitoring of the secondary substation quantities [25].

Unlike in the transmission systems, the scarcity of the measured information brings formidable challenge to the state estimator to provide a reasonably meaningful estimate of the system states. This introduces bottlenecks in carrying out a range of substation and feeder automation tasks that rely on the quality of the estimated values of the states.

1.7 DSE Applications

DSSE renders initial state for Distribution Management System (DMS) and enhances real-time distribution grid supervision. Highly accurate DSSE will have highly positive impact to the overall network operation and vice-versa. DMS is expanding their range of operation rapidly that includes but not limited to capacitor switching, distribution transformer optimization, voltage magnitude/reactive power control (*V/Var*), reduced energy loss, recloser and switching control, reconfiguration of distribution feeder, restoration, load demand management, fault locating and price signal estimation. Highly accurate and consistent DSSE also help finding potential irregularity of the electric usage and the factor related to unbalanced voltage in the network. In unwanted cases when model can't present the actual state of the network; DSE can repair, locate and determine erroneous data.

1.8 Chapter Outline

Chapter 2 describes the evolution of DSSE and proposed methods that are presented in this thesis report. It talks about the metering and measurement concern in distribution network, pseudo measurements, AMI topology, problem statement and distribution state estimation challenges. Before performing the DSSE, line modeling and power flow calculation is necessary to define the base case of a distribution network. Chapter 3 represents formation of three-phase unbalanced line

modeling equations, backward/forward sweep power flow framework that are used for the DSSE. Chapter 4 defines detail structure of the WLS based DSSE that are proposed in this thesis. WLS state estimation theory and related equations are presented such as measurement function, Jacobian matrix, measurement residuals, gradient etc. Bad data identification and pseudo measurements are also incorporated with the WLS DSSE. Chapter 5 is about load correction based DSSE. Equations and formation of the load correction based DSSE is presented in steps with a detailed flow-chart of the method. Finally, chapter 6 shows the simulation output for IEEE 13 bus system case for both the proposed methods. Output results are compared in table and graphs. Voltage magnitude, voltage angle, current, active power flow, reactive power flow and total loss of the network is estimated with analogical figures to validate the accuracy of the methods.

Chapter 2: Background

2.1 Literature Review

Real-time measurement is limited in distribution network and observability of the network is not determined without pseudo measurements. DSSE research was pioneered in the 1990's even with low measurement reporting. Because of the lack of the observability downstream of the distribution substation, only a small number of utilities implemented the DSSE at the beginning. As mentioned earlier, with the increased Smart Distribution Management System (SDSM) that contains AMI has encouraged utilities to implement DSSE in recent years. Practical test proved that the DSSE be the most feasible, reliable and accurate enough for real time distribution network management. Existing DSSE techniques are different depending on the evolution and execution timing of the estimator, state variables, bad data detection etc. Until today, three-phase unbalanced distribution state estimation is an open research topic due to computational complexity involved with it. Some existing methods are discussed in this chapter.

2.1.1 Node Voltage Based DSSE Technique

Bus voltage is used as state variable for this method. If the polar form of the phasor representation is used of the bus voltage, Jacobean and gain matrices must recalculate in each iteration. On the other hand, by using rectangular form of bus voltage as state variable, Jacobian matrices of the converted bus current injection measurements become constant. Bus injection power and voltage magnitude measurements are changed into equivalent voltage measurements and bus injection current in rectangular forms relying on the calculated bus voltage measurement in last iteration. Rectangular branch currents are obtained by converting actual current magnitude and branch

power [21]. Only single factorization of the gain matrix is necessary in the rectangular bus voltage DSSE method. This technique is highly effective for balanced distribution systems.

2.1.2 Load adjustment Based DSSE Technique

Loads are adjusted based on load modeling method from the customer load profile. Customer loads can be modeled as a mixture of constant power, constant current, and constant impedance elements. Generally, the power factor is fixed separately for each of the three load components. Load adjustment state estimation methods usually use the bus current injection / power injection so that the values adapt the measured data. Measurements data are used as constraints for the algorithm solution. Bus loads are adjusted through an iterative process using Gauss-Seidel power flow algorithm [1]. Substation voltage and current magnitude measurements on the feeder are treated entirely correct during the process [15]. However, the algorithm is only implemented for balanced distribution network.

2.1.3 Particle Swarm Optimization (PSO) DSSE Technique

A hybrid particle swarm optimization method was tested due to the nonlinear characteristics of unbalanced distribution network. The proposal is very similar to the WLS state estimation considering the objective function. The approach is to minimize the measured voltages, calculated voltages and currents by utilizing load value and distributed energy resources [4]. PSO takes longer to converge which is a concern. To improve the convergence reliability and timing, a Hybrid Particle Swarm Optimization (HPSO) is investigated. This method has also addressed the transformer taps estimation in the context of DSSE. It was the very first DSSE approach that estimates transformer tap positions without any assumption in unbalanced three-phase system

using HPSO. The HPSO estimation found to be more accurate estimation of losses in the network that facilitates proper allocation of cost of the electricity. However, bad tap error detection is still a subject to investigate for this approach before implementing.

2.1.4 Dynamic DSSE Technique

Dynamic DSSE method is a recursive technique relying on few measurement snapshots over a time period. It is also known as forecasting-aided state estimation (FASE) [5]. For larger distribution system with measurements of various frequencies, newly received measurement is combinedly processed with available analytical estimate. It is used eventually to forecast state variations within all DSSE executions. No loss of higher order information in this method improves the overall properties of the estimator. It offers computation advantages over few other methods since it does not require to calculate Jacobian or hessian matrix. However, Bandwidth and speed limitation in SCADA and AMI makes it really challenging to use large heterogeneous measurement containing various data for establishing contiguous past and future feeder models of the operating network.

2.1.5 Distributed DSSE Technique

Distributed DSSE basically split up the distribution network into several sub division based on topological points, geographical location and metering points. This method is also known as multi-area State Estimation (SE) and it solves the network condition in local estimators [9]. A second state estimation is initiated on all sub-areas by utilizing previous estimation outputs and the estimates of quantities supplied by neighboring areas as measurement data. Number sequential or parallel estimation are executed in distributed DSSE [6]. This technique not implemented

practically because of some constraints such as lack of real and synchronized measurement, communication delay which are key factor for accurate solution of distributed DSE method.

2.2 Measurement Placement in Distribution Systems

Grid sensing and monitoring is widespread at the transmission level. In the transmission network, the common measurements are voltage magnitude at buses and the complex power flow on the lines. These measurements don't rely on the communication of phase angle relationships between substations. Since the 1990's, synchrophasor measurements have gradually been added to the portfolio. Accurate GPS time clocks have enabled better timing and phasor accuracy between substation measurements. The importance of bulk power transmission justifies the cost of measurements. However, this is not the case in distribution where the immense size and relative less importance makes transmission style measurements too costly. On the other hand, the growth of AMI has added a new class of voltage magnitude and complex power measurements to multiple customer connection points in the distribution network. Supervisory control and data acquisition (SCADA) systems rely on real-time PMU and power measurements to control the network. Such measurements are usually available down to substations. Because of the larger size of the distribution network, it is hard to monitor each customer location online. The online monitoring is done only at the main substation locations usually. This limits the automation and control operation of the distribution systems. Interruptions are attended manually in most cases. Since the state estimator requires the measurements online, the limited number of real measurements available at the main substations do not serve the purpose. Hence many pseudo measurements are introduced. With the evolution of AMI and smart grid, load demand and voltage measurements are available these days to work with DSE [14]. Loads are derived from the regular behavior of various

customers, historical data of the feeders, distribution transformer loadings etc. The loads modelled in this way have generalized uncertainty however it estimated at best possible way. Recently many utilities started installing AMI which can be utilized for online monitoring of the network. Again, due to the larger size of the distribution network supplying thousands of customers, it might not be feasible economically to install the smart meters in all the locations [16]. Consequently, a large part of the network remains unmonitored and the measurement provided by the installed smart meter is not enough for state estimation [17]. Hence, many pseudo measurements need to be introduced in order to make the system observable. Since pseudo measurements are high-variance estimates of the loads, the quality of the estimated voltages and angles at each bus is poor if the number of pseudo measurements is large. Estimation errors are often too high for effective network control; so, it is necessary to deploy more real measurements. Choices then need to be made regarding the locations, types and number of measurements. These issues have been addressed in past research works, at the transmission level. But little attention has been paid to measurement placement at the distribution level [17]. Research reported in the literature concerning measurement placement falls, broadly speaking, into two categories:

- Improvement of network observability.
- Minimization of errors in the estimates.

2.3 Pseudo Measurements Formulation

The quality of the estimate heavily relies on the realistic modelling of the estimated loads. In the absence of any real measurement of loads which are highly distributed and diverse, they are considered as pseudo measurements (random variables) with apropos variance and mean. Because of pseudo measurement's compatibility with WLS based on Maximum Likelihood Estimation

(MLE), it is usual to model them by normal distribution. Gaussian distribution is the most common technique to model the loads. However, single Gaussian probability density assumption is not well justified for all kinds of loads [11]. The research work on statistical methods for load research data analysis states that the statistical distribution of electric load variation does not follow any defined probability distribution function pattern [12] [13]. Several attempts have been carried out to model the loads through different probability distributions.

2.4 Advanced Metering Infrastructure (AMI) in Smart Distribution Systems

Advanced Metering Infrastructure (AMI) is one of the most essential elements of smart grid (SG) that combines data from smart meters (SM) and sends them to the utility center to be analyzed and stored. Distribution networks increasingly using the AMI which is spiraling the workforce and operational cost for utilities. AMI smart meter data transmission can be through a wireless communication and nearly readily available (every 15 minutes or more). AMI smart meters transmit customer load information to the computing unit in an integrated bidirectional way. However; increased supervision, intelligence and control is needed to utilize the smart meters with full efficiency. Advanced *V/Var* optimization, demand response, fault location and restoration schemes require more accurate and reliable information about the current system state, which is increasing with the ongoing expansion of advanced metering infrastructure (AMI) in smart grid [11]. Accurate utilization of AMI in DSSE should be a cornerstone of future smart distribution systems in US. AMI smart meters provide load, voltage and current at the installed node. However, this research work focused on distribution system state estimation DSE based on weighted least square (WLS) and Load Correction (LC) method. Normally distributed noise component has been

used for modeling measurement errors into the AMI load measurements. Figure 1.3 resembles the modern AMI topology in distribution system.

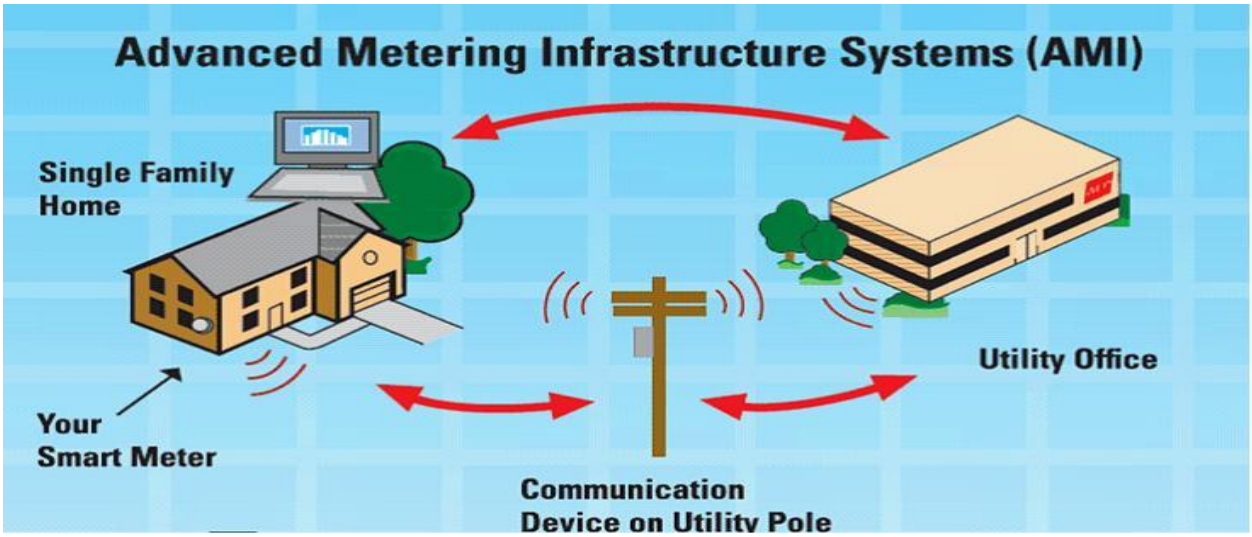

Figure 2. 1: AMI systems topology

Chapter 3: Distribution Systems Modeling and Power Flow

3.1 Line Modeling

Distribution networks consist of both overhead and underground transmission line segments. Most line segments can be categorized into several typical or standardized configurations. These configurations cover the spacing of the phase conductors, wire sizes, and phasing arrangements. Conductor data for overhead and underground distribution lines are given in Appendix A. Distribution network is large in size with shorter lateral branches and unbalanced loads. It makes the system highly nonlinear to model and analyze. Very first step towards analyzing a distribution feeder network is modelling impedance and admittance matrices for lateral branches.

3.1.1 Phase Impedance Matrix for Overhead Line

Modified Carson's equations are used for the line modeling [2]. Carson's equation for self and mutual impedance are as below:

Self-Impedance:

$$\hat{Z} = r_i + 0.09530 + j0.12134\left(\ln\frac{1}{GMR_i} + 7.93402\right)\Omega/\text{mile} \tag{3.1}$$

Mutual Impedance:

$$\hat{Z}_{ij} = 0.09530 + j0.12134\left(\ln\frac{1}{D_{ij}} + 7.93402\right)\Omega/\text{mile} \tag{3.2}$$

Where, r_i is the resistance of conductor *i* (Ω/mile), GMR_i is the geometric mean radius of conductor *i* (ft) and D_{ij} is the distance between conductors *i* and *j* (ft).

The primitive impedance matrix for a three- phase line consisting of *m* neutrals are in following form:

$$\left[\hat{Z}_{primitive}\right]=\left[\begin{array}{ccc|ccc} \hat{Z}_{aa} & \hat{Z}_{ab} & \hat{Z}_{ac} & \hat{Z}_{an1} & \hat{Z}_{an2} & \hat{Z}_{anm} \\ \hat{Z}_{ba} & \hat{Z}_{bb} & \hat{Z}_{bc} & \hat{Z}_{bn1} & \hat{Z}_{bn2} & \hat{Z}_{bnm} \\ \hat{Z}_{ca} & \hat{Z}_{cb} & \hat{Z}_{cc} & \hat{Z}_{cn1} & \hat{Z}_{cn2} & \hat{Z}_{cnm} \\ \hline \hat{Z}_{n1a} & \hat{Z}_{n1b} & \hat{Z}_{n1c} & \hat{Z}_{n1a1} & \hat{Z}_{n1n2} & \hat{Z}_{n1nm} \\ \hat{Z}_{n2a} & \hat{Z}_{n2b} & \hat{Z}_{n2c} & \hat{Z}_{n2a1} & \hat{Z}_{n2n2} & \hat{Z}_{n2nm} \\ \hat{Z}_{nma} & \hat{Z}_{nmb} & \hat{Z}_{nmc} & \hat{Z}_{nmn1} & \hat{Z}_{nmn2} & \hat{Z}_{nmnm} \end{array}\right] \tag{3.3}$$

And,

$$\left[\hat{Z}_{primitive}\right]=\begin{bmatrix}[\hat{Z}_{ij}] & [\hat{Z}_{in}] \\ [\hat{Z}_{nj}] & [\hat{Z}_{nm}]\end{bmatrix} \tag{3.4}$$

Final equation after Kron's reduction [2] for the phase impedance matrix is as follow:

$$[Z_{abc}]=[\hat{Z}_{ij}]-[\hat{Z}_{in}][\hat{Z}_{nn}]^{-1}.[\hat{Z}_{nj}] \tag{3.5}$$

Or,

$$[Z_{abc}]=\begin{bmatrix} Z_{aa} & Z_{ab} & Z_{ac} \\ Z_{ba} & Z_{bb} & Z_{bc} \\ Z_{ca} & Z_{cb} & Z_{cc} \end{bmatrix}\Omega/\text{mile}. \tag{3.6}$$

3.1.2 Phase Impedance Matrix for Underground Line

Most of the new residential distribution lines are built underground now-a-days. The modified Carson's equations are also applicable to underground cables in the same way [7]. Two popular types of underground cables are the "concentric neutral cable" and the "tape shield cable." Impedances for these cables are:

$$r_{cn} = \frac{r_s}{k} \Omega / \text{mile}$$

And

$$r_{shield} = 7.9385.10^{8}.\frac{\rho}{d_s.T} \Omega / \text{mile}$$

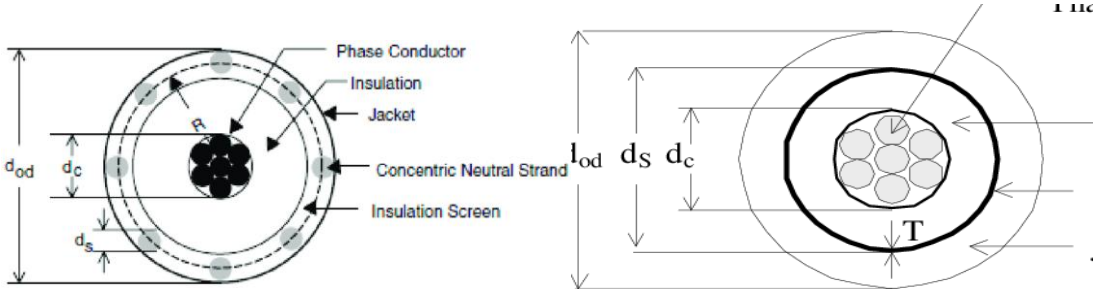

Figure 3. 1: Concentric neutral (left) and tape shielded (right) underground distribution cable

3.1.3 Shunt Admittance for Overhead lines

Conductance and the capacitive susceptance forms the shunt admittance over a distribution line. Same concept is used for the overhead shunt admittance determination. Neglecting the shunt conductance, the phase shunt admittance matrix is as below:

$$[y_{abc}] = 0 + j.\omega.[C_{abc}]\mu S/\text{mile}$$

Where,

$$\omega = 2.\pi.f = 376.9911$$

3.1.4 Shunt Admittance Matrix for Underground Lines

The equation for the shunt admittance of the underground concentric neutral cable and tape shield cable are:

$$y_{ag} = 0 + j\frac{77.3619}{\ln(R_b/RD_c) - (1/k)\ln(k.RD_s/R_b)}\mu S/\text{mile}$$

And,

$$y_{ag} = 0 + j\frac{77.3619}{\ln(R_b/RD_c)}\mu S/\text{mile}$$

3.2 Line Modeling Database

For managing the vast amounts of data associated with distribution networks, a database structure has been adopted in this work. For convenience and compatibility with other research efforts, the numbering system for line configurations, developed by W. H. Kersting was employed. See reference [2] for a description of the numbering system. This system is also used in describing the transmission line segments of the IEEE Power and Energy Society's set of distribution network test cases [23]. Each configuration number resembles a database that represents “phase impedance matrix”, “shunt admittance matrix”, “symmetrical components matrix of the line impedance” and

"symmetrical components matrix of the line shunt admittance", "Transformer impedance and admittance matrix". Conductor data are obtained from the table described in Appendix B section and the MATLAB script for the line modeling are given in Appendix section. The function asks for user input for conductor, spacing ID, Phasing, Neutral conductor, transformer data, configuration number etc. Line configuration number needed for a certain test case can be quickly commanded in the load flow input to be executed.

3.3 Power Flow Calculation Techniques

In power system analysis, the operating state of the network is paramount to all other studies. Solving for the voltage profile of the operating state is performed using a power flow algorithm. The power flow analysis is a root-solving problem of a nonlinear system, where the complex power injections are the given values. There are several iterative power-flow algorithms are available for transmission systems such as Newton-Raphson, Gauss-Seidel, Fast-decoupled method etc. However, these iterative techniques are not welcomed for radial distribution network because of poor convergence characteristics. A special iterative technique is used that is more suitable for radial distribution network named backward/forward sweep (BFS) or ladder iterative technique [24]. The biggest advantage of this method is execution time, simplicity and robustness of the algorithm.

3.4 Backward/Forward Sweep Power Flow (BFS)

The backward/forward sweep is a method best suited for three-phase unbalanced distribution systems power flow problem. It is an iterative method, which typically converges within a few iterations. This method involves two sweeps of calculations. In the backward sweep, the end

voltages are initialized for the first iteration, and currents are calculated starting at the buses at the load end of the radial branch and solved up to the source bus by applying the current summation method [8]. The forward sweep starts at the source bus and calculates voltages using the current calculated from the backward sweep until the load end of the radial branches. The voltages from the forward sweep are used for the next iteration in the backward sweep calculations.

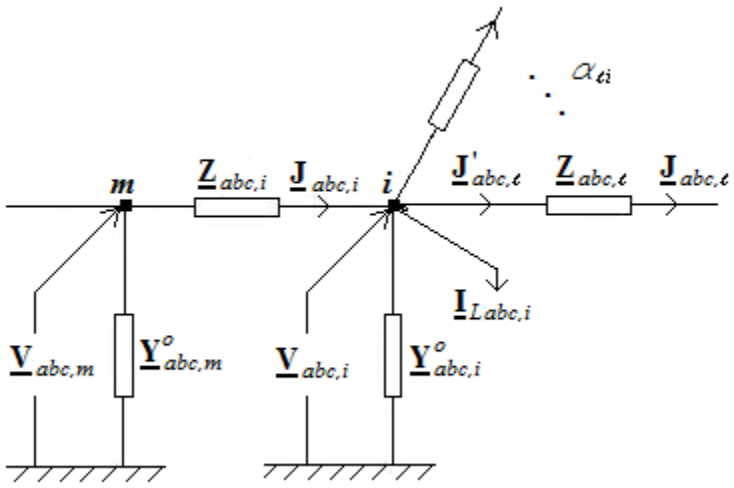

Figure 3. 2: A part of distribution network

The power flow calculation for a radial distribution networks (Figure 3.2) using backward/forward sweep method is carried out through the following iterative steps:

Step 1. Read input data: Define network configuration, line parameters, transformer parameters, load data.

Step 2. Initialization: Set the voltage at the root bus and assuming a flat symmetrical profile for the initial voltages at all other network buses.

Step 3. Backward sweep: At iteration *k*, starting from the branch in the last layer (branch

corresponding to last bus N_{bus}) and moving towards the branches connected to the root bus. The current in branch i, $\underline{J}_{abci}$ according to Figure 3.2, is calculated as:

$$\underline{J}_{abc,i}^{(k)} = \underline{I}_{Labci}^{(k)} + \underline{I}_{Cabc,i}^{(k)} + \underline{Y}_{abc,i}^{o} \cdot \underline{V}_{abc,i}^{(k-1)} + \sum_{\substack{\ell \in \alpha_{\ell i} \\ \ell \neq i}} \underline{J}_{abc,\ell}^{(k)} \qquad i = NB, NB\text{-}1, \ldots, 0; \;\; k = 1,2,\ldots \tag{3.7}$$

Where, k is the index of iteration; $\underline{I}_{Labc,i}$ is three-phase complex current of load at bus i; $\underline{I}_{Cabc,i}$ is three phase complex current of a var compensator at bus i; $\underline{J}_{abc,\ell}$ is three-phase complex current in branch ℓ emanating from bus i; $\underline{Y}_i^o$ is the shunt admittance at bus i; $\alpha_{\ell i}$ is the set of buses connected with bus i; $\underline{V}_{abc,i}$ is the complex voltage at bus i.

For a specified power of load, $\underline{S}_{Labc,i} = P_{Labc,i} + jQ_{Labc,i}$. The current of load is calculated in accordance with load type, and phase connection [2].

Step 4. Forward sweep: Bus voltages are updated in a forward sweep starting from branches connected to the root bus toward those in the last. For each branch, i, the voltage at bus i is calculated using the updated voltage at bus m (Figure 3.2) and the branch current calculated in the preceding backward sweep:

$$\underline{V}_{abc,i}^{(k)} = \underline{V}_{abc,m}^{(k)} - \underline{Z}_{abc,i} \underline{J}_{abc,i}^{(k)} \tag{3.8}$$

Step 5. Check convergence criteria: steps 2 and 3 are repeated until convergence achieved. For example, a convergence criteria can be adopted as follows:

$$\max \left| V_{abc,i}^{(k)} - V_{abc,i}^{(k-1)} \right| \leq \varepsilon_V = (10^{-3} \div 10^{-5}) \tag{3.8}$$

3.4.1 Transformer Modeling for Unbalanced Power Flow

The symmetrical components models of three-phase distribution transformers for common transformer connections in the backward/forward sweep-based power flow algorithm is used. A matrix block model of three-phase transformer is presented in Figure 3.3. As shown in Figure 3.3, a series block represents the transfer matrix of transformer for currents $\underline{M}_J$, the transfer matrix of transformer for voltages $\underline{M}_V$ and the matrix of phase impedances of transformer $\underline{Z}_{Tabc}$. A shunt block $\underline{Y}^m_{abc}$ models magnetizing admittance of the transformer. The shunt block should be placed on the side which windings are connected in the grounded way (Y_n). For all other cases, the shunt block can be connected on either side of the transformer (arbitrarily selected). In the backward sweep, starting from the branches connected to the far ends and moving toward a certain swing bus, the currents at the sending end of the branch are calculated as a function of the currents at its receiving end. In the forward sweep, starting from the branches connected to the source bus and moving toward to the branches connected to the far ends, the voltages at the receiving end of the branch are calculated as a function of the voltages at its sending end and the currents at its receiving end.

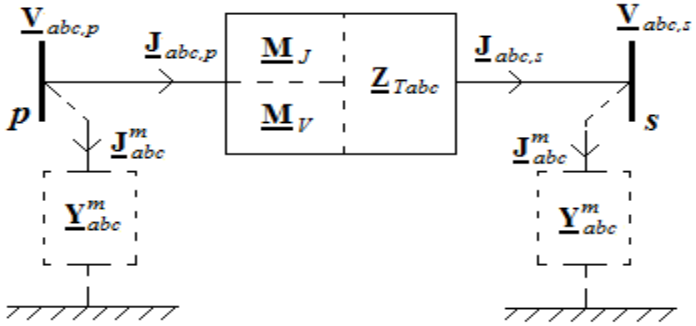

Figure 3. 3: Three-phase transformer model

Therefore, when the branch represents a three-phase transformer, the currents at the primary (*p*) side of the transformer are calculated as a function of the currents at its secondary (*s*) side. The

voltages at the secondary side of the transformer are calculated as a function of the voltages at its primary side and the currents at its secondary side. The relations between the symmetrical components of the voltages and currents of a three-phase transformer can be expressed in matrix form as follows:

$$\underline{\boldsymbol{J}}_{\boldsymbol{di0,p}} = \underline{\boldsymbol{m}}_{\boldsymbol{J}} \cdot \underline{\boldsymbol{J}}_{\boldsymbol{di0,s}} \tag{3.9}$$

$$\underline{\mathbf{V}}_{di0,s} = \underline{\mathbf{m}}_{V} \cdot \underline{\mathbf{V}}_{di0,p} - \underline{\mathbf{Z}}_{Tdi0} \cdot \underline{\mathbf{J}}_{di0,s} \tag{3.10}$$

Where,

$\underline{\mathbf{J}}_{di0,p} = \left[\underline{J}_{d,p} \quad \underline{J}_{i,p} \quad \underline{J}_{0,p}\right]^{T}$ is the vector of symmetrical components (*d*-positive sequence, *i*-negative sequence and 0-zero sequence) of three-phase currents at the primary side of the transformer;

$\underline{\mathbf{J}}_{di0,s} = \left[\underline{J}_{d,s} \quad \underline{J}_{i,s} \quad \underline{J}_{0,s}\right]^{T}$ is the vector of symmetrical components of three-phase currents at the secondary side of the transformer;

$\underline{\mathbf{V}}_{di0,p} = \left[\underline{V}_{d,p} \quad \underline{V}_{i,p} \quad \underline{V}_{0,p}\right]^{T}$ is the vector of symmetrical components of three-phase voltages at the primary side of the transformer; and

$\underline{\mathbf{V}}_{di0,s} = \left[\underline{V}_{d,s} \quad \underline{V}_{i,s} \quad \underline{V}_{0,s}\right]^{T}$ is the vector of symmetrical components of three-phase voltages at the secondary side of the transformer.

The transfer matrices $\underline{\mathbf{m}}_{J}$ and $\underline{\mathbf{m}}_{V}$, as well as the matrix of symmetrical components of the transformer impedance $\underline{\mathbf{Z}}_{Tdi0}$ are given in Table 3.1. From Table 3.1, transfer of the positive and negative sequences of the voltages and currents do not depend on the type of transformer connections. Transfer of the zero sequences of the currents and voltages, the form of the matrix of symmetrical components of the transformer impedance $\underline{\mathbf{Z}}_{Tdi0}$ depend on the type of transformer

connections and grounding of the neutral point.

Connection	$\underline{\mathbf{m}}_J$	$\underline{\mathbf{m}}_V$	$\underline{\mathbf{Z}}_{Tdi0}$
Y_nY_n (k=0,4,8)	$\begin{bmatrix} 1/\underline{m}_T^* & 0 & 0 \\ 0 & 1/\underline{m}_T & 0 \\ 0 & 0 & 1/m_T \end{bmatrix}$	$\begin{bmatrix} 1/\underline{m}_T & 0 & 0 \\ 0 & 1/\underline{m}_T^* & 0 \\ 0 & 0 & 1/m_T \end{bmatrix}$	$\begin{bmatrix} \underline{Z}_T & 0 & 0 \\ 0 & \underline{Z}_T & 0 \\ 0 & 0 & \underline{Z}_T \end{bmatrix}$
Y_nY_n (k=2,6,10)	$\begin{bmatrix} 1/\underline{m}_T^* & 0 & 0 \\ 0 & 1/\underline{m}_T & 0 \\ 0 & 0 & -1/m_T \end{bmatrix}$	$\begin{bmatrix} 1/\underline{m}_T & 0 & 0 \\ 0 & 1/\underline{m}_T^* & 0 \\ 0 & 0 & -1/m_T \end{bmatrix}$	$\begin{bmatrix} \underline{Z}_T & 0 & 0 \\ 0 & \underline{Z}_T & 0 \\ 0 & 0 & \underline{Z}_T \end{bmatrix}$
Yy_n (k=0,2,4,6,8,10) Dy_n (k=1,3,5,7,9,11)	$\begin{bmatrix} 1/\underline{m}_T^* & 0 & 0 \\ 0 & 1/\underline{m}_T & 0 \\ 0 & 0 & 0 \end{bmatrix}$	$\begin{bmatrix} 1/\underline{m}_T & 0 & 0 \\ 0 & 1/\underline{m}_T^* & 0 \\ 0 & 0 & 0 \end{bmatrix}$	$\begin{bmatrix} \underline{Z}_T & 0 & 0 \\ 0 & \underline{Z}_T & 0 \\ 0 & 0 & \underline{Z}_T \end{bmatrix}$
Y_ny (k=0,2,4,6,8,10) Yy (k=0,2,4,6,8,10) Y_nd (k=1,3,5,7,9,11) Yd (k=1,3,5,7,9,11) Dy (k=1,3,5,7,9,11) Dd (k=0,2,4,6,8,10)	$\begin{bmatrix} 1/\underline{m}_T^* & 0 & 0 \\ 0 & 1/\underline{m}_T & 0 \\ 0 & 0 & 0 \end{bmatrix}$	$\begin{bmatrix} 1/\underline{m}_T & 0 & 0 \\ 0 & 1/\underline{m}_T^* & 0 \\ 0 & 0 & 0 \end{bmatrix}$	$\begin{bmatrix} \underline{Z}_T & 0 & 0 \\ 0 & \underline{Z}_T & 0 \\ 0 & 0 & 0 \end{bmatrix}$

Where, $\underline{m}_T = m_T \cdot e^{jk30^\circ}$ is the complex transmission ratio and $\underline{Z}_T$ is the transformer impedance

Table 3. 1: Transfer matrices for different connection types of the transformer

3.4.2 Implementation of The Transformer Model into BFS algorithm

Backward sweep – calculation of three-phase currents at the primary side of the transformer. Based on symmetrical component theory, the phase currents at secondary side of three-phase transformer can be represented through their symmetrical components, as follow:

$$\underline{\mathbf{J}}_{di0,s} = \mathbf{T}^{-1} \cdot \underline{\mathbf{J}}_{abc,s} \tag{3.11}$$

Substituting from (3.11) into (3.9), and using the Fortescue transformation, phase currents at primary side of the transformer can be computed as a function of phase currents at secondary side:

$$\underline{\mathbf{J}}_{abc,p} = \underline{\mathbf{M}}_J \cdot \underline{\mathbf{J}}_{abc,s} \tag{3.12}$$

Where, $\underline{\boldsymbol{M}}_J = \boldsymbol{T} \cdot \underline{\boldsymbol{m}}_J \cdot \boldsymbol{T}^{-1}$ is the transformation matrix of the transformer for currents, T is the Fortescue's transformation matrix.

Forward sweep **-** calculation of three-phase voltages at the secondary side of the transformer. Firstly, the symmetrical components of the voltage at primary side should be determined:

$$\underline{\mathbf{V}}_{di0,p} = \mathbf{T}^{-1} \cdot \underline{\mathbf{V}}_{abc,p} \tag{3.13}$$

Substituting from (3.11) and (3.13) into (3.10) and using the Fortescue transformation gives an expression for calculation of the voltages at the secondary side of the transformer as a function of the voltages at its primary side and the currents at its secondary side.

$$\underline{\mathbf{V}}_{abc,s} = \underline{\mathbf{M}}_V \cdot \underline{\mathbf{V}}_{abc,p} - \underline{\mathbf{Z}}_{Tabc} \cdot \underline{\mathbf{J}}_{abc,s} \tag{3.14}$$

Where, $\underline{\boldsymbol{M}}_V = \boldsymbol{T} \cdot \underline{\boldsymbol{m}}_V \cdot \boldsymbol{T}^{-1}$ is the transformation matrix of the transformer for voltages; and $\underline{\boldsymbol{Z}}_{Tabc} = \boldsymbol{T} \cdot \underline{\boldsymbol{Z}}_{Tdi0} \cdot \boldsymbol{T}^{-1}$ is the impedance matrix of the transformer.

3.5 Implementation and Validation of the Power-Flow Algorithm

The modeling and analysis techniques of this chapter have been implemented in a MATLAB package. This software and data set package has been validated, using the IEEE 13-bus and 37-bus test cases. IEEE 13 and 37 bus-feeders are used for simulation purposes of this thesis to validate the results of the proposed method. 13 and 37 Bus feeders are three-phase unbalanced distribution networks. Figure 3.4 and figure 3.5 are the layout of IEEE 13 and IEEE 37 bus-feeder systems. Parameters of these systems are given in Appendix section. IEEE 13 systems displays practical features of a radial distribution network including nominal voltage of 4.16 kV,

comparatively highly loaded, one in-line transformer, voltage regulator, unbalanced loading, both overhead and underground lines and shunt capacitors. IEEE 37 bus-feeder is an actual feeder located in Arizona having nominal voltage of 24.9 kV, long and lightly loaded, shunt capacitors, unbalanced loads, two in-line voltage regulators and an in-line transformer [22]. Three-phase loads are connected in delta or wye and single-phase loads are connected in line-to-line or line-to-ground [23]. The validation of the power flow with published package is given in Appendix C that conform IEEE standard which can be seen in [23].

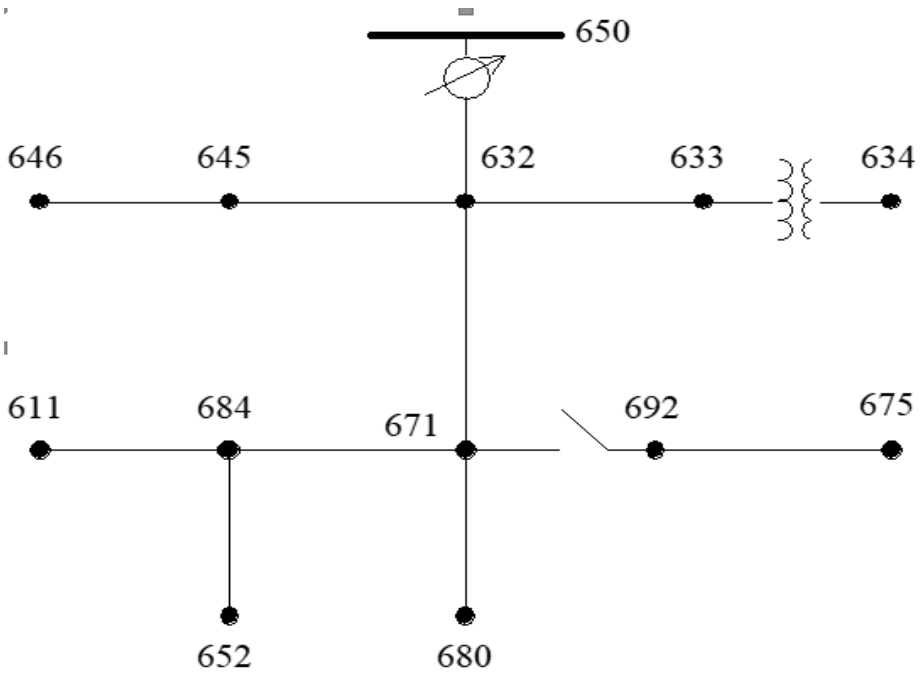

Figure 3. 4: IEEE 13bus-feeder system layout

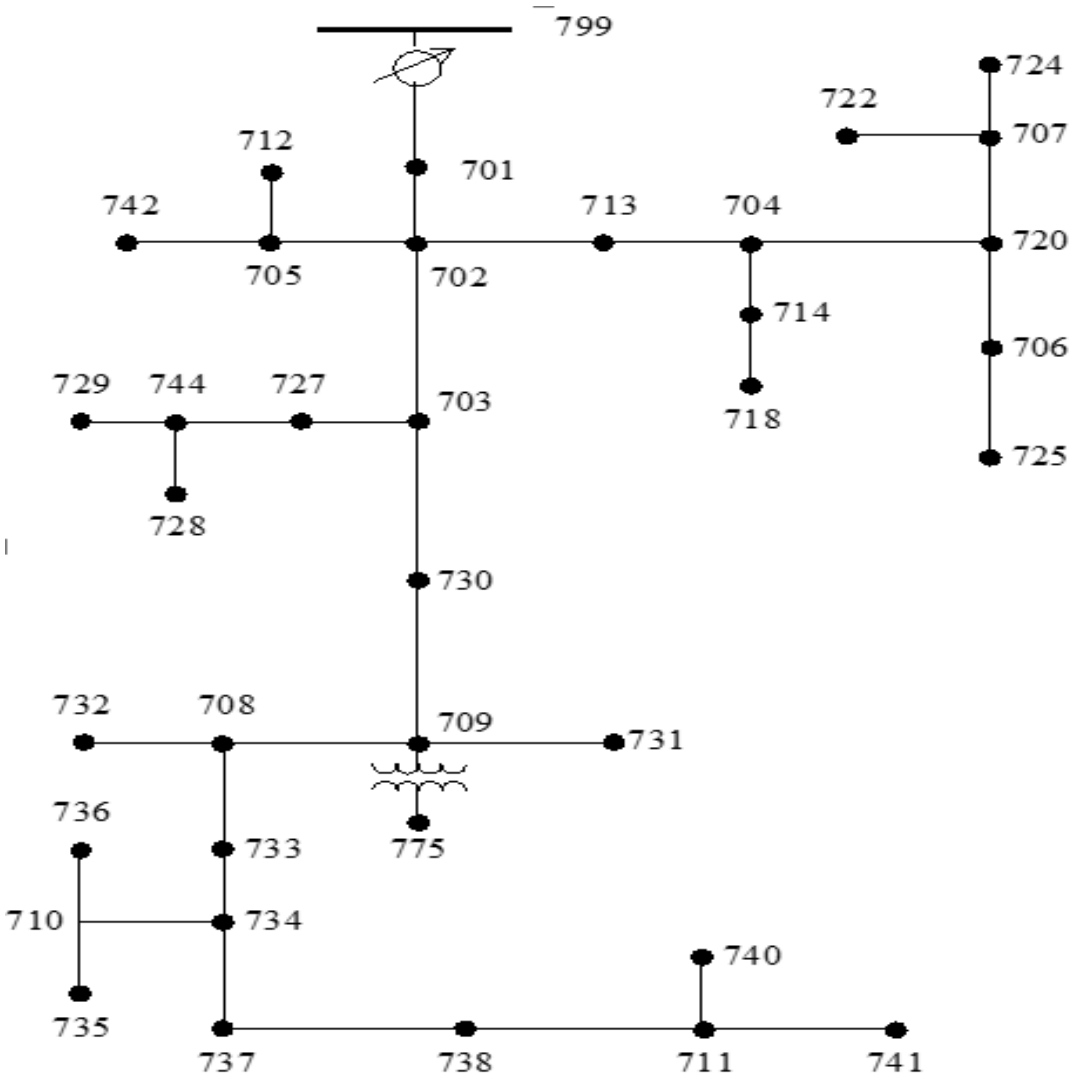

Figure 3. 5: IEEE 37 bus-feeder system layout

Chapter 4: Distribution Systems State Estimation Based on WLS

4.1 Introduction to State Estimation

The power flow analysis finds the state variables of a system for a given set of power injection inputs. This translates into solving a nonlinear system with a one-to-one correspondence between unknown and given values. Such is the case when conducting engineering studies. On the other hand, when measurements are made of the system, a state estimator becomes necessary. The state estimator addresses several issues that don't occur in power flow analysis. Generally, measurements contain additive noise or errors to the input data. Multiple measurements are made to reduce the impact of noise and errors. The measurements don't have to represent the same data inputs as found in power flow analysis. The least squares method finds wide spread use as a state estimator. This is due in part to the Gaussian nature of most noise and errors. Even when the error distributions are not Gaussian, the numerical calculations are often enough to transform the error impacts under the Central Limit Theorem.

The Weighted Least Squares (WLS) method [21] is popular in power system applications in part due to the variability of measurement devices and the ability to assign weights based on the measurement quality. This chapter explores the application of the WLS to the distribution network, which poses additional challenges over the bulk power transmission network with single-phase, balanced-circuit modeling.

4.2 The Weighted Least Squares (WLS)

WLS method is one of the most commonly used methods for power systems state estimators' tool. This thesis explains how state estimation methods aim to predict the closest possible

approximation for the state variable of branch current for radial distribution network. Objective of the WLS is to minimize the sum of the squares of the measurement's errors. Brach currents are considered as the state variable in this method. Appropriate equations are represented in the following sections.

4.3 Measurement Model for DSSE WLS Method

The measurement model used for DSSE is:

$$y = h(x) + e \tag{4.1}$$

- *y* is the matrix of the available measurements that are used as input for the DSSE algorithm; measurements can be voltages on the nodes and currents or active and reactive powers either on the branches or on the node injections. Load bus P and Q are the measurements used from AMI smart meters for this thesis work.
- *x* is the matrix of the chosen state variables, which is branch current in this case. Typical distribution state estimators are usually composed by the voltage magnitudes and angles at all the network buses. State of the system is defined as set of known variables that allows computing all the electrical parameters of the network. Hence, different options for the selection of the state variable are possible.

- h(x) is the matrix of nonlinear measurement functions connecting measurements *y* to the state variables *x*. Usually all functions represent the associated measured quantity in terms of the adopted state variables.

- e is the matrix of the errors associated with measurements; Typically, these are assumed as zero mean errors (E(ei)=0, decorrelated (E(ei,ej)=0, for $i \neq j$) resulting to a diagonal covariance matrix ($\sum y = E(ee^T) = diaa(\sigma_i^2)$, σ_i is the standard deviation involved with *i*-th measurement and square term is the variance for the respective measurement).

4.4 Measurement Residuals

In WLS calculation, objective is to minimize the sum of the following objective function:

$$J(x) = \sum_{i=1}^{M} \frac{\omega i[y_i - h_i(x)]^2}{e_i^2} \quad (4.2)$$

Where, w_i is the weight defined for the *i*-th measurement. M is total number of measurements available for the estimator input. The term {y-h(x)} is the difference between measured value and corresponding parameter as a function of the state vector, is commonly known as measurement residual [3]. Equation 4.2 can be generalized in matrix form as follow:

$$J(x) = [y - h(x)]^T W[y - h(x)] \quad (4.3)$$

Where, W is a resulting M×M weighting covariance matrix, having the weights $1/\omega_i \wedge 2$ on the diagonal elements. The weighting matrix plays a critical role in the WLS approach. In fact, it allows considering the different reliability of measurements, giving more importance to those with higher accuracy. For a proper modeling of the WLS method, it should be chosen as the inverse of the covariance matrix $\sum_y$ of the measurement errors.

The minimization of the objective function J(x) is usually obtained using an iterative Gauss-Newton Method. At each iteration k, to the following equation system to be solved:

$$G(X_k)\Delta X_k = H_K^T W[y - h(X_k)] \quad (4.4)$$

Where, H_k=H(X_k) is the Jacobian of the measurement functions h(x), G(X_k)=$H_K^T W H_k$ is the so-called Gain matrix, and ΔX_k is the updating state vector used to compute the new state according to the following:

$$X_{k+1} = X_k + \Delta x_k \quad (4.5)$$

The iterative process continues until a specified convergence criterion is achieved. Usually, the largest absolute element in the updating state vector Δx is compared to a defined tolerance threshold ε, and the algorithm stops when max $(|\Delta x|) < \varepsilon$. the state vector obtained at the last iteration is the estimation outcome provided by the WLS algorithm.

4.5 Measurement Function h(x)

Measurements included in the WLS DSSE are: active and reactive power (a branch or node injection), voltage magnitude on a node and current magnitude on a branch. To solve the WLS problem, all the corresponding measurement functions, which express the measured quantity in terms of the state variable, must be defined.

4.5.1 Active and Reactive Power Flow Measurement

As described in the previous subsection, in BC-DSSE active and reactive powers are converted in equivalent current measurements. Thus, indicating with

$$h_{i_l^T}^{eq} + j h_{i_l^x}^{eq} = \alpha\left(i_{l\varphi}^r + j i_{l\varphi}^x\right) \quad (4.6)$$

Where, $\alpha = 1$ if the measured power is in the same direction of the corresponding branch current used in the state vector and α=-1 if the power is in the opposite verse. As it can be observed, obviously, the transformation of the powers in equivalent currents leads to a linear relationship for this measurement function. Moreover, these functions are only related to state variables $\left(i_{l\varphi}^{T} and i_{l\varphi}^{x}\right)$ belonging to the same phase of the measurement, thus, there is no coupling among the different phases.

4.5.2 Active and Reactive Power Injection Measurement

Similarly, to the previous case, the power injections are converted in equivalent current injections. The associated measurement functions, for the equivalent current injection on phase φ of node *i*, are:

$$h_{i_{ln\,j,l\varphi}^{T}}^{eq} + jh_{i_{ln\,j,i\varphi}^{x}}^{eq} = \alpha\left[\sum_{ken}\left(i_{k\varphi}^{T} + ji_{k\varphi}^{x}\right) - \sum_{m\in}\left(i_{m\varphi}^{T} + ji_{m\varphi}^{x}\right)\right] \quad (4.7)$$

Where, Ω is the set of branches incoming on node *i* and A is the set of branches outgoing from node *i*. The variable α in this case, instead, is equal to l if the considered power injection is drawn from the network (like for a load), while it is equal to -1 in the opposite case (like for a generator). Even in this case, it is possible to observe that the obtained measurement functions are linearly related to the state variables and that no coupling exists among the different phases.

4.5.3 Current Magnitude Measurement

The function associated to a current magnitude measurement $I_{l\varphi}$ on phase φ of a generic line l is:

$$h_{I_{l\varphi}} = \sqrt{i_{l\varphi}^{x\ 2}} \quad (4.8)$$

It is possible to notice that current magnitude measurements introduce nonlinearities in the estimator model and lead to the coupling between real and imaginary state variables. However, they are still related to state variables belonging only to the same phase φ of the measurement, thus, no coupling among the different phases is introduced.

4.5.4 Voltage Magnitude Measurement Function

The voltage phasor:

$$\left[v_{i\varphi} = v_{1\varphi} - \sum_{k\in T} Z_{k\,1\varphi} i_k\right] e^{-j^{\delta i\varphi}} \tag{4.9}$$

Where, $\delta_{i\delta}$ is the angle of the considered voltage on the phase φ of node *i*. With further modifications, it is possible to write:

$$V_{i\phi} = \mathrm{Re}\left[V_{1\phi} e^{j^{(\delta 1\phi - \delta 1\phi)}} - \sum_{k\in T} Z_{k,\phi} i_k e^{-j\delta 1\phi} \right] \tag{4.10}$$

And, the final function of the voltage magnitude measurement is:

$$hv_{i\phi} = V_{1\phi}\cos\left(\delta_{1\phi} - \delta_{i\phi}\right) - \sum_{keT}\left(R_{k,\phi} i_k^r - X_{k,\phi} i_k^x\right)\cos\left(\delta_{i\phi}\right) - \sum_{keT}\left(X_{k,\phi} i_k^T + R_{k,\phi} i_k^x\right)\sin\left(\delta_{i\phi}\right) \tag{4.11}$$

Where, $R_{k,\varphi}$ and $X_{k,\varphi}$ are the real and imaginary part respectively of the considered row vector of the three-phase impedance matrix $Z_{k,\varphi}$ for branch *k*. It can be seen that the relationship for the voltage magnitude measurement is nonlinear and introduces in the estimator model coupling both between real and imaginary components of the currents and between the different phases of the system.

To solve the WLS problem, the computation of their derivatives with respect to each state variable has to be developed in order to achieve the Jacobian matrix other than the definition of the measurement functions. Details on the resulting Jacobian terms for each measurement function are provided in next section**.**

4.6 Jacobian Matrix formation of WLS BCDSSE

The Jacobian of the BCDSSE includes all the derivatives of the traditional measurements with respect to the real and imaginary components of the branch currents. The relationships associated to the different Jacobian terms are given below as resembling the same scheme of measurement function:

4.6.1 Active and Reactive Power Flow

$$\frac{\partial h_{i_{l\varphi}^{r}}^{eq}}{\partial i_{j\psi}^{r}} = \begin{cases} 0 \text{ for phase } \psi \neq \varphi \\ 0 \text{ for phase } \psi = \varphi \text{ and branch } j \neq l \\ \alpha \text{ for phase } \psi = \varphi \text{ and branch } j = l \end{cases}$$

$$\frac{\partial \mathrm{h}_{\mathrm{i}_{\mathrm{l}\phi}^{\mathrm{r}}}^{\mathrm{eq}}}{\partial \mathrm{i}_{\mathrm{j}\psi}^{\mathrm{x}}} = 0 \text{ for each phase } \psi \text{ and branch j}$$

$$\frac{\partial \mathrm{h}_{\mathrm{i}_{\mathrm{l}\phi}^{\mathrm{x}}}^{\mathrm{eq}}}{\partial \mathrm{i}_{\mathrm{j}\psi}^{\mathrm{r}}} = 0 \text{ for each phase } \psi \text{ and branch j}$$

$$\frac{\partial \mathrm{h}_{\mathrm{i}_{\mathrm{l}\phi}^{\mathrm{x}}}^{\mathrm{eq}}}{\partial \mathrm{i}_{\mathrm{j}\psi}^{\mathrm{x}}} = \begin{cases} 0 \text{ for phase} \psi \neq \phi \\ 0 \text{ for phase} \psi = \phi \text{ and branch j} \neq \mathrm{l} \\ \alpha \text{ for phase} \psi = \phi \text{ and branch j} = \mathrm{l} \end{cases}$$

Where, α is +1 or -1 depending on the direction of the measured power with respect to the conventional direction assumed for the branch current.

4.6.2 Active and Reactive Power Injection

$$\frac{\partial h^{eq}_{i^{x}_{l\phi}}}{\partial i^{x}_{j\psi}} = \begin{cases} 0 \quad \text{for phase } \psi \neq \phi \\ 0 \quad \text{for phase } \psi = \phi \text{ and branch j not converging in node i} \\ \alpha \quad \text{for phase } \psi = \phi \text{ and branch j incoming in node i} \\ -\alpha \text{ for phase } \psi = \phi \text{ and branch j outgoing from node i} \end{cases}$$

$$\frac{\partial h^{eq}_{i^{r}_{ln\,j,i\phi}}}{\partial i^{x}_{j\psi}} = 0 \quad \text{for each phase } \psi \text{ and branch j}$$

$$\frac{\partial h^{eq}_{i^{x}_{ln\,j,i\phi}}}{\partial i^{r}_{j\psi}} = 0 \quad \text{for each phase } \psi \text{ and branch j}$$

$$\frac{\partial h^{eq}_{i^{x}_{l\phi}}}{\partial i^{x}_{j\psi}} = \begin{cases} 0 \quad \text{for phase } \psi \neq \phi \\ 0 \quad \text{for phase } \psi = \phi \text{ and branch j not converging in node i} \\ \alpha \quad \text{for phase } \psi = \phi \text{ and branch j incoming in node i} \\ -\alpha \text{ for phase } \psi = \phi \text{ and branch j outgoing from node i} \end{cases}$$

Where, α is +1 for positive powers drawn by loads and -1 for positive power generation.

4.6.3 Current Magnitude

$$\frac{\partial h_{I_{i\phi}}}{\partial i^{r}_{j\psi}} = \begin{cases} 0 \quad \text{for phase } \psi \neq \phi \\ 0 \quad \text{for phase } \psi = \phi \text{ and branch } j \neq l \\ \cos\theta_{l\phi} \text{ for phase } \psi = \phi \text{ and branch } j = l \end{cases}$$

$$\frac{\partial h_{I_{i\phi}}}{\partial i^{x}_{j\psi}} = \begin{cases} 0 & \text{for phase } \psi \neq \phi \\ 0 & \text{for phase } \psi = \phi \text{ and branch } j \neq l \\ \sin\theta_{l\phi} & \text{for phase } \psi = \phi \text{ and branch } j = l \end{cases}$$

Where, $\theta_{l\varphi}$ is the angle of the current in branch l and for phase φ.

4.6.4 Voltage Magnitude

T is the set of branches linking the chosen slack bus to the bus *i*. the voltage measurement is as follow:

$$\frac{\partial h_{V_{i\phi}}}{\partial i^{r}_{j\psi}} = \begin{cases} 0 & \text{for } j \notin \Gamma \\ -r_j^{\phi\phi}\,\mathrm{Cos}\,\delta_{i\phi} - x_j^{\phi\phi}\,\mathrm{Sin}\,\delta_{i\phi} & \text{for phase } \psi = \phi \text{ and branch } j \in \Gamma \\ -r_j^{\phi\phi}\,\mathrm{Cos}\,\delta_{i\phi} - x_j^{\phi\phi}\,\mathrm{Sin}\,\delta_{i\phi} & \text{for phase } \psi \neq \phi \text{ and branch } j \in \Gamma \end{cases}$$

$$\frac{\partial h_{V_{i\phi}}}{\partial i^{x}_{j\psi}} = \begin{cases} 0 & \text{for } j \notin \Gamma \\ -x_j^{\phi\phi}\,\mathrm{Cos}\,\delta_{i\phi} - r_j^{\phi\phi}\,\mathrm{Sin}\,\delta_{i\phi} & \text{for phase } \psi = \phi \text{ and branch } j \in \Gamma \\ -x_j^{\phi\phi}\,\mathrm{Cos}\,\delta_{i\phi} - r_j^{\phi\phi}\,\mathrm{Sin}\,\delta_{i\phi} & \text{for phase } \psi \neq \phi \text{ and branch } j \in \Gamma \end{cases}$$

Where, $r_j^{\varphi\varphi}$ and $x_j^{\varphi\varphi}$ are the real and the imaginary part of the self-impedance in branch $j_{i.}$ $r_j^{\varphi\varphi}$ and $x_j^{\varphi\varphi}$ are the real and the imaginary part of the mutual-impedance in branch *j* between phases φ and ψ; $\delta_{i\varphi}$ is the voltage angle of bus *i* for phase φ.

4.7 WLS BCDSSE Algorithm

BCDSSE constructs the Jacobian and gain matrices and solves the update equations iteratively formulated earlier. The algorithm involves the following steps at each iteration k:

- Step 1: convert all measurements into equivalent current measurements using equations provided in previous section.
- Step 2: Use current measurements to obtain an estimate of branch currents by solving the update equations (4.4) for each phase $\phi = a,b,c$.
- Step 3: Given the branch currents, update the node voltages V by the forward sweep procedure.
- Step 4: Check for convergence; if two successive updates of branch currents are less than permissible convergence tolerance then stop, otherwise go back to step 1.

4.8 Bad Data Detection

Bad measurement data detection is an important element at this point of the distribution state estimation. If bad data is enormously present as an input to the state estimators, then the system's state variables will be way out from the expected estimates. An algorithm is incorporated with the state estimation method in order to distinguish bad measurements and eliminate them. Chi-Square testing method is one of many data identification techniques which is used in this thesis. The identification is performed by the largest normalized residual test, which is widely used for this purpose. One indication for the presence of corrupted data in the set of measurements is the magnitude of the residual, *J(x),* which is the product of state estimation as discussed previously. Comparatively small value of *J(x)* indicates that the measurement set does not contain significant corrupted measurements. However, there is a possibility for the presence of corrupted data if the residual converges to a big number. To figure out the boundary or the range of residuals to be considered a good or a bad number, the residual must follow a specific distribution as the measurement function. Therefore, the residual *J(x)* is supposed to have a probability distribution

function (PDF) of Chi-Square distribution, $\chi 2$ (K). K is the degree of freedom of this distribution, which is the difference between the number of measurements (Nm) and the number of states (Ns) as shown below:

$$K = N_m - N_s = N_m - (2n - 1) \quad 4.12$$

A hypothesis test is performed to figure out if the residual is in acceptable state or not. As the hypothesis test is performed on the residual value, it is not necessary to define a threshold value as long as the significant figure α is known. Significant figure is the probability in which the residual would be larger than a specified threshold LJ. An example is presented in the next section for further clarification.

4.8.1 Chi-Square Distribution for Bad data Detection

Assuming six independent measurements are received from a substation feeder for that single bus for the variables given in Table 4.1, considering that they have been taken from a sample following a normal distribution.

Variable	**x1**	**x2**	**x3**	**x4**	**x5**	**x6**
Meas.value	1.8	0.9	0.4	-.25	-1.8	2.9

Table 4. 1: Arbitrary measured data in an arbitrary bus for chi-square test

To solve the problem, 95% confidence is considered for the bad data detection using Chi-Square distribution. From the problem statement, it is concluded that the significant figure α is 5 (100-95), and that the calculation of degree of freedom as follow:

$$K=Nm - (2n - 1) = 6 – (2 \text{ x } 1 -1) = 6 – 1 = 5$$

Where, *n* is 1 as a single bus data was considered and *Nm* is 6. Therefore; to obtain the probability of finding this value using the Chi-Square method, the sum of the squares of all six measurements has to be calculated as below:

$$J(x) = \sum_{i=1}^{6} x_i^2$$

$$J(x) = 3.24+ 0.81+ 0.16+ 0.0625+ 3.24+ 8.41 = 15.9225$$

By using the Chi-Square distribution table and the calculated values, the degree of freedom and the significant figure, a value for the threshold is extracted randomly, where LJ = 12.139. Therefore, from the Figure 4.1 below, the sum of the squares found to be lying in the rejected area. It happened because L was bigger than the threshold LJ; since $J(x)$ = 154.9225 > LJ =11.070. This concludes that the data collected failed the test and it contains "bad" data. For the WLS method, following residual matrix as mentioned in 4.2 is used to compare with LJ:

$$J(x) = \sum_{i=1}^{M} \frac{\omega i[y_i - h_i(x)]^2}{e_i^2}$$

According to the pre-stated confidence percentage and degree of freedom in the problem statement, a value from the Chi-Square distribution table is registered for that probability as threshold (LJ). Both $J(x)$ and LJ are compared to examine the existence of bad data in the system. Therefore, if $J(x) \geq LJ$, then corrupted data is present. Otherwise, the measurements set is assumed to be acceptable.

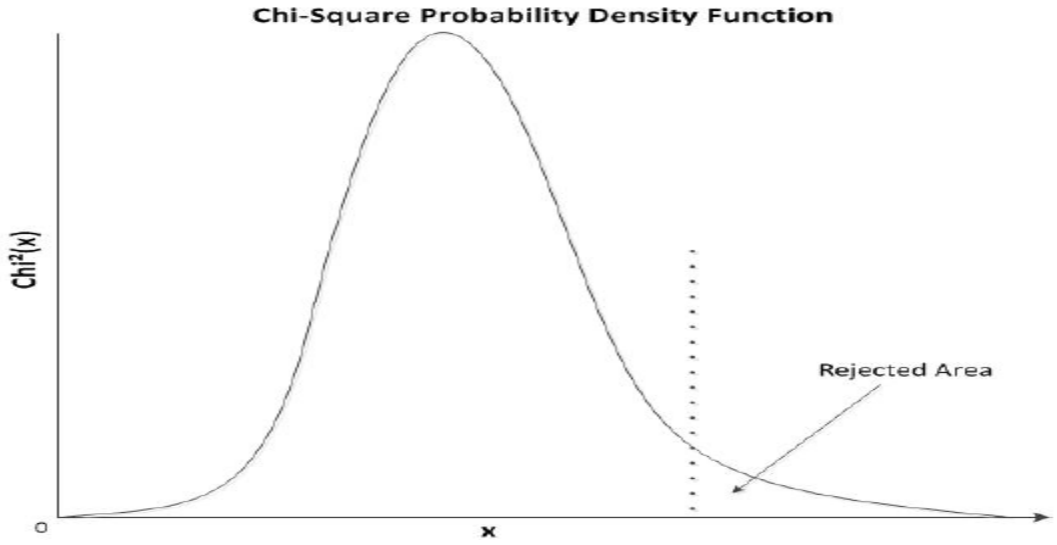

Figure 4. 1: Chi-Square PDF testing for bad data detection

Chapter 5: Unbalanced DSSE Based on Load Correction Method

5.1 Introduction to Load Correction Based DSSE

This chapter presents a state estimation technique in the radial distribution network based on load flow calculation algorithm. Iterative backward/forward sweep algorithm is used to calculate load flow of the radial network. Unlike WLS, Load correction technique does not require to calculate Jacobian matrices and is applicable to both balanced and unbalanced distribution network. This technique is found to be a very practical approach due to its rigid performance with minimum available measurements.

5.2 Load Correction Based DSSE

The load correction approach for state estimation in radial distribution networks is a practical algorithm based on the adjustment of the load (active and reactive power at network buses) so that the values conform the real-time measurement data. Through iterative procedure, the bus loads are adjusted based on backward/forward sweep power flow computation by treating voltage and power measurements in a substation as real-time (true) information. A practical method for DSSE in the distribution network must include the real conditions of the network. Due to the insufficient number of real-time (telemetric) measurements, it is necessary to make the system observable in some way with the introduction of so-called pseudo-measurements. The pseudo-measurements are the load data taken from historical load profiles in the network buses.

5.3 Measurements for Load Correction DSSE

The results of the state estimation in a distribution network are the estimated values of voltages at all buses, currents, active and reactive power in all branches and power losses in the network. In order to begin the process of state estimation using this simple algorithm, the next set of data must be available for the moment in which the state estimation is performed:

- The voltage at root bus (source substation) as real-time measurement.
- The active and reactive powers (or current magnitudes and power factors) at source substation feeder as real-time measurements.
- The loads at all buses of the network as pseudo-measurements.

5.4 Load Correction Based DSSE Algorithm

The DSSE algorithm for unbalanced radial distribution networks based on iterative load correction consists three main steps described below. General flow chart of the load correction state estimation algorithm is presented in Figure 5.1.

- Initial Calibration of active and reactive power of loads based on the normalized daily load diagrams and load weights. The normalized daily load profiles for active (LP) and reactive (LQ) power are established based on historical load data in the network. For the load weight can be used nominal powers ($P_{[nom]}$ and $Q_{[nom]}$) of the loads. Therefore, the initial loads at moment (hour) T, at bus *i*, can be obtained using following equations:

$$P_i(T) = P_{[nom]^i} * LP(T) \quad (5.1)$$

$$Q_i(T) = Q_{[nom]^i} * LQ(T) \quad (5.2)$$

- Generate Measurements as an input to the state estimator. There are two types of measurements:

  (i) Real-time (true) measurements: Voltage (for all three phases) at the source substation, and three-phase active and reactive powers at the source substation (in feeding line of the distribution system).

  (ii) Pseudo-measurements for load data: The measurements were generated using three-phase backward/forward sweep power flow program with addition of uniformly distributed random component to generate measurement error. Measurements have been produced by adding uniformly distributed random component to load flow results as true, where the power flow is performed with the values of loads given by (5.1) and (5.2).

  For example, measured value of voltage at source substation $V_0^{[meas]}$ is generated as follows:

$$V_0^{[meas]} = V_0^{[true]}\left(1 - \frac{E_v}{100}\right) + 2 \cdot rand \cdot V_0^{[true]} \cdot \frac{E_v}{100} \tag{5.3}$$

  Where, $V_0^{[meas]}$ is the measured value of voltage, $V_0^{[true]}$ is the true value of voltage, E_v is the error of voltage measurement in (%), *rand* is uniformly distributed random number in the interval (0,1).

- State Estimation: Iterative correction of the power of loads based on the calculated and measured values of active and reactive power at source substation (in feeding branch). After power flow calculation, it compares the calculated and the measured quantities (active and reactive power at source substation). If difference between calculated and measured quantity is higher than permitted convergence criterion value, the load correction at buses is performed using the following equations:

$$\mathbf{P}_{L,i}^{(k+1)} = \frac{\mathbf{P}_0^m}{\mathbf{P}_0^{c(k)}} \cdot \mathbf{P}_{L,i}^{(k)} \tag{5.4}$$

$$\mathbf{Q}_{L,i}^{(k+1)} = \frac{\mathbf{Q}_0^m}{\mathbf{Q}_0^{c(k)}} \cdot \mathbf{Q}_{Li}^{(k)} \tag{5.5}$$

Where,

$\mathbf{P}_{L,i} = \begin{bmatrix} P_{L,ia} \\ P_{L,ib} \\ P_{L,ic} \end{bmatrix}$ And $\mathbf{Q}_{L,i} = \begin{bmatrix} Q_{L,ia} \\ Q_{L,ib} \\ Q_{L,ic} \end{bmatrix}$ are active and reactive power of load at bus *I;*

$\mathbf{P}_0^m = \begin{bmatrix} P_{0a}^m \\ P_{0b}^m \\ P_{0c}^m \end{bmatrix}$ And $\mathbf{Q}_0^m = \begin{bmatrix} Q_{0a}^m \\ Q_{0b}^m \\ Q_{0c}^m \end{bmatrix}$ are measured value of active and reactive powers in source substation (feeding line);

$\mathbf{P}_0^c = \begin{bmatrix} P_{0a}^c \\ P_{0b}^c \\ P_{0c}^c \end{bmatrix}$ And $\mathbf{Q}_0^c = \begin{bmatrix} Q_{0a}^c \\ Q_{0b}^c \\ Q_{0c}^c \end{bmatrix}$ are calculated value of active and reactive powers in source substation, *k* is the iteration index and *a*, *b*, *c* are phases.

- Calculate "true" values of variables in the system at moment T (hour) using true voltage at substation $V_0^{[true]}$ and load given by (5.1) and (5.2) to compare with estimated values.

This DSSE technique is very simple, robust and applicable to all radial distribution networks with minimum real measurements. It can be applied to both balanced and unbalanced distribution network using similar algorithm. Another important advantage of this method over WLS is that, there is no need of differential equations of Jacobian matrices.

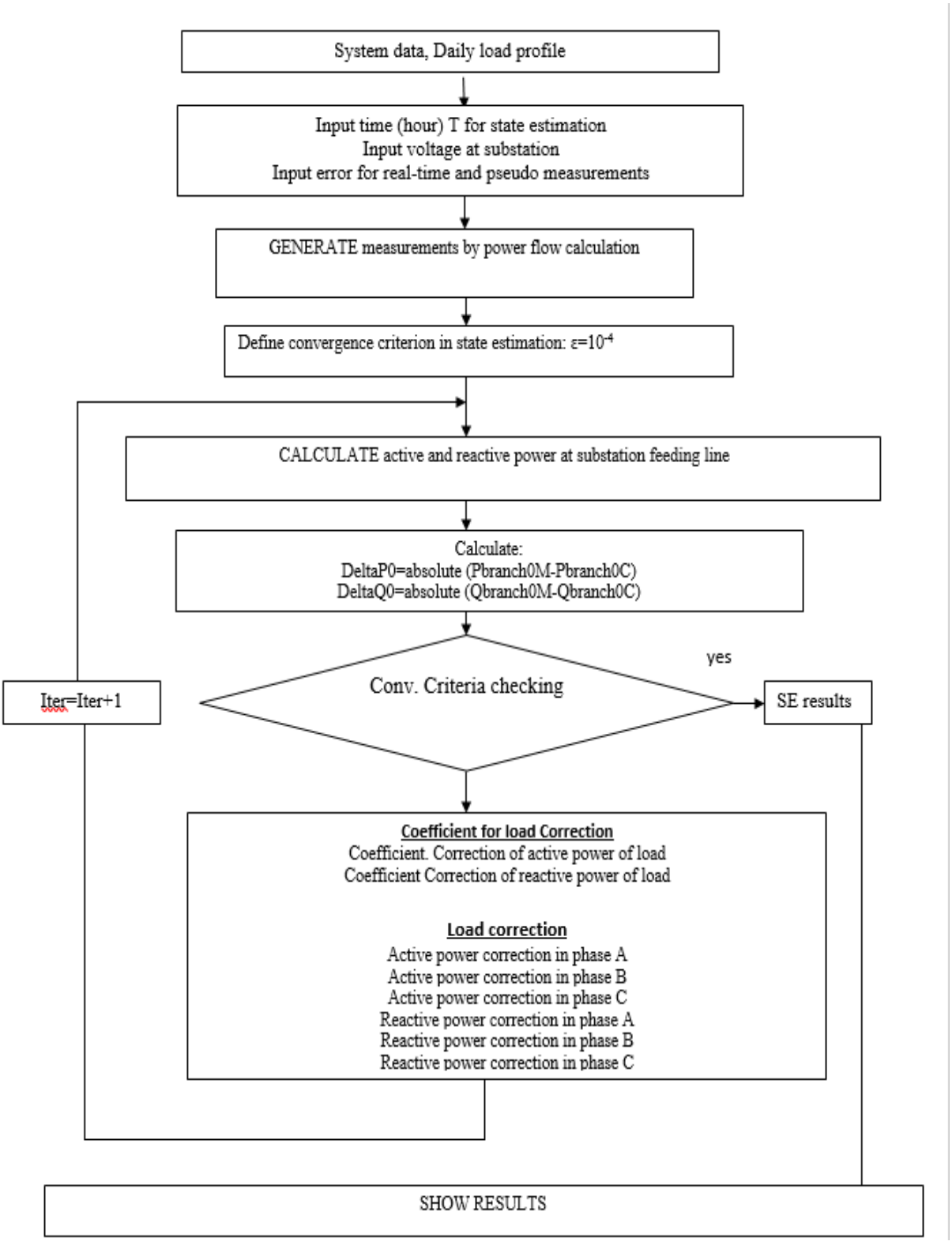

Figure 5. 1: Load correction based DSSE flow chart

Chapter 6: Performance Analysis

6.1 Case Study on IEEE 13 Bus Network System

6.1.1 WLS DSSE Performance

Branch currents are used as state variable which is described in previous chapter on WLS DSSE. The state vector is solved iteratively until the convergence criteria is satisfied. To verify if the WLS DSSE is converging closer value to the measured value, the algorithm is compiled in MATLAB platform for two cases. The test feeder presented here is a 13 bus, 4.16kv three-phase radial network [23]. The base case power flow calculation conforms the IEEE standard validity for the network. Two kind of measurements are used; AMI load measurements and real measurements on the substation feeder. Feeder real (true) measurements are power flow and voltage in the substation feeder line. Load measurements are noised by adding 35% error for the simulation. Series of data tables and graphs are shown to compare the true and estimated value. The measurement standard deviation (σ) of 0.03 (20% accuracy of measured value) is selected for power and current measurements from a normal distribution. Standard deviation (σ) of 0.0095 (3% accuracy of measured value) is selected for voltage magnitude to add measurement errors. Table 6.1 and Table 6.2 represent the estimation of bus voltage magnitudes and angles respectively. Figure 6.1 represents the graphical view of the voltage magnitudes with percentage of errors for all three phases in the estimation process.

BUS No	Phase A (pu)		Phase B (pu)		Phase C (pu)	
	Estim.	True	Estim.	True	Estim.	True
650	1.0650	1.0625	1.0525	1.0500	1.0712	1.0687
632	1.0237	1.0211	1.0445	1.0420	1.0201	1.0174

633	1.0209	1.0180	1.0429	1.0401	1.0177	1.0148
634	0.9988	0.9941	1.0270	1.0218	1.0006	0.9960
645	0.0000	0.0000	1.0353	1.0328	1.0182	1.0155
646	0.0000	0.0000	1.0336	1.0311	1.0161	1.0134
671	0.9924	0.9901	1.0546	1.0529	0.9801	0.9779
680	0.9924	0.9901	1.0545	1.0529	0.9801	0.9779
684	0.9907	0.9881	0.0000	0.0000	0.9779	0.9759
611	0.0000	0.0000	0.0000	0.0000	0.9758	0.9738
652	0.9854	0.9826	0-0000	0.0000	0.0000	0.0000
692	0.9924	0.9901	1.0545	1.0529	0.9801	0.9779
675	0.9861	0.9836	1.0569	1.0553	0.9783	0.9759

Table 6. 1: Estimated voltage magnitude for 13 bus network in pu using WLS

BUS	**Phase A (dg)**		**Phase B (dg)**		**Phase C (dg)**	
No	**Estim.**	**True**	**Estim.**	**True**	**Estim.**	**True**
650	0.000	0.000	-120.000	-120.000	120.000	120.000
632	-2.475	-2.489	-121.710	-121.720	117.842	117.829
633	-2.536	-2.554	-121.750	-121.765	117.842	117.825
634	-3.152	-3.230	-122.151	-122.221	117.419	117.345
645	0.000	0.000	-121.891	-121.899	117.867	117.856
646	0.000	0.000	-121.967	-121.975	117.911	117.901
671	-5.274	-5.295	-122.352	-122.342	116.013	116.025
680	-5.274	-5.295	-122.352	-122.342	116.012	116.025
684	-5.296	-5.318	0.000	0.000	115.907	115.924
611	0.000	0.000	0.000	0.000	115.759	115.777
652	-5.223	-5.242	0.000	0.000	0.000	0.000
692	-5.274	-5.295	-122.352	-122.342	116.012	116.025
675	-5.517	-5.543	-122.528	-122.517	116.027	116.038

Table 6. 2: Estimated bus voltage angles for 13 bust network in degree using WLS

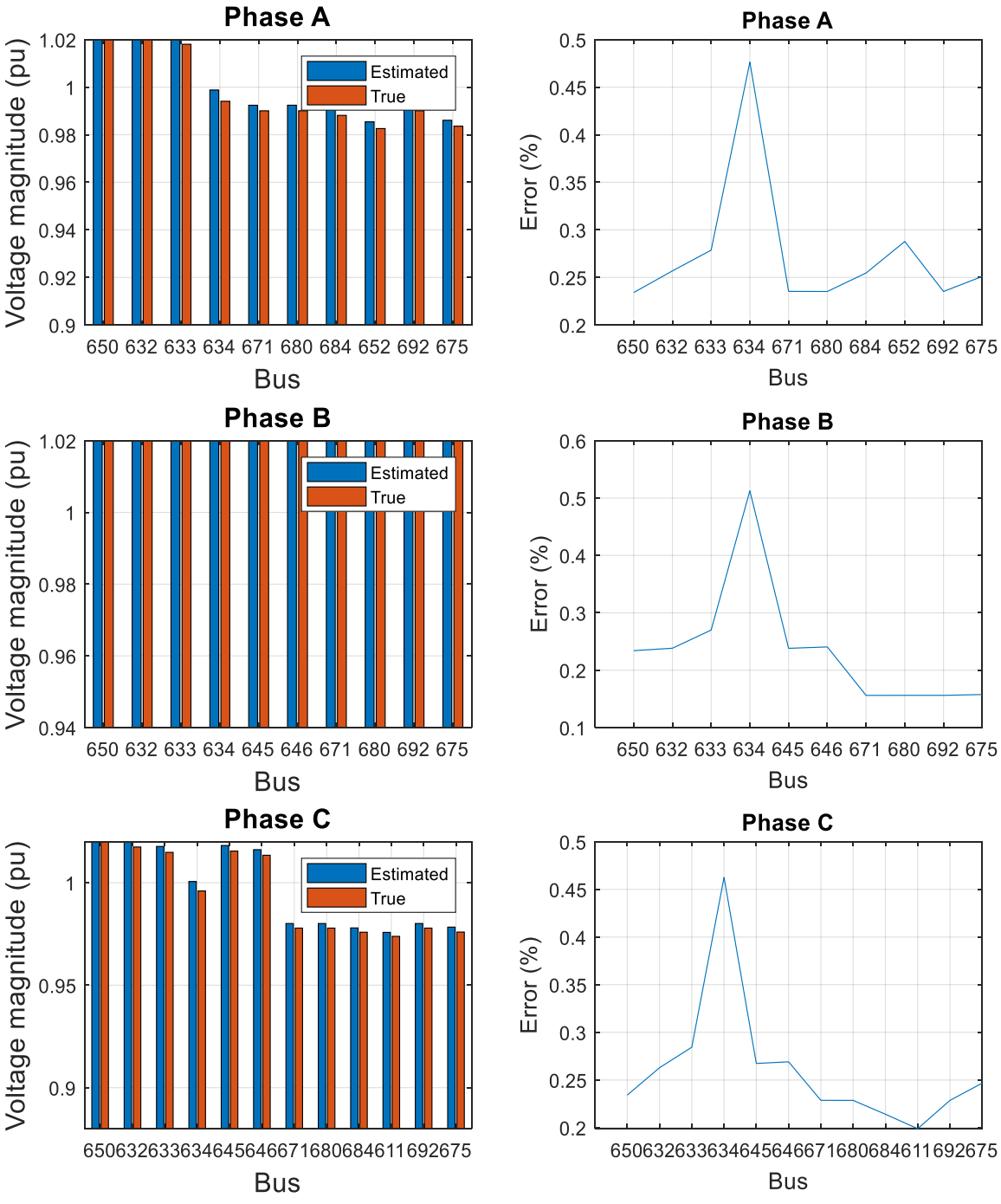

Figure 6. 1: True and estimated voltage magnitude with percentage of estimation errors for using WLS

The voltage estimation is for all the phases are very close to the true base case value. Maximum error is recorded for phase 'A' in bus 634 which is about 0.5%. Minimum error is recorded for phase c in bus 652 which is about 0.2%. Bus voltage angle estimation providing good response as it can be seen the angle deviation is higher in the far end buses from substation which is understandable. Table 6.3 and Figure 6.2 represent the branch current magnitude for all the phases.

BRANCH		**Phase A**		**Phase B**		**Phase C**	
Bus_i	**to Bus_J**	**Estim.**	**True**	**Estim.**	**True**	**Estim.**	**True**
650	632	559.867	558.331	416.014	414.867	588.160	586.557
632	633	82.329	81.323	61.739	61.123	63.524	62.703
633	634	713.518	704.802	535.073	529.739	550.549	543.433
632	645	0.000	0.000	132.881	143.025	60.693	65.206
645	646	0.000	0.000	60.694	65.207	60.694	65.207
632	671	470.867	470.132	198.088	186.409	427.440	420.610
671	680	0.002	0.002	0.002	0.002	0.001	0.001
671	692	221.101	229.053	70.189	69.600	174.939	178.360
692	675	196.874	205.292	70.178	69.589	117.170	124.059
671	684	59.372	63.074	0.000	0.000	68.855	71.150
684	611	0.000	0.000	0.000	0.000	68.855	71.150
684	652	59.381	63.083	0.000	0.000	0.000	0.000

Table 6. 3Table: Estimated branch currents (A) for 13 bus network using WLS

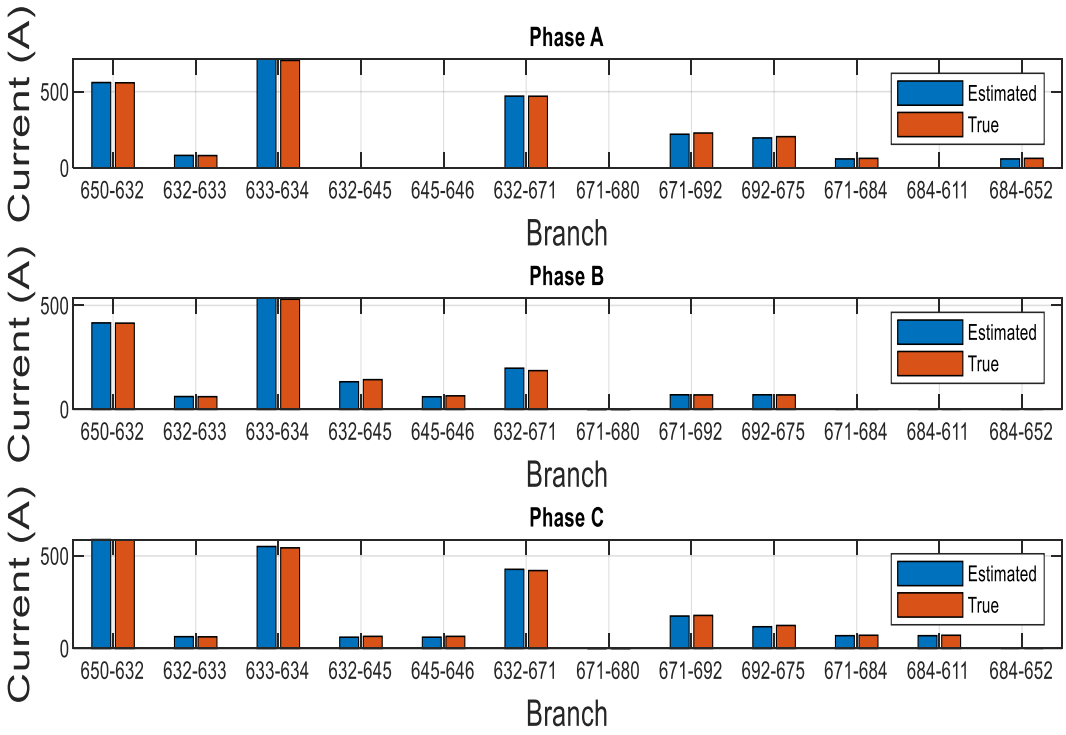

Figure 6. 2: Estimated vs true Brach current magnitude for 13 bus network using WLS

Following Table 6.4 and Figure 6.3 shows are active power estimation based on WLS method for 13 bus system.

BRANCH		Phase A		Phase B		Phase C	
Bus_i to Bus_J		Estim.	True	Estim.	True	Estim.	True
000	650	1254.258	1251.353	979.620	977.334	1351.548	1348.441
650	632	1232.631	1229.846	982.884	980.581	1309.875	1306.994
632	633	165.692	162.515	122.927	121.424	122.239	121.495
633	634	163.112	159.998	121.475	120.001	120.703	119.999
632	645	0.000	0.000	308.746	331.753	4.339	79.445
645	646	0.000	0.000	150.353	161.481	74.105	79.175
632	671	1039.419	1039.483	491.960	464.877	970.260	957.016
671	680	-0.000	-0.000	0.001	0.001	-0.000	-0.000

671	692	512.124	531.020	65.044	68.343	408.278	416.110
692	675	464.660	484.971	64.693	68.000	274.147	289.997
671	684	117.904	124.403	-0.000	-0.000	160.285	165.939
684	611	0.000	0.000	0.000	0.000	159.924	165.553
684	652	117.189	123.595	0.000	0.000	0.000	0.000

Table 6. 4: Estimation of active power flow (kw) for 13 bus network using WLS

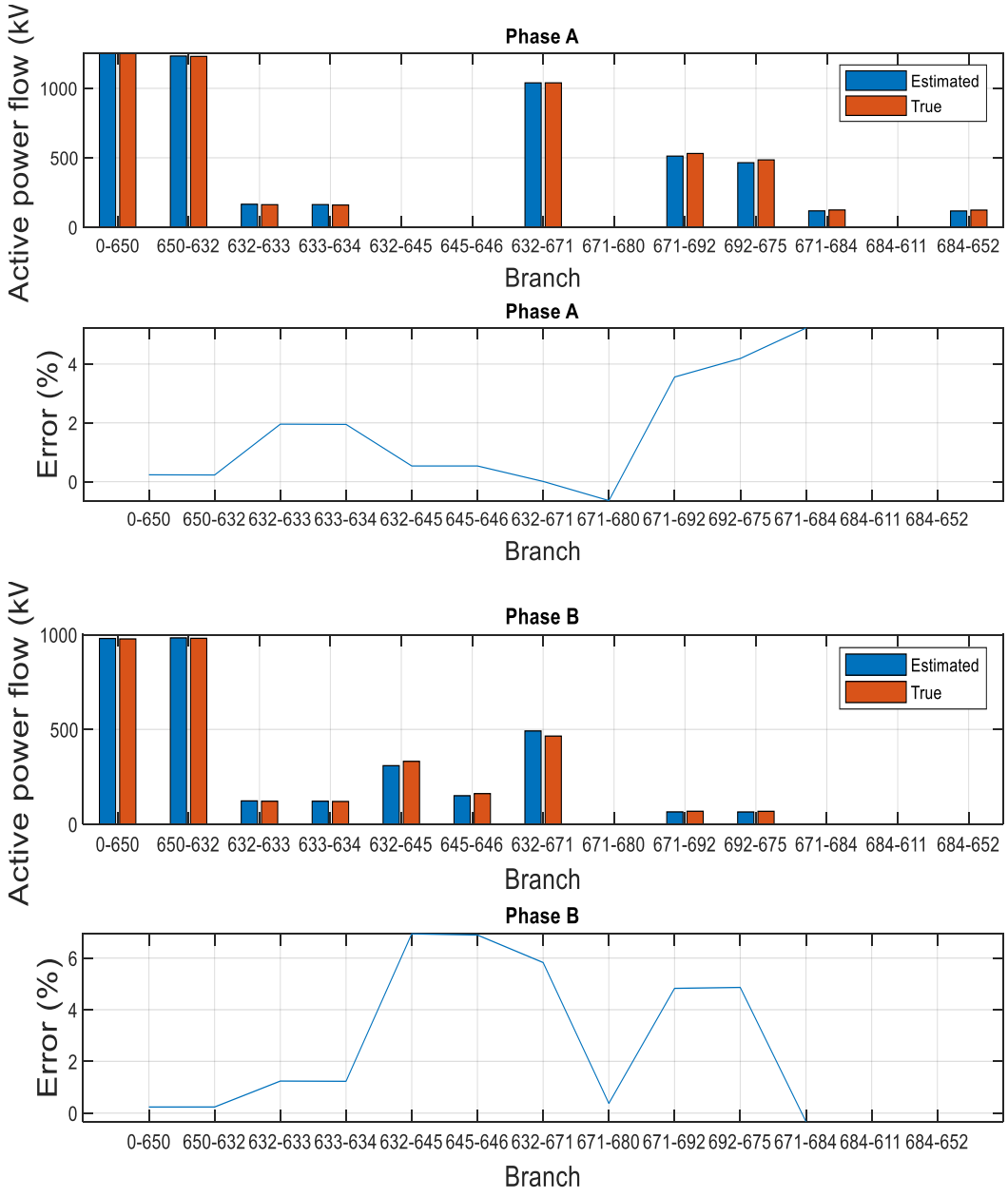

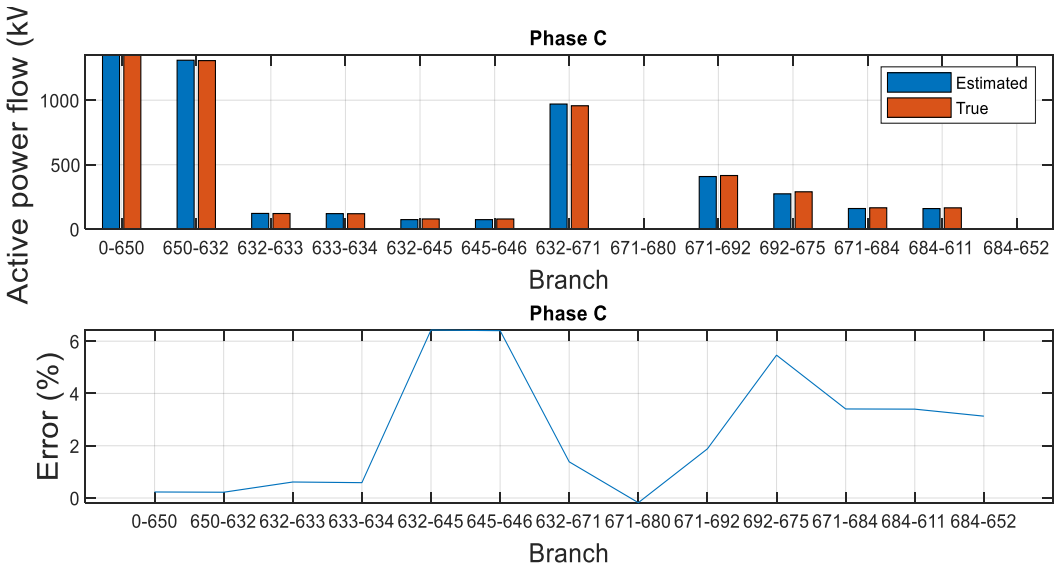

Figure 6. 3: Estimated vs true active power flow (kw) comparison for 13 bus network using WLS

Active power estimation is under acceptable range for measurement variance of 100. Figure 6.4 and Table 6.5 illustrates the estimation accuracy for reactive power flow for the 13-bus network below.

BRANCH		**Phase A**		**Phase B**		**Phase C**	
Bus_i to Bus_J		**Estim.**	**True**	**Estim.**	**True**	**Estim.**	**True**
000	650	682.887	681.303	374.278	373.410	671.192	669.651
650	632	603.024	601.878	341.984	341.295	589.536	588.438
632	633	114.110	114.573	93.032	92.583	94.869	92.718
633	634	109.421	109.997	90.395	89.998	92.078	89.998
632	645	0.000	0.000	115.644	125.774	127.926	137.766
645	646	0.000	0.000	0.073	0.562	27.741	137.552
632	671	414.169	411.406	89.982	78.150	254.675	244.887
671	680	-0.004	-0.004	-0.004	-0.004	-0.004	-0.004
671	692	117.348	121.206	-164.839	-162.196	43.159	48.280
692	675	-15.795	-3.572	-165.375	-162.741	13.556	21.486
671	684	77.013	83.258	0.000	0.000	-17.813	-16.540

684	611	0.000	0.000	0.000	0.000	-18.177	-16.927
684	652	76.783	82.993	0.000	0.000	0.000	0.000

Table 6. 5: Estimation of reactive power flow (kvar) for 13 bus network using WLS

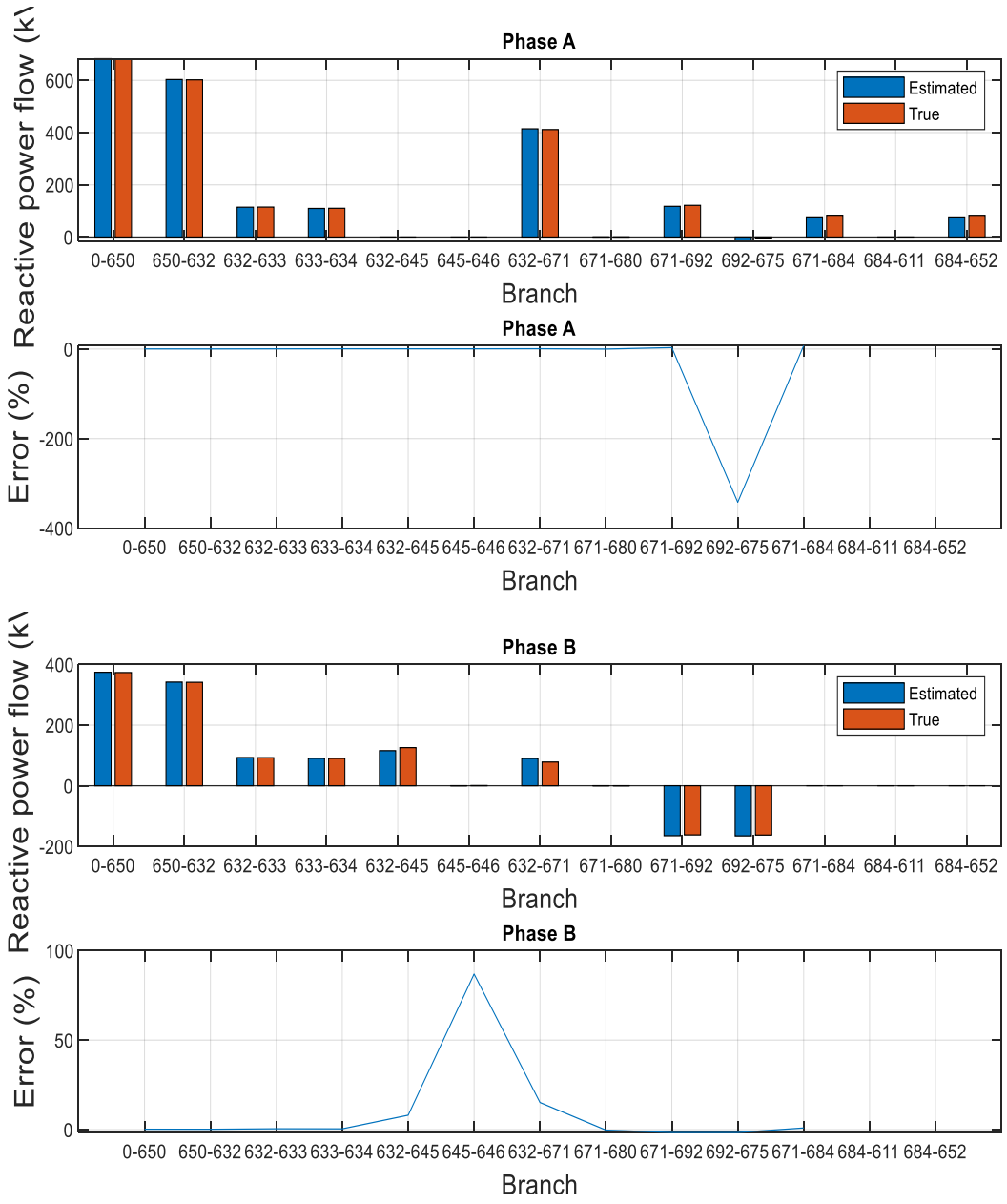

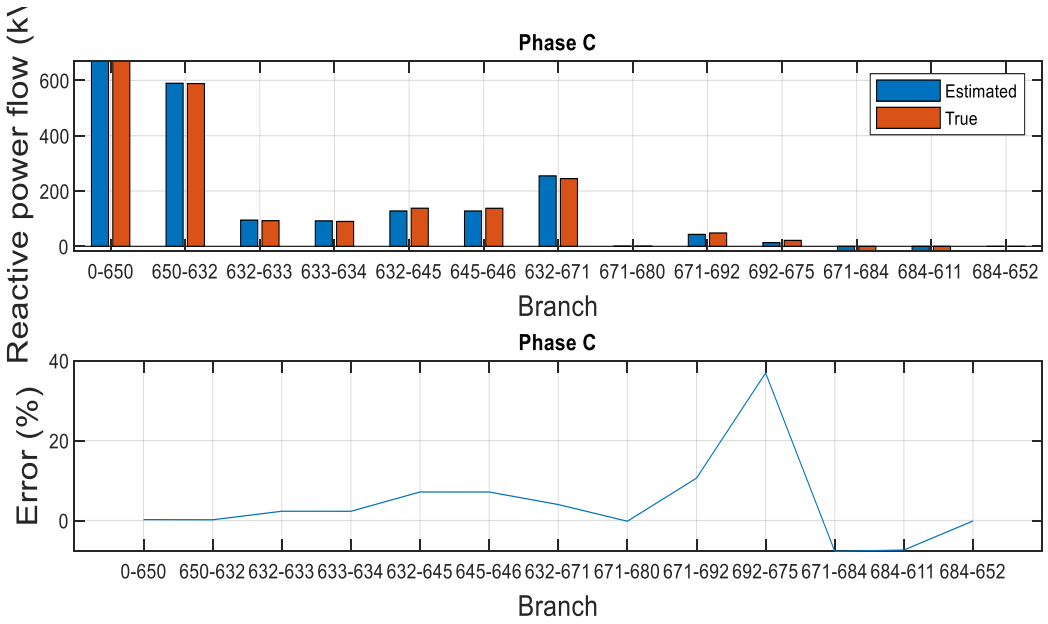

Figure 6. 4: Estimated vs true reactive power flow (kvar) with estimation error for 13 bus network using WLS

Total estimated active Power (kw)	Total true active power (kw)	Total estim. reactive power (kvar)	Total true reactive power (kvar)
111.045	110.985	327.087	324.703

Table 6. 6: Total estimated vs true active and reactive power loss for 13 bus network using WLS

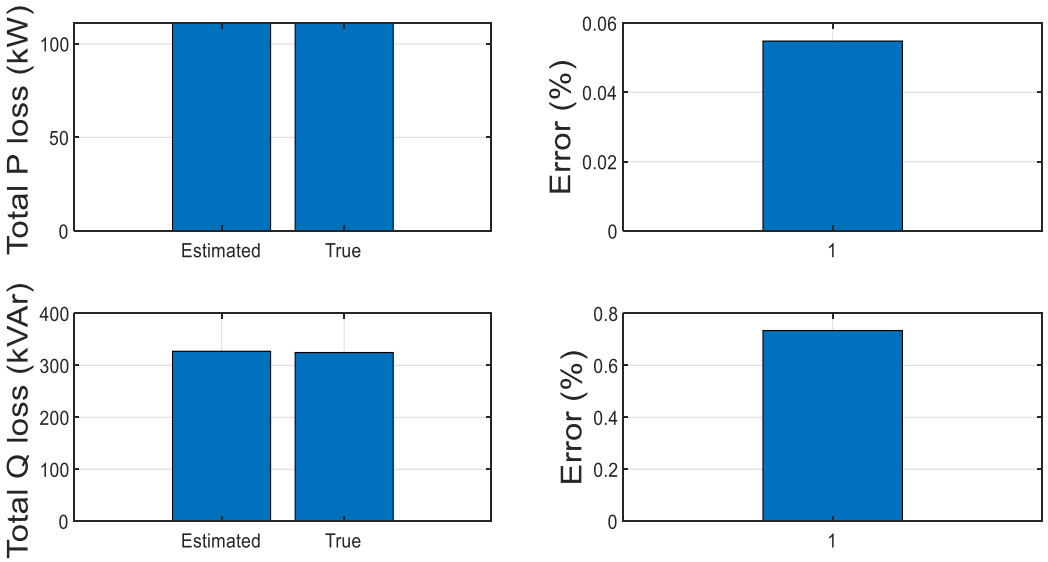

Figure 6. 5: Total active (kw) and reactive (kvar) power loss estimation for 13 bus network based on WLS DSSE

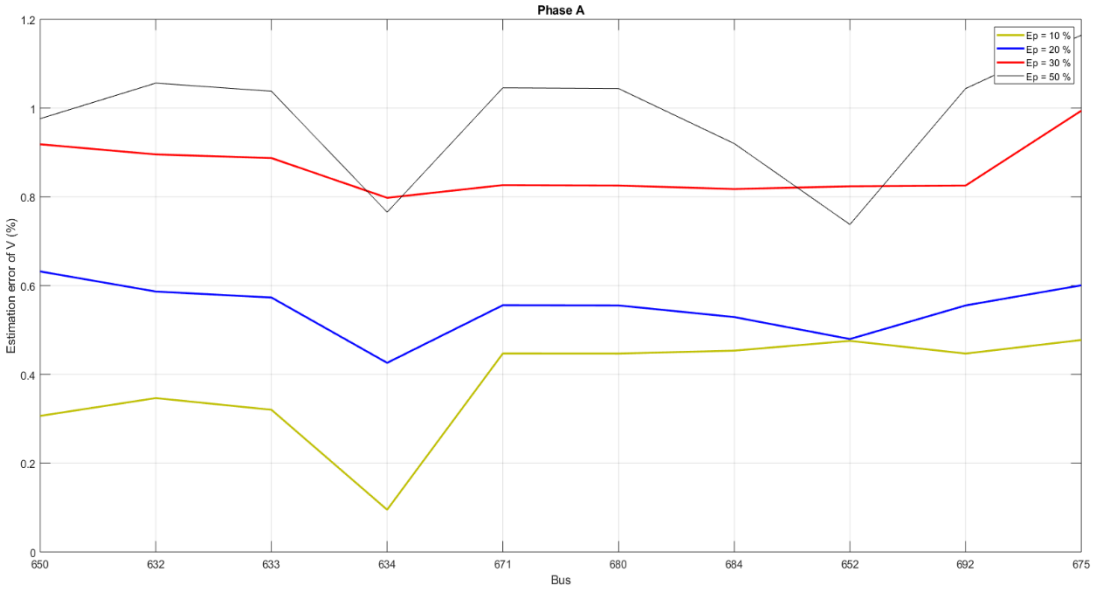

Figure 6. 6: Estimation error comparison for bus voltage magnitudes in phase A for different load measurement errors

When the measurement error is high, estimation error is supposed to be higher. Figure 6.6 shows the estimation error characteristics for bus voltage in phase a using load measurement error of 10%, 20%, 30% and 50%. Estimation graph for measurement error 50% has the most accurate estimation. On the other hand, estimation with measurement error 10% has the lowest amount of estimation error. However, the range of estimation falls under a narrow margin which makes the method very effective.

6.1.2 Load Correction DSSE Performance

The LC DSSE analysis was performed on standard IEEE 13-bustest feeder with voltage measurements at the substation and power flow measurements in substation feeding line. All loads are considered as pseudo measurements. It is assumed that the active and reactive power of loads are changed in same manner with normalized daily load diagram given in Figure 6.6. The load

weights are nominal powers for IEEE 13-bus system. Based on these data, initial calibration of load for a given moment (T) is performed as described. The error of real-time (true) measurement for voltage was assumed up to 1%. The error of real-time (true) measurements for three-phase active and reactive power in feeding line was assumed up to 3 %, whereas the error in pseudo-measurement of load was considered to vary up to 50 %. For the simulation output presented below; voltage error is 1%, feeding line active and reactive power error is 3% and metered load error is 30%.

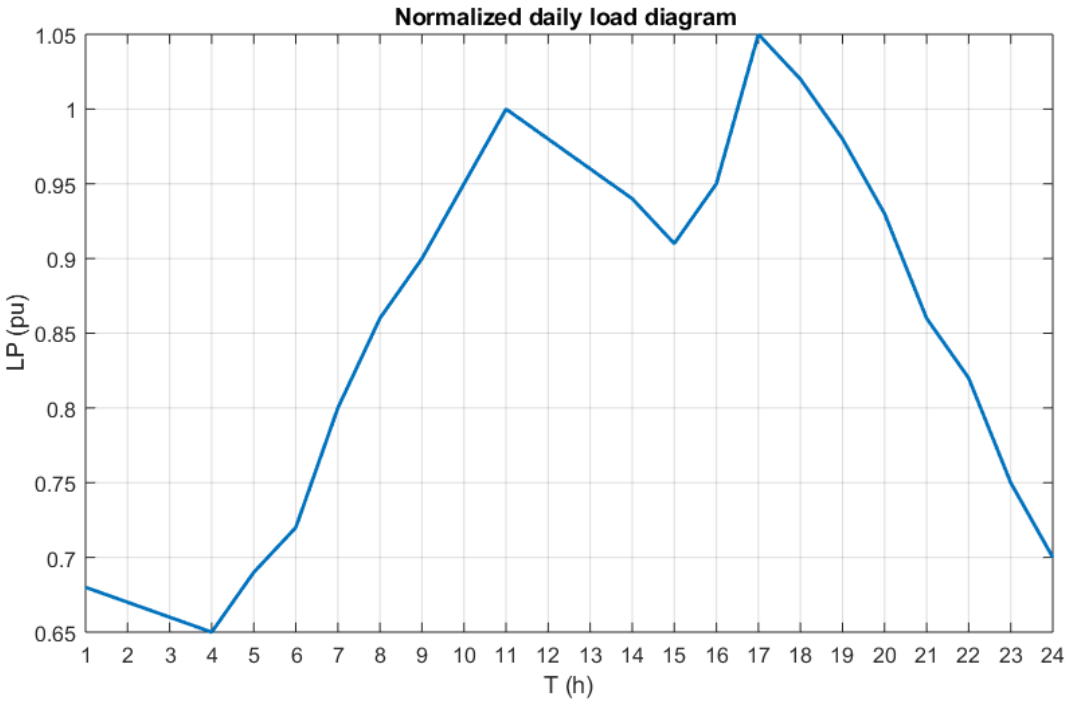

Figure 6. 7: Normalized daily load diagram

Table 6.7 and Figure 6.8 represent the estimated vs true voltage magnitude in pu based on load correction method for 13 bus network system. Table 6.8 shows the voltage angle estimation in degree for 13 bus network system using load correction method.

BUS No	Phase A (pu)		Phase B (pu)		Phase C (pu)	
	Estim.	**True**	**Estim.**	**True**	**Estim.**	**True**
650	1.0546	1.0625	1.0422	1.0500	1.0608	1.0687
632	1.0118	1.0211	1.0340	1.0420	1.0078	1.0174
633	1.0090	1.0180	1.0321	1.0401	1.0049	1.0148
634	0.9852	0.9941	1.0142	1.0218	0.9848	0.9960
645	0.0000	0.0000	1.0246	1.0328	1.0053	1.0155
646	0.0000	0.0000	1.0227	1.0311	1.0030	1.0134
671	0.9792	0.9901	1.0441	1.0529	0.9684	0.9779
680	0.9792	0.9901	1.0441	1.0529	0.9684	0.9779
684	0.9772	0.9881	0.0000	0.0000	0.9672	0.9759
611	0.0000	0.0000	0.0000	0.0000	0.9660	0.9738
652	0.9720	0.9826	0-0000	0.0000	0.0000	0.0000
692	0.9792	0.9901	1.0441	1.0529	0.9684	0.9779
675	0.9728	0.9836	1.0466	1.0553	0.9660	0.9759

Table 6. 7: Estimated voltage magnitude (pu) for 13 bus network using load correction method

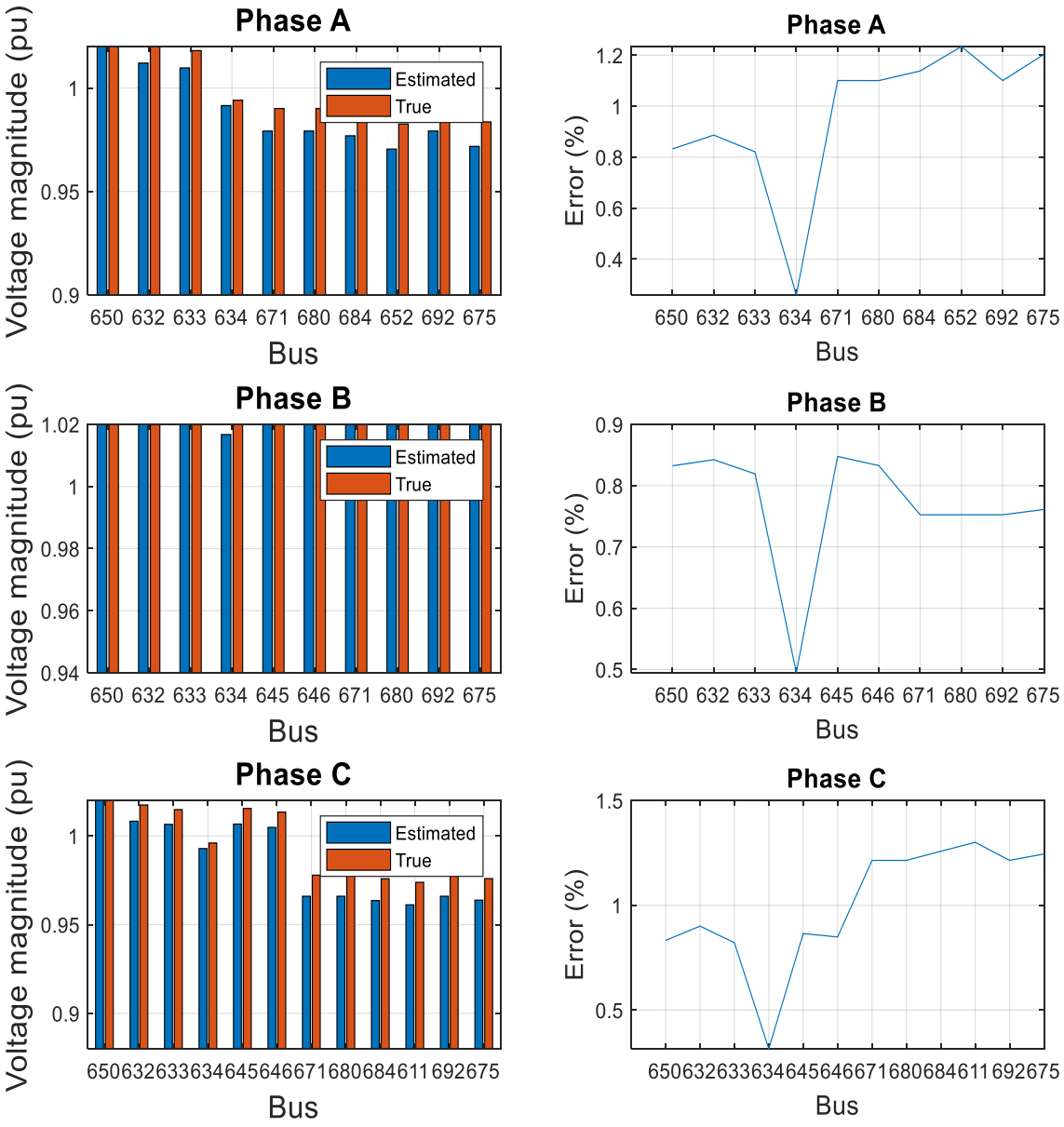

Figure 6. 8: Estimated voltage vs true voltage with estimation error for 13 bus network using load correction method

BUS No	Phase A (dg)		Phase B (dg)		Phase C (dg)	
	Estim.	True	Estim.	True	Estim.	True
650	0.000	0.000	-120.000	-120.000	120.000	120.000
632	-2.525	-2.489	-121.744	-121.720	117.797	117.829
633	-2.565	-2.554	-121.786	-121.765	117.792	117.825
634	-3.050	-3.230	-122.167	-122.221	117.429	117.345
645	0.000	0.000	-121.919	-121.899	117.815	117.856
646	0.000	0.000	-121.989	-121.975	117.855	117.901
671	-5.515	-5.295	-122.401	-122.342	115.973	116.025
680	-5.515	-5.295	-122.401	-122.342	115.973	116.025
684	-5.540	-5.318	0.000	0.000	115.867	115.924
611	0.000	0.000	0.000	0.000	115.709	115.777
652	-5.443	-5.242	0.000	0.000	0.000	0.000
692	-5.515	-5.295	-122.401	-122.342	115.973	116.025
675	-5.772	-5.543	-122.587	-122.517	115.989	116.038

Table 6. 8: Estimated bus voltage angles (dg) for 13 bust network in degree using LC method

Estimated branch currents are presented below in Table 6.9 and Figure 6.9 for IEEE 13 bus network. Specific amount of error being added with the measurements as mentioned earlier.

BRANCH Bus_i to Bus_J		Phase A		Phase B		Phase C	
		Estim.	True	Estim.	True	Estim.	True
650	632	561.347	558.331	417.111	414.867	589.729	586.557
632	633	61.010	81.323	49.768	61.123	45.690	62.703
633	634	528.760	704.802	431.322	529.739	395.985	543.433
632	645	0.000	0.000	140.939	143.025	59.180	65.206
645	646	0.000	0.000	59.181	65.207	59.181	65.207
632	671	491.369	470.132	190.607	186.409	431.039	420.610
671	680	0.002	0.002	0.002	0.002	0.001	0.001

671	692	250.996	229.053	67.216	69.600	183.769	178.360
692	675	229.509	205.292	67.206	69.589	139.074	124.059
671	684	73.363	63.074	0.000	0.000	80.294	71.150
684	611	0.000	0.000	0.000	0.000	80.294	71.150
684	652	73.372	63.083	0.000	0.000	0.000	0.000

Table 6. 9: Estimated branch currents (A) for 13 bus network using LC method

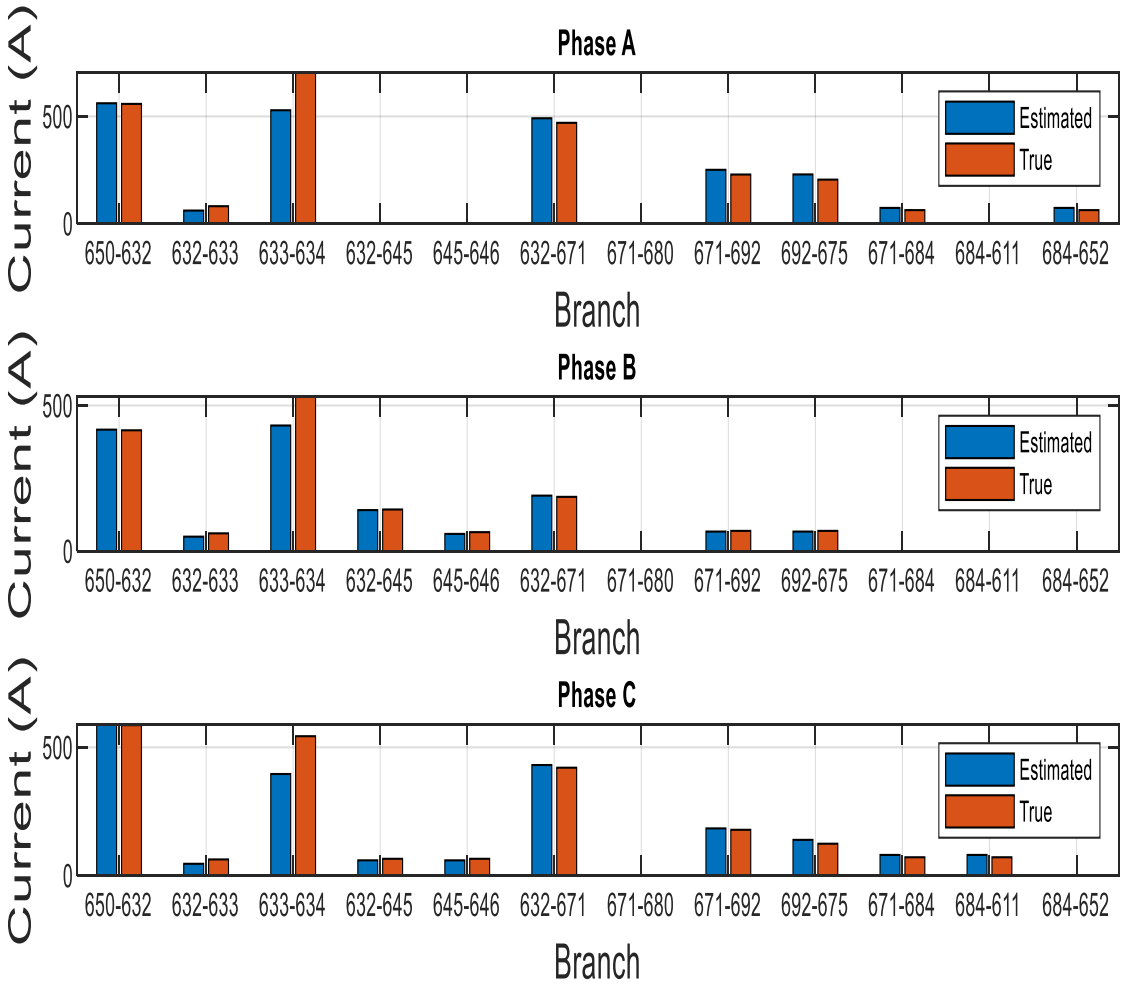

Figure 6. 9: Estimated vs true Brach current magnitude for 13 bus network using LC method

Active power and reactive power flow estimation is one of the parameters to understand the efficiency of a DSSE. Load correction method does a decent job to estimate power flow the

network. Table 6.10, Figure 6.10 and Table 6.11 and Figure 6.11 resembles are estimation of active power flow and reactive power flow respectively based on LC method for 13 bus network system.

BRANCH		Phase A		Phase B		Phase C	
Bus_i to Bus_J		Estim.	True	Estim.	True	Estim.	True
000	650	1247.636	1251.353	974.438	977.334	1344.441	1348.441
650	632	1225.896	1229.846	977.719	980.581	1302.544	1306.994
632	633	118.961	162.515	98.729	121.424	88.834	121.495
633	634	117.545	159.998	97.785	120.001	88.040	119.999
632	645	0.000	0.000	322.318	331.753	72.358	79.445
645	646	0.000	0.000	145.339	161.481	72.136	79.175
632	671	1074.368	1039.483	471.545	464.877	963.610	957.016
671	680	-0.000	-0.000	0.001	0.001	-0.000	-0.000
671	692	574.895	531.020	83.452	68.343	421.905	416.110
692	675	534.689	484.971	83.154	68.000	319.295	289.997
671	684	140.563	124.403	-0.000	-0.000	185.689	165.939
684	611	0.000	0.000	0.000	0.000	185.204	165.553
684	652	139.471	123.595	0.000	0.000	0.000	0.000

Table 6. 10: Estimation of active power flow (kw) for 13 bus network using LC method

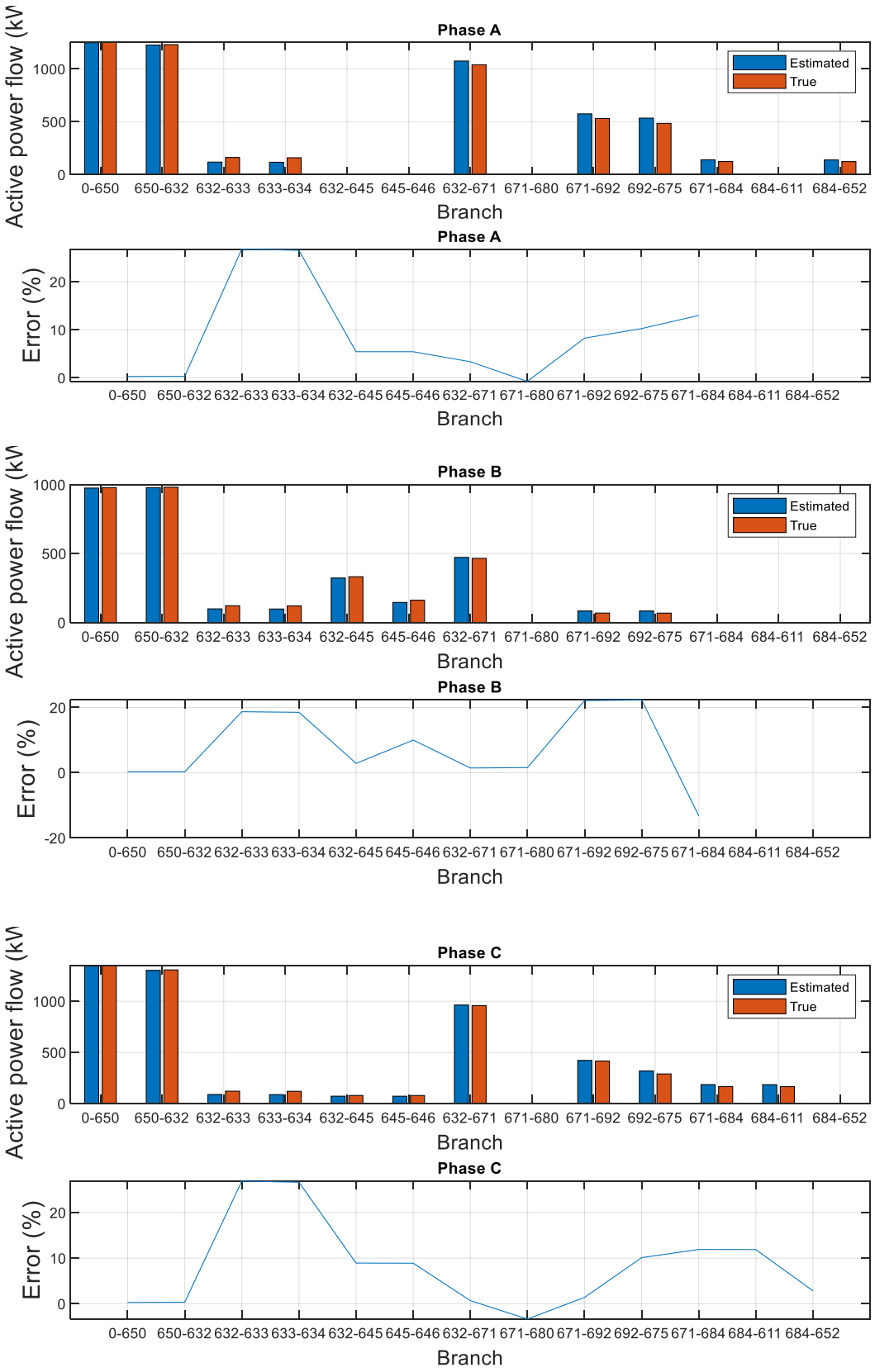

Figure 6. 10: Estimated active power flow (kw) comparison for 13 bus network using LC method

BRANCH		Phase A		Phase B		Phase C	
Bus_i	to Bus_J	Estim.	True	Estim.	True	Estim.	True
000	650	679.289	681.303	372.317	373.410	667.684	669.651
650	632	599.004	601.878	339.853	341.295	585.590	588.438
632	633	87.965	114.573	73.873	92.583	65.632	92.718
633	634	85.391	109.997	72.161	89.998	64.188	89.998
632	645	0.000	0.000	127.597	125.774	123.444	137.766
645	646	0.000	0.000	-0.459	0.562	123.267	137.552
632	671	425.538	411.406	80.644	78.150	267.523	244.887
671	680	-0.004	-0.004	-0.004	-0.004	-0.004	-0.004
671	692	133.922	121.206	-146.613	-162.196	61.514	48.280
692	675	32.417	-3.572	-147.173	-162.741	41.112	21.486
671	684	99.352	83.258	0.000	0.000	-7.164	-16.540
684	611	0.000	0.000	0.000	0.000	-7.658	-16.927
684	652	98.974	82.993	0.000	0.000	0.000	0.000

Table 6. 11: Estimation of reactive power flow (kvar) for 13 bus network using LC method

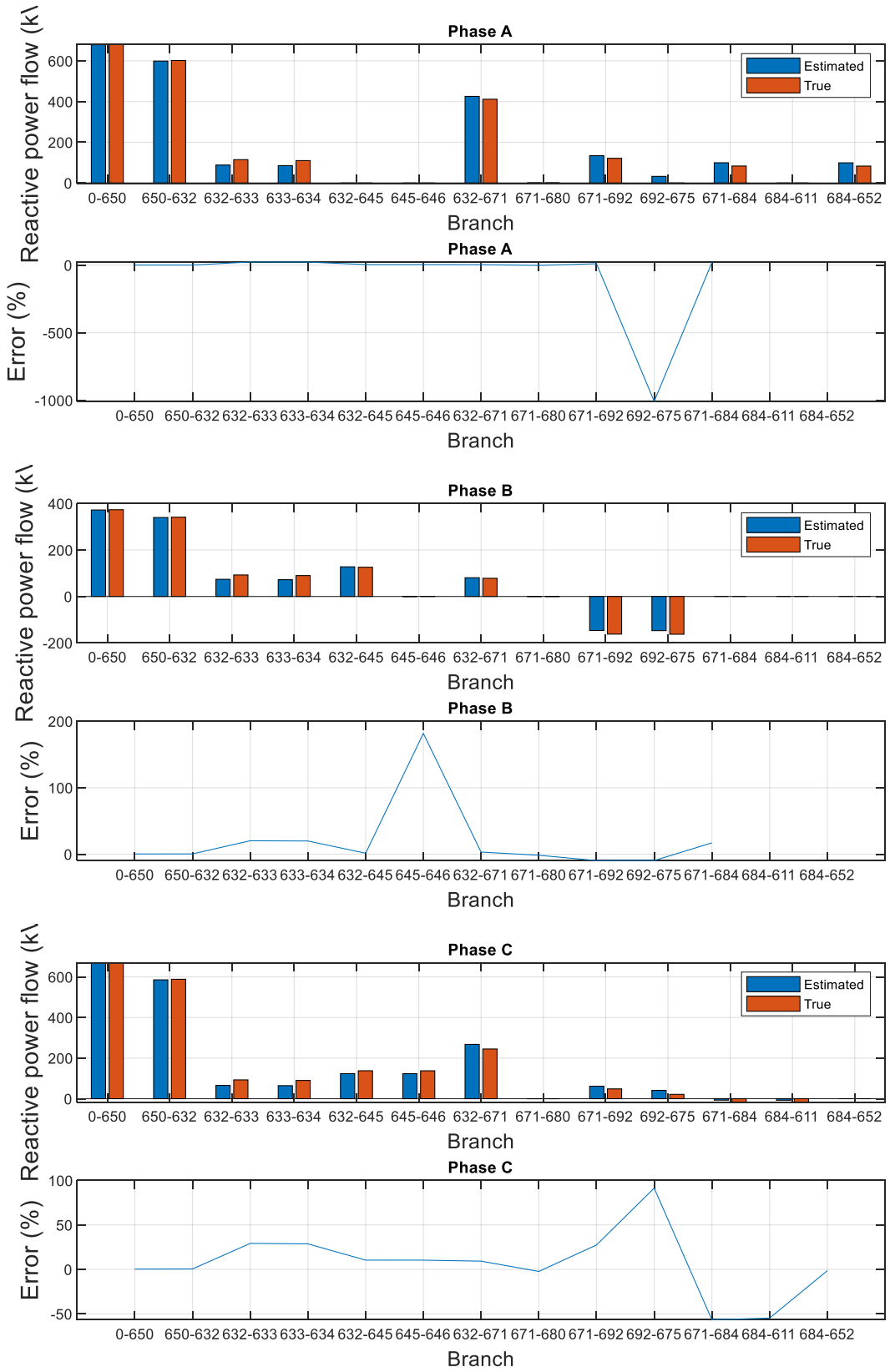

Figure 6. 11: Estimated vs true reactive power flow (kvar) for 13 bus network using LC method

Total active power loss of the network is estimated with an estimation error of about 2.3% and total reactive power loss estimation got an error of about 3%. Following Table 6.12 and Figure 6.12 illustrate the total power loss estimation using load correction method.

Total estimated active Power (kw)	Total true active power (kw)	Total estim. reactive power (kvar)	Total true reactive power (kvar)
113.595	110.985	333.720	324.703

Table 6. 12: Total estimated vs true active and reactive power loss for 13 bus network using LC

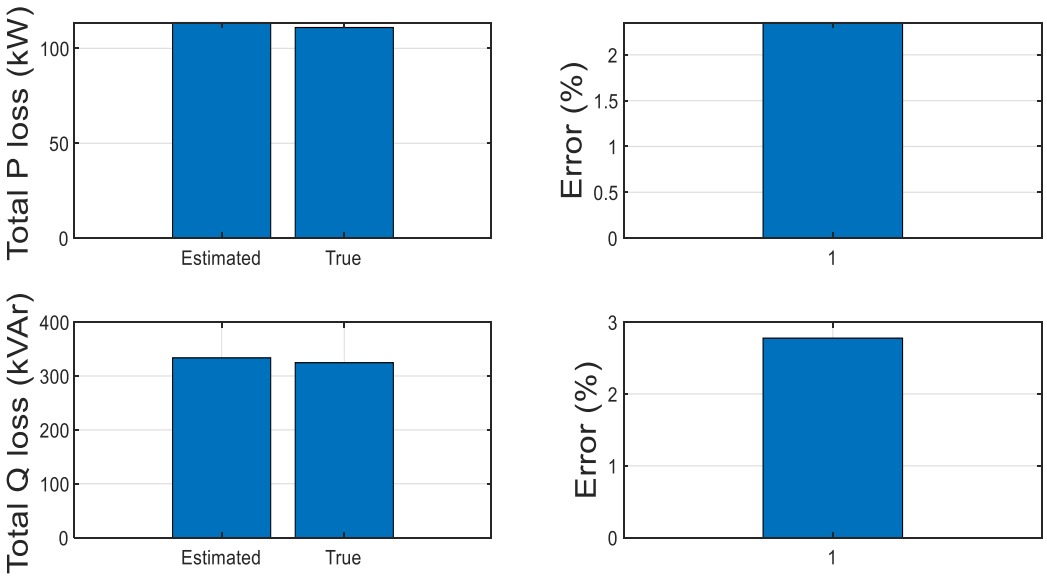

Table 6. 12: Total active (kw) and reactive (kvar) power loss estimation for 13 bus network based on LC DSSE

The MATLAB simulation was performed for different measurement errors for substation voltage measurements and load (P and Q) measurements. Figure 6.13 and Figure 6.14 Shows are estimation errors for different amount of noised measurements. These figures clearly depict the consistency of the estimation process. Higher amount of measurement error created larger estimation error which is understandable. Figure 6.14 is showing the measurements used for the 13-bus case simulation.

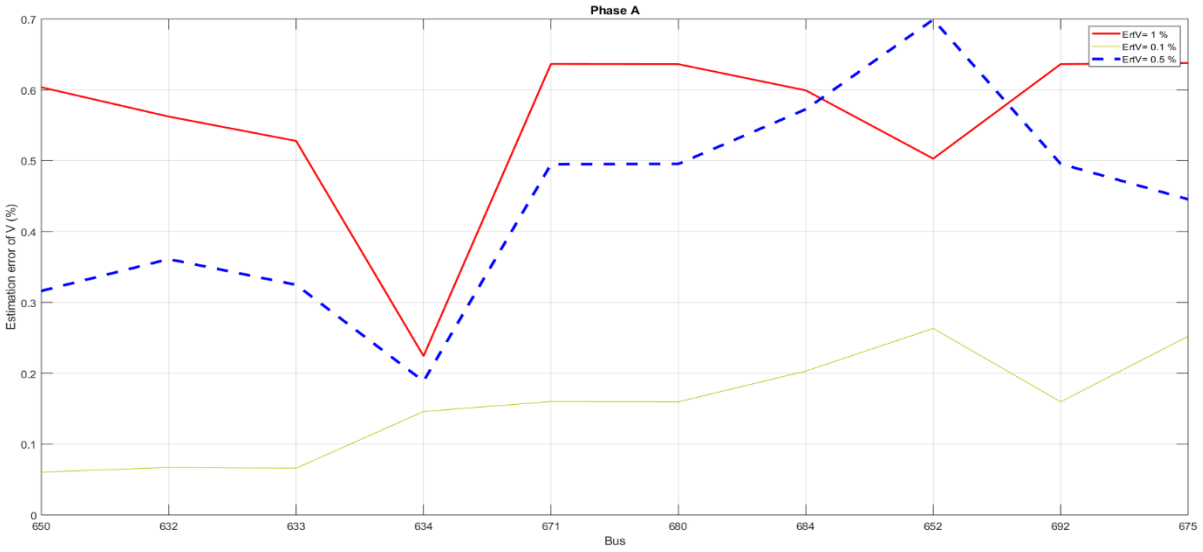

Figure 6. 12: Estimation errors of voltage magnitudes in phase A for different measurement errors for voltage at substation bus using LC method

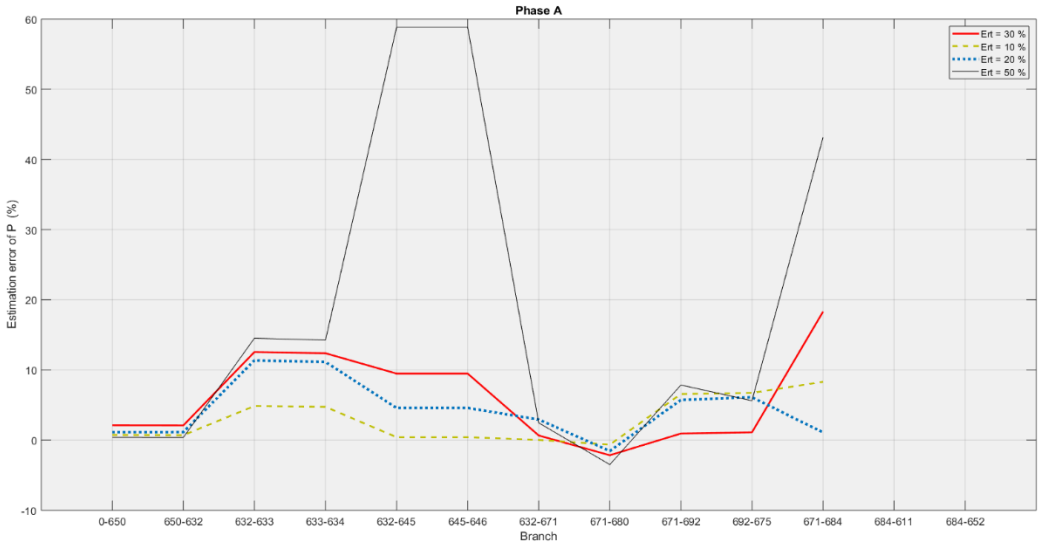

Figure 6. 13: Estimation errors of active power flow in phase A for different load bus (P and Q) measurement errors using LC method

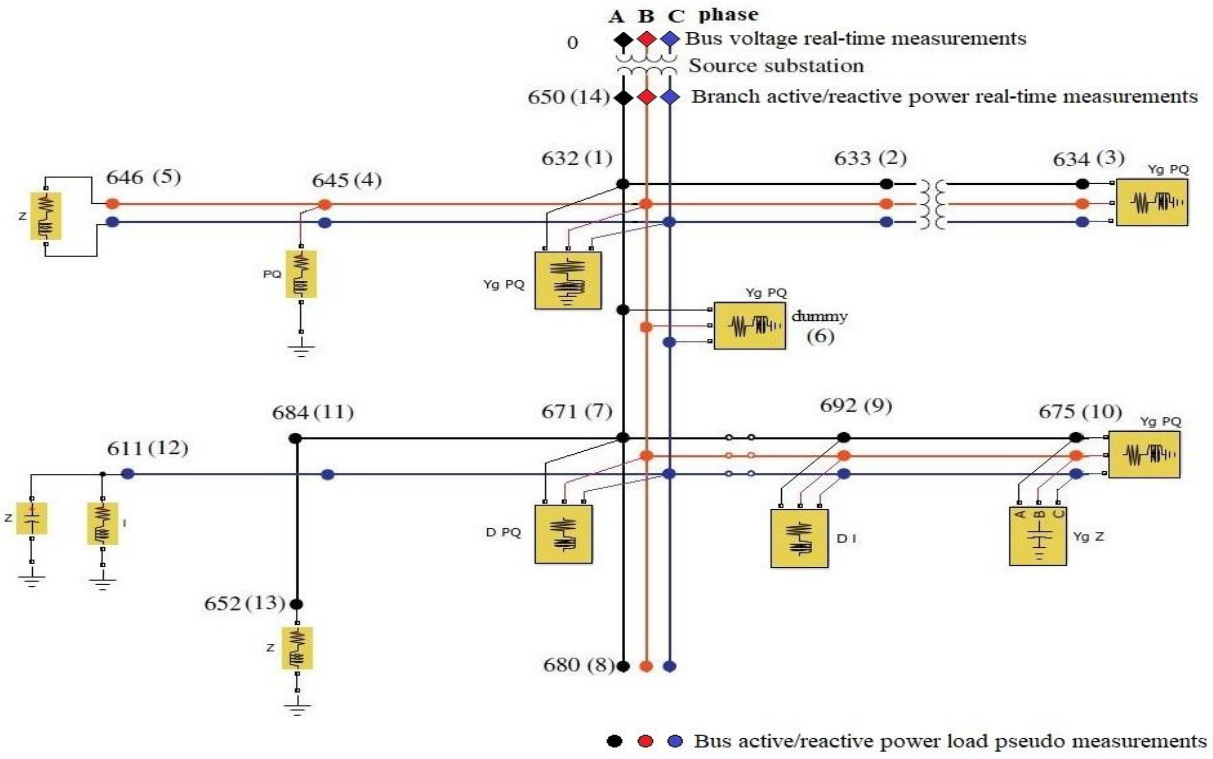

Figure 6. 14: Measurements for 13 bus network distribution system state estimation

6.2 Case Study on IEEE 37 Bus Network System

6.2.1 WLS DSSE Performance

Branch currents are used as state variable which is described in previous chapter on WLS DSSE. The state vector is solved iteratively until the convergence criteria is satisfied. To verify if the WLS DSSE is converging closer value to the measured value, the algorithm is compiled in MATLAB platform for two cases. The test feeder presented here is a 37 bus, 29.6kv three-phase radial network [23]. The base case power flow calculation conforms the IEEE standard validity for the network. Two kind of measurements are used; AMI load measurements and real measurements on the substation feeder. Feeder real (true) measurements are power flow and voltage in the substation feeder line. Load measurements are noised by adding 35% error for the

simulation. Series of data tables and graphs are shown to compare the true and estimated value. The measurement standard deviation (σ) of 0.026 (20% accuracy of measured value) is selected for power and current measurements from a normal distribution. Standard deviation (σ) of 0.0095 (3% accuracy of measured value) is selected for voltage magnitude to add measurement errors. Table 6.13 through Table 6.17 represent the estimation of bus voltage magnitudes, current, active power and reactive power respectively. Figure 6.15 through 6.19 represents the graphical view of the estimated parameters for IEEE 37 bus-feeder network.

BUS	**Phase A (pu)**		**Phase B (pu)**		**Phase C (pu)**	
Node No	**Estim.**	**True**	**Estim.**	**True**	**Estim.**	**True**
799	1.0008	1.0000	1.0008	1.0000	1.0008	1.0000
701	0.9850	0.9845	0.9907	0.9902	0.9864	0.9859
702	0.9766	0.9762	0.9850	0.9845	0.9792	0.9789
703	0.9686	0.9683	0.9800	0.9794	0.9746	0.9742
730	0.9624	0.9624	0.9763	0.9757	0.9707	0.9704
709	0.9606	0.9606	0.9751	0.9745	0.9697	0.9693
775	0.9604	0.9604	0.9753	0.9747	0.9697	0.9693
708	0.9578	0.9578	0.9734	0.9729	0.9684	0.9680
732	0.9575	0.9575	0.9734	0.9729	0.9681	0.9677
733	0.9551	0.9552	0.9718	0.9713	0.9672	0.9668
734	0.9511	0.9513	0.9696	0.9690	0.9652	0.9648
737	0.9478	0.9480	0.9674	0.9668	0.9643	0.9639
738	0.9465	0.9467	0.9667	0.9662	0.9638	0.9633
711	0.9459	0.9460	0.9667	0.9662	0.9633	0.9627
741	0.9458	0.9458	0.9668	0.9662	0.9631	0.9626
740	0.9456	0.9457	0.9668	0.9662	0.9629	0.9624
710	0.9499	0.9503	0.9692	0.9685	0.9635	0.9633
735	0.9495	0.9500	0.9692	0.9685	0.9631	0.9629

736	0.9500	0.9503	0.9681	0.9672	0.9627	0.9623
731	0.9606	0.9606	0.9744	0.9739	0.9690	0.9687
727	0.9675	0.9671	0.9792	0.9785	0.9739	0.9734
744	0.9670	0.9665	0.9787	0.9779	0.9736	0.9732
728	0.9666	0.9661	0.9783	0.9775	0.9733	0.9728
729	0.9667	0.9662	0.9785	0.9777	0.9736	0.9732
713	0.9750	0.9747	0.9834	0.9829	0.9772	0.9769
704	0.9735	0.9732	0.9810	0.9806	0.9748	0.9745
720	0.9721	0.9719	0.9786	0.9784	0.9712	0.9711
706	0.9721	0.9718	0.9783	0.9781	0.9709	0.9707
725	0.9721	0.9718	0.9780	0.9778	0.9707	0.9705
707	0.9716	0.9713	0.9743	0.9743	0.9672	0.9672
722	0.9715	0.9713	0.9739	0.9738	0.9668	0.9668
724	0.9716	0.9713	0.9735	0.9735	0.9666	0.9666
714	0.9733	0.9730	0.9808	0.9804	0.9747	0.9745
718	0.9723	0.9720	0.9799	0.9796	0.9748	0.9745
705	0.9758	0.9753	0.9840	0.9836	0.9777	0.9773
712	0.9754	0.9749	0.9840	0.9836	0.9773	0.9768
742	0.9757	0.9753	0.9832	0.9829	0.9771	0.9768

Table 6. 13: Estimated voltage magnitude for 37 bus network in pu using WLS

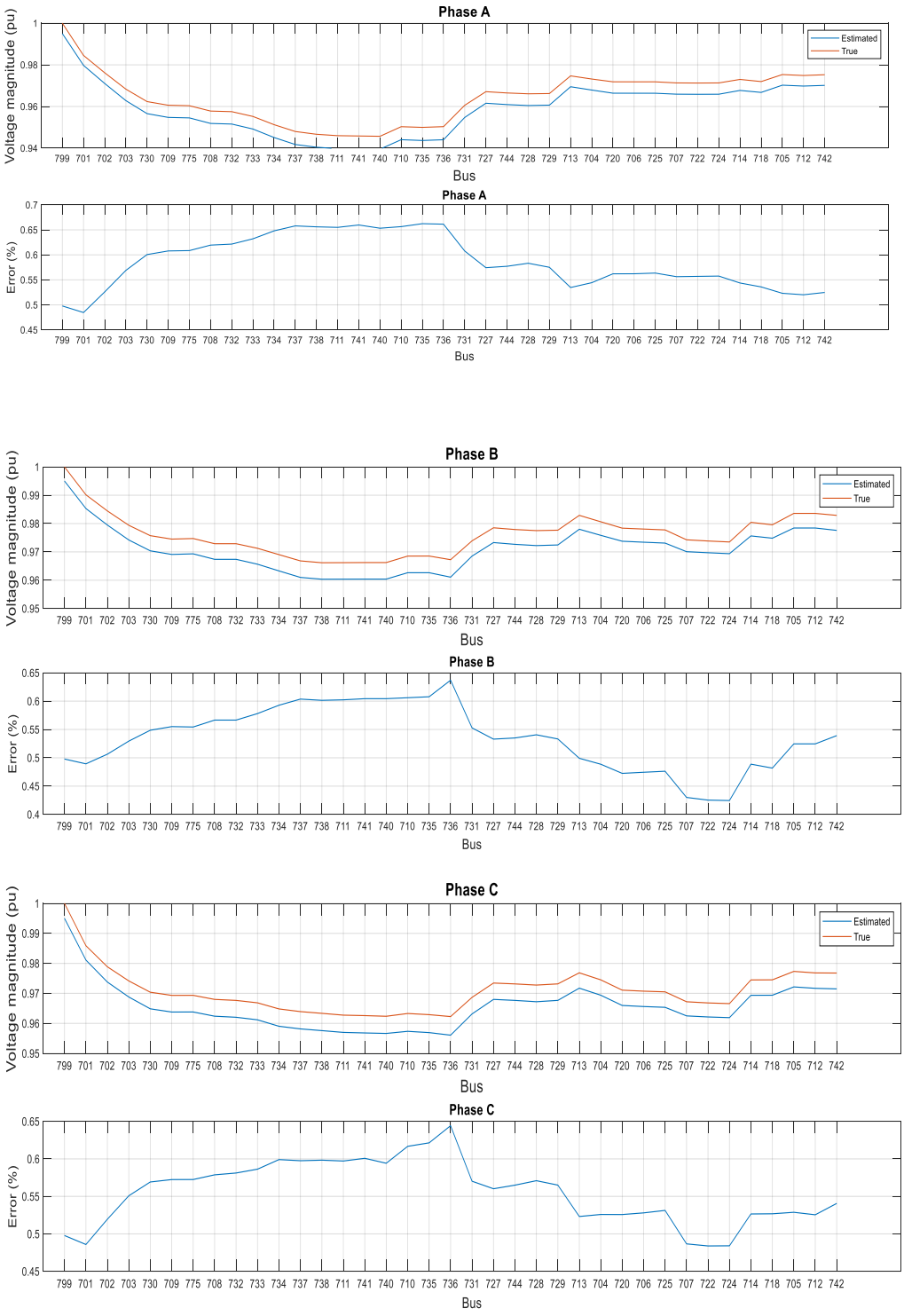

Figure 6. 15: Estimated voltage vs true voltage with estimation error for 37 bus network using WLS method

BRANCH		Phase A		Phase B		Phase C	
Bus_i	Bus_J	Estim.	True	Estim.	True	Estim.	True
799	701	380.438	373.318	281.657	276.391	362.395	355.642
701	702	273.868	271.323	221.870	219.250	256.553	252.801
702	703	194.261	192.612	133.652	136.184	134.865	134.025
703	730	154.948	149.344	101.700	100.201	110.009	107.488
730	709	136.613	133.055	101.711	100.211	89.497	89.302
709	775	0.004	0.004	0.004	0.004	0.004	0.004
709	708	136.621	133.062	89.447	87.991	77.136	76.515
708	732	9.247	10.198	0.005	0.005	9.251	10.202
708	733	129.023	124.700	89.465	88.008	67.917	66.367
733	734	109.862	107.477	67.691	68.528	67.917	66.368
734	737	81.370	82.555	63.226	63.216	28.670	30.393
737	738	52.295	52.655	31.825	30.623	28.668	30.392
738	711	28.641	30.365	0.029	0.029	28.667	30.390
711	741	7.966	9.777	0.008	0.008	7.972	9.783
711	740	20.692	20.605	0.003	0.003	20.695	20.607
734	710	23.899	20.511	7.923	9.491	28.503	26.466
710	735	23.940	20.552	0.003	0.003	23.942	20.554
710	736	0.019	0.019	7.922	9.489	7.905	9.472
709	731	0.011	0.011	19.196	19.084	19.186	19.074
703	727	39.518	43.560	31.991	36.027	25.014	26.678
727	744	31.958	35.976	31.997	36.033	15.947	17.422
744	728	16.332	17.428	16.282	17.429	15.955	17.430
744	729	8.561	9.783	8.557	9.779	0.004	0.004
702	713	62.541	59.892	74.486	71.777	91.531	87.912
713	704	42.097	41.514	74.490	71.780	74.374	72.263
704	720	25.283	24.960	54.105	52.135	69.424	67.665
720	706	0.020	0.020	10.222	10.034	10.204	10.016
706	725	0.004	0.004	10.221	10.033	10.217	10.030

720	707	5.070	4.812	43.882	42.099	46.415	44.580
707	722	5.102	4.844	33.890	32.609	36.517	35.179
707	724	0.012	0.012	9.990	9.488	9.980	9.477
704	714	23.314	23.021	26.408	25.822	5.198	4.832
714	718	18.959	19.106	18.952	19.099	0.008	0.008
702	705	18.969	21.092	23.056	20.160	34.207	34.022
70S	712	17.777	20.108	0.004	0.004	17.781	20.111
705	742	2.154	1.826	23.057	20.160	21.901	19.205

Table 6. 14: Table: Estimated branch currents (A) for 37 bus network using WLS

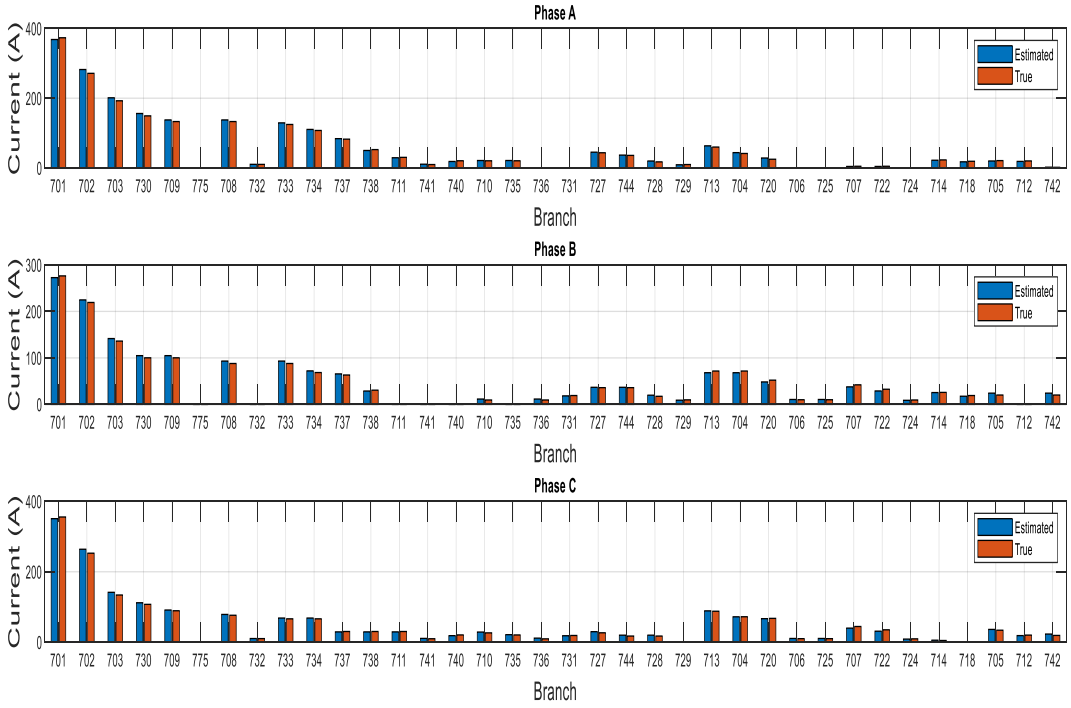

Figure 6. 16: Estimated vs true Brach current magnitude for 37 bus network using WLS method

BRANCH		Phase A		Phase B		Phase C	
Bus_i to Bus_J		Estim.	True	Estim.	True	Estim.	True
799	701	871.227	854.521	679.495	666.434	946.807	928.673
701	702	641.345	635.880	531.159	523.532	658.667	649.269
702	703	468.112	465.553	268.635	276.022	359.802	356.153
703	730	366.956	353.679	203.226	203.016	293.357	285.644
730	709	334.253	324.768	202.907	202.706	236.403	234.919
709	775	0.000	0.000	-0.000	-0.000	-0.000	-0.000
709	708	333.303	323.866	150.741	150.932	207.000	205.153
708	732	13.445	14.697	-0.000	-0.000	24.758	27.302
708	733	319.010	308.375	150.345	150.549	182.020	177.638
733	734	260.375	255.753	116.155	119.963	181.639	177.276
734	737	207.861	209.998	94.490	94.122	76.330	80.931
737	738	125.383	124.368	47.750	45.790	76.285	80.879
738	711	42.019	44.113	0.000	0.000	76.238	80.825
711	741	11.386	13.849	0.000	0.000	21.228	26.045
711	740	30.609	30.238	0.000	0.000	54.985	54.753
734	710	35.644	30.379	21.262	25.435	75.221	68.797
710	735	35.613	30.356	0.000	0.000	63.620	54.638
710	736	0.000	0.000	21.239	25.401	11.546	14.103
709	731	0.000	0.000	51.737	51.358	29.087	29.456
703	727	98.725	109.581	64.377	71.982	65.325	69.434
727	744	84.073	94.749	64.333	71.926	38.651	42.197
744	728	39.263	41.675	39.097	42.144	38.636	42.180
744	729	22.886	26.141	12.882	14.662	-0.000	-0.000
702	713	136.400	131.122	198.010	190.897	215.531	207.092
713	704	101.828	100.194	197.565	190.483	155.003	152.463
704	720	39.075	38.240	146.593	141.118	146.580	144.477
720	706	0.000	0.000	27.685	27.152	14.827	14.865
706	725	0.000	0.000	27.677	27.143	14.818	14.857

720	707	7.837	7.375	118.366	113.467	76.856	74.915
707	722	7.836	7.374	91.378	87.857	62.412	60.904
707	724	0.000	0.000	26.924	25.551	14.375	13.948
704	714	62.645	61.849	50.593	49.014	7.839	7.431
714	718	50.889	51.276	29.590	29.727	-0.000	-0.000
702	705	33.287	35.725	62.865	54.953	81.266	84.018
705	712	27.451	30.769	-0.000	-0.000	47.943	54.231
705	742	5.812	4.925	62.814	54.914	33.255	29.723

Table 6. 15: Estimation of active power flow (kw) for 37 bus network using WLS

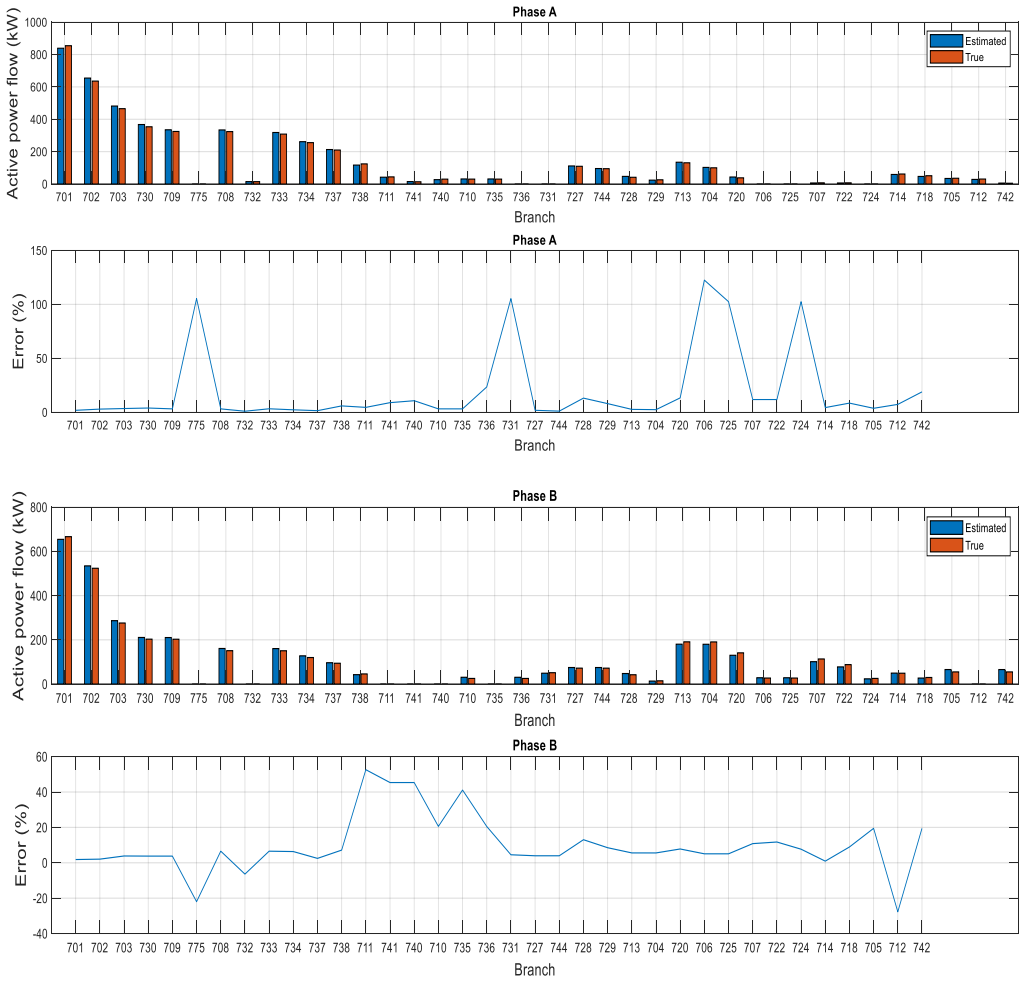

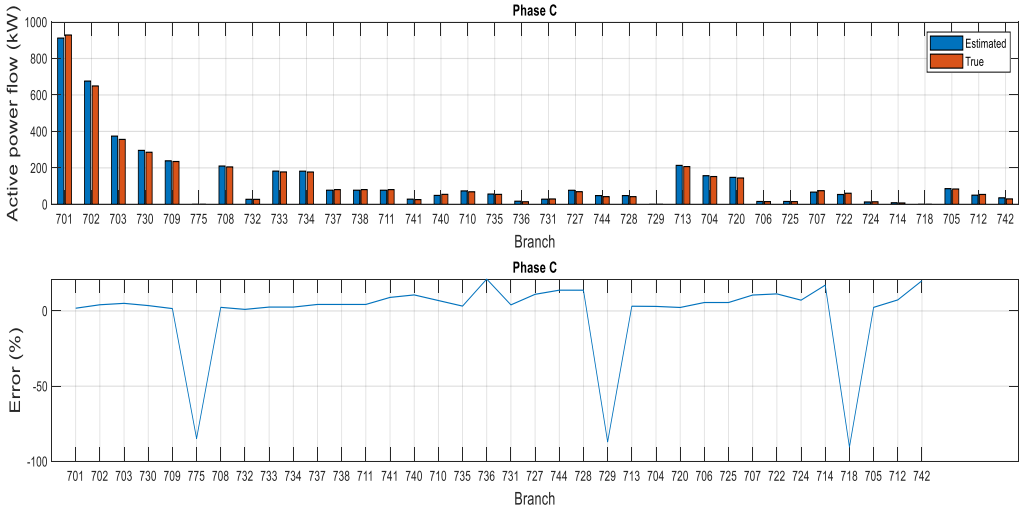

Figure 6. 17: Estimated active power flow (kw) comparison for 37 bus network using WLS method

BRANCH		Phase A		Phase B		Phase C	
Bus_i to Bus_J		Estim.	True	Estim.	True	Estim.	True
799	701	565.152	554.298	369.194	362.016	291.363	285.863
701	702	371.534	366.643	290.953	289.329	225.590	220.764
702	703	229.768	224.550	244.104	245.833	56.715	63.792
703	730	190.103	183.172	185.505	179.432	39.061	44.285
730	709	143.340	141.380	185.381	179.313	44.238	48.577
709	775	-0.010	-0.010	-0.010	-0.010	-0.010	-0.010
709	708	142.851	140.920	188.418	183.033	1.506	6.495
708	732	20.525	22.721	-0.013	-0.013	-1.739	-1.748
708	733	121.889	117.793	188.273	182.895	3.127	8.132
733	734	126.678	121.942	139.967	139.554	2.898	7.915
734	737	49.777	54.224	140.720	140.816	-6.650	-6.468
737	738	55.647	60.124	70.633	68.017	-6.632	-6.454
738	711	62.220	66.264	-0.077	-0.077	-6.622	-6.449
711	741	17.501	21.562	-0.020	-0.020	-1.480	-1.653
711	740	44.759	44.741	-0.008	-0.008	-5.104	-4.759

734	710	51.843	44.665	-0.877	-1.387	11.595	16.083
710	735	51.963	44.787	-0.008	-0.008	-5.990	-4.807
710	736	-0.051	-0.051	-0.793	-1.307	17.648	20.954
709	731	-0.030	-0.030	-3.237	-3.914	42.527	41.881
703	727	38.479	40.279	58.242	66.052	17.039	18.926
727	744	16.302	17.549	58.243	66.048	18.910	20.665
744	728	19.298	20.987	20.493	21.283	18.951	20.705
744	729	-1.525	-1.690	19.300	22.069	-0.012	-0.012
702	713	99.764	94.759	44.670	42.226	122.403	117.270
713	704	50.293	49.970	44.486	42.058	127.820	121.825
704	720	55.792	55.288	-6.549	-8.247	115.892	110.837
720	706	-0.054	-0.054	-1.228	-1.579	23.107	22.475
706	725	-0.012	-0.012	-1.187	-1.539	23.147	22.515
720	707	11.177	10.648	-5.371	-6.705	97.838	93.092
707	722	11.282	10.754	-4.076	-5.122	75.352	71.935
707	724	-0.031	-0.031	-1.238	-1.526	22.539	21.212
704	714	-5.482	-5.300	50.915	50.200	11.647	10.725
714	718	-4.461	-4.401	42.109	42.478	-0.022	-0.022
702	705	39.030	44.429	0.901	-0.044	44.567	37.840
705	712	39.440	44.772	-0.010	-0.010	-4.519	-4.792
705	742	-0.378	-0.313	0.937	-0.005	49.103	42.650

Table 6. 16: Estimation of reactive power flow (kw) for 37 bus network using WLS

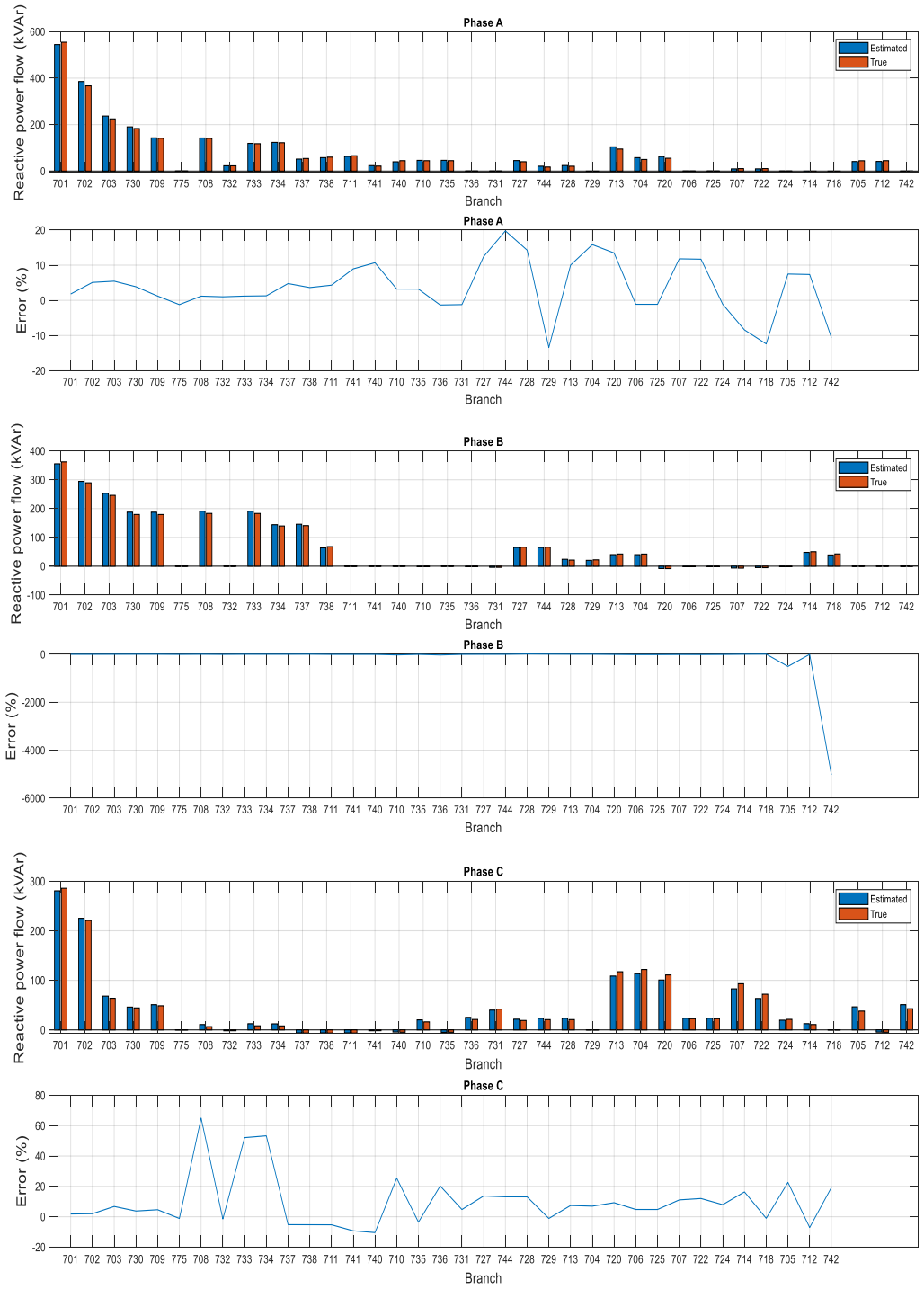

Figure 6. 18: Estimated vs true reactive power flow (kvar) for 37 bus network using WLS method

Total estimated active Power (kw)	Total true active power (kw)	Total estim. reactive power (kvar)	Total true reactive power (kvar)

63.855	62.413	56.135	54.947

Table 6. 17: Total estimated vs true active and reactive power loss for 37 bus network using WLS

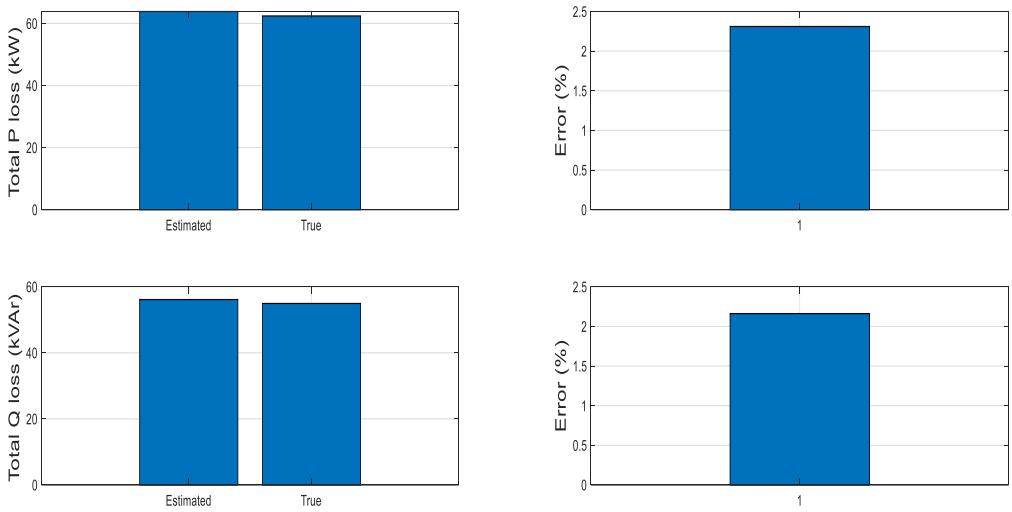

Figure 6. 19: Total active (kw) and reactive (kvar) power loss estimation for 37 bus network based on WLS DSSE

6.2.2 Load Correction DSSE Performance

The LC DSSE analysis was performed on standard IEEE 37-bus test feeder with voltage measurements at the substation and power flow measurements in substation feeding line. All loads are considered as pseudo measurements. It is assumed that the active and reactive power of loads are changed in same manner with normalized daily load diagram given in Figure 6.6. The load weights are nominal powers for IEEE 37-bus system. Based on these data, initial calibration of load for a given moment (T) is performed as described. The error of real-time (true) measurement for voltage was assumed up to 1%. The error of real-time (true) measurements for three-phase active and reactive power in feeding line was assumed up to 3 %, whereas the error in pseudo-measurement of load was considered to vary up to 50 %. For the simulation output presented

below; voltage error is 1%, feeding line active and reactive power error is 3% and metered load error is 30%. Table 6.18 through Table 6.22 represent the estimation of bus voltage magnitudes, current, active power and reactive power respectively. Figure 6.20 through 6.24 represents the graphical view of the estimated parameters for 37 bus-feeder network.

BUS	**Phase A (pu)**		**Phase B (pu)**		**Phase C (pu)**	
Node No	**Estim.**	**True**	**Estim.**	**True**	**Estim.**	**True**
799	0.9998	1.0000	0.9998	1.0000	0.9998	1.0000
701	0.9843	0.9845	0.9899	0.9902	0.9857	0.9859
702	0.9762	0.9762	0.9844	0.9845	0.9789	0.9789
703	0.9685	0.9683	0.9794	0.9794	0.9743	0.9742
730	0.9627	0.9624	0.9758	0.9757	0.9707	0.9704
709	0.9610	0.9606	0.9746	0.9745	0.9696	0.9693
775	0.9608	0.9604	0.9749	0.9747	0.9697	0.9693
708	0.9582	0.9578	0.9731	0.9729	0.9683	0.9680
732	0.9579	0.9575	0.9731	0.9729	0.9680	0.9677
733	0.9557	0.9552	0.9715	0.9713	0.9672	0.9668
734	0.9519	0.9513	0.9693	0.9690	0.9653	0.9648
737	0.9487	0.9480	0.9672	0.9668	0.9643	0.9639
738	0.9474	0.9467	0.9666	0.9662	0.9637	0.9633
711	0.9467	0.9460	0.9666	0.9662	0.9631	0.9627
741	0.9465	0.9458	0.9666	0.9662	0.9630	0.9626
740	0.9463	0.9457	0.9666	0.9662	0.9627	0.9624
710	0.9510	0.9503	0.9688	0.9685	0.9638	0.9633
735	0.9507	0.9500	0.9688	0.9685	0.9635	0.9629
736	0.9510	0.9503	0.9676	0.9672	0.9629	0.9623
731	0.9610	0.9606	0.9741	0.9739	0.9690	0.9687
727	0.9673	0.9671	0.9785	0.9785	0.9736	0.9734
744	0.9667	0.9665	0.9779	0.9779	0.9733	0.9732

728	0.9663	0.9661	0.9775	0.9775	0.9729	0.9728
729	0.9665	0.9662	0.9777	0.9777	0.9733	0.9732
713	0.9748	0.9747	0.9829	0.9829	0.9769	0.9769
704	0.9733	0.9732	0.9807	0.9806	0.9747	0.9745
720	0.9721	0.9719	0.9786	0.9784	0.9714	0.9711
706	0.9720	0.9718	0.9783	0.9781	0.9711	0.9707
725	0.9720	0.9718	0.9780	0.9778	0.9709	0.9705
707	0.9716	0.9713	0.9747	0.9743	0.9678	0.9672
722	0.9715	0.9713	0.9743	0.9738	0.9674	0.9668
724	0.9716	0.9713	0.9740	0.9735	0.9672	0.9666
714	0.9732	0.9730	0.9805	0.9804	0.9747	0.9745
718	0.9722	0.9720	0.9797	0.9796	0.9747	0.9745
705	0.9754	0.9753	0.9834	0.9836	0.9774	0.9773
712	0.9750	0.9749	0.9834	0.9836	0.9769	0.9768
742	0.9753	0.9753	0.9827	0.9829	0.9768	0.9768

Table 6. 18: Estimated voltage magnitude for 37 bus network in pu using LC method

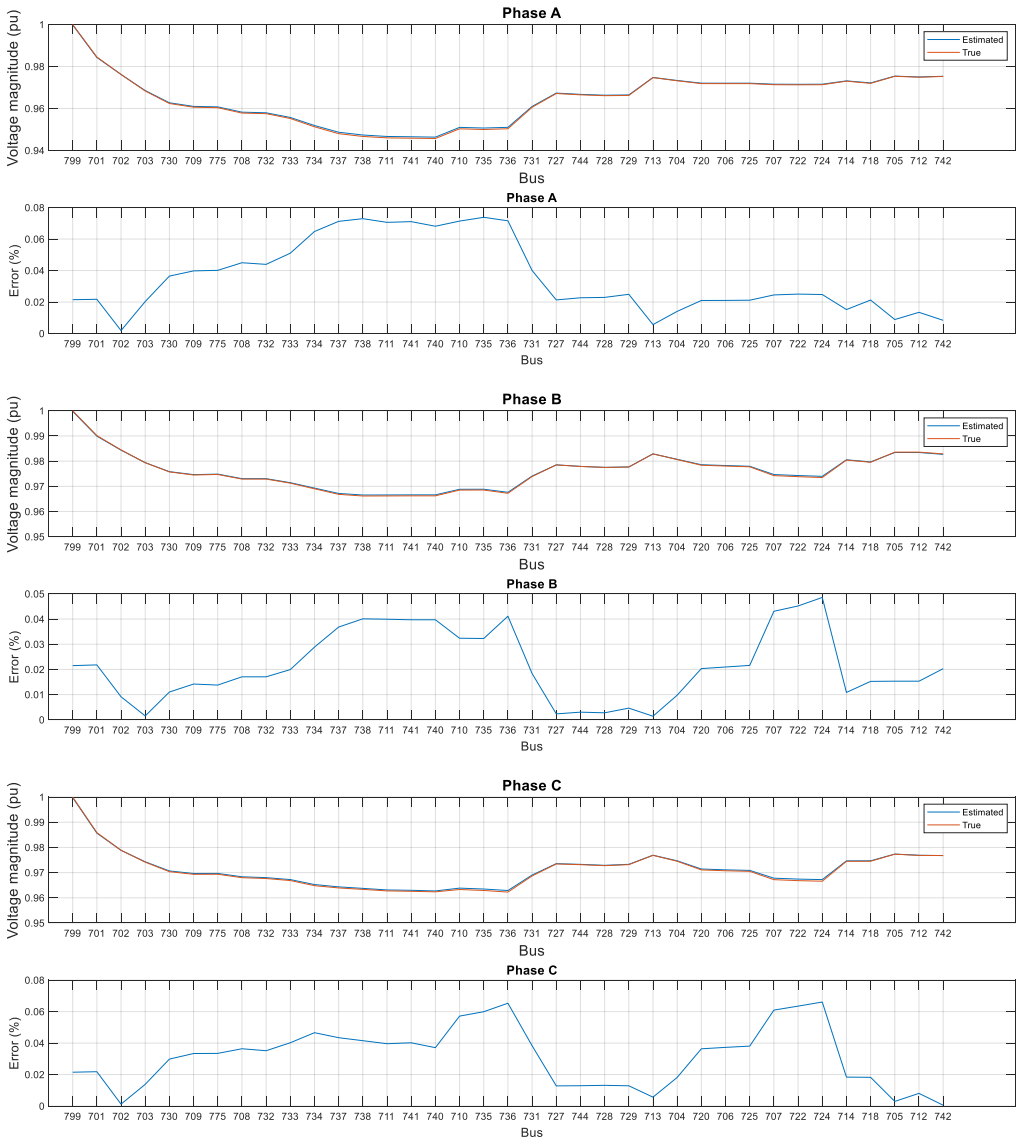

Figure 6. 20: Estimated voltage vs true voltage with estimation error for 37 bus network using load correction method

BRANCH		Phase A		Phase B		Phase C	
Bus_i to Bus_J		Estim.	True	Estim.	True	Estim.	True
799	701	373.302	373.318	276.421	276.391	355.640	355.642
701	702	264.097	271.323	214.317	219.250	245.396	252.801
702	703	188.583	192.612	133.341	136.184	130.293	134.025
703	730	145.615	149.344	97.836	100.201	103.424	107.488

730	709	130.805	133.055	97.847	100.211	86.790	89.302
709	775	0.004	0.004	0.004	0.004	0.004	0.004
709	708	130.812	133.062	86.439	87.991	75.085	76.515
708	732	10.576	10.198	0.005	0.005	10.581	10.202
708	733	122.171	124.700	86.456	88.008	64.555	66.367
733	734	103.979	107.477	65.830	68.528	64.556	66.368
734	737	80.747	82.555	60.805	63.216	31.196	30.393
737	738	51.903	52.655	29.052	30.623	31.194	30.392
738	711	31.167	30.365	0.029	0.029	31.193	30.390
711	741	9.478	9.777	0.008	0.008	9.484	9.783
711	740	21.707	20.605	0.003	0.003	21.709	20.607
734	710	19.258	20.511	8.848	9.491	24.770	26.466
710	735	19.299	20.552	0.003	0.003	19.302	20.554
710	736	0.019	0.019	8.847	9.489	8.830	9.472
709	731	0.011	0.011	17.751	19.084	17.741	19.074
703	727	43.201	43.560	35.544	36.027	27.022	26.678
727	744	35.249	35.976	35.550	36.033	17.343	17.422
744	728	17.313	17.428	17.539	17.429	17.351	17.430
744	729	9.086	9.783	9.082	9.779	0.004	0.004
702	713	58.501	59.892	68.258	71.777	84.933	87.912
713	704	39.270	41.514	68.261	71.780	68.551	72.263
704	720	23.736	24.960	49.562	52.135	64.239	67.665
720	706	0.020	0.020	9.808	10.034	9.791	10.016
706	725	0.004	0.004	9.808	10.033	9.804	10.030
720	707	4.500	4.812	39.751	42.099	42.048	44.580
707	722	4.532	4.844	30.940	32.609	33.320	35.179
707	724	0.012	0.012	8.810	9.488	8.799	9.477
704	714	21.742	23.021	24.412	25.822	4.534	4.832
714	718	18.078	19.106	18.070	19.099	0.008	0.008
702	705	19.180	21.092	21.529	20.160	33.390	34.022

705	712	18.133	20.108	0.004	0.004	18.136	20.111
705	742	1.943	1.826	21.530	20.160	20.493	19.205

Table 6. 19: Estimated Current magnitude for 37 bus network using load correction method

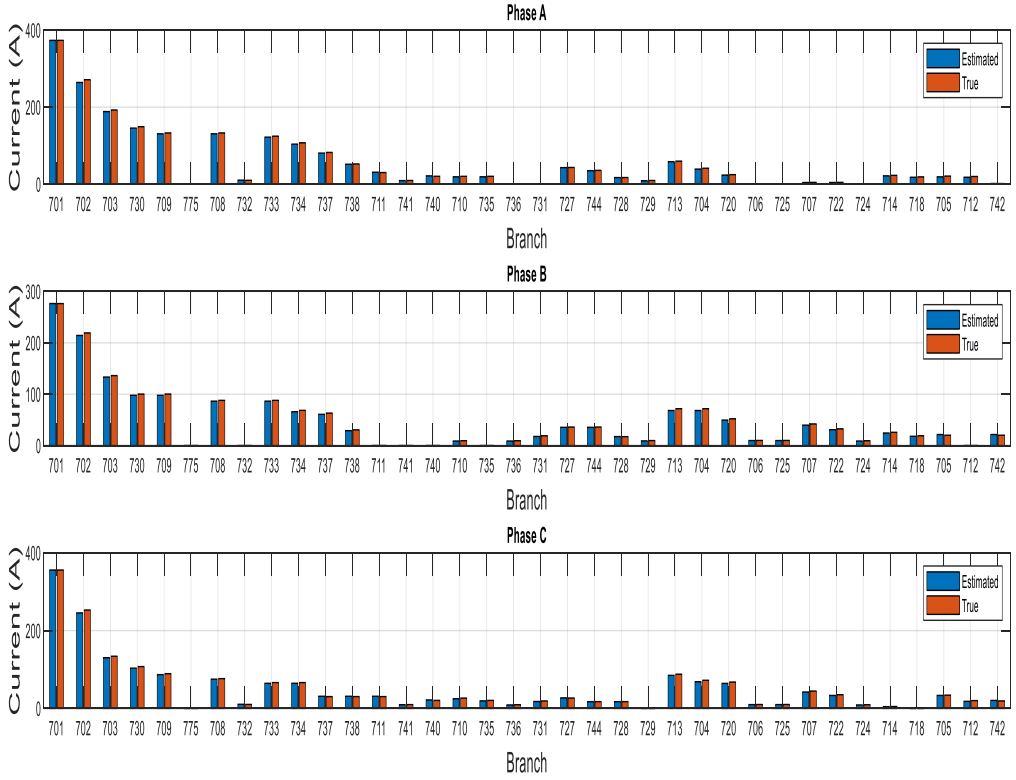

Figure 6. 21: Estimated vs true Brach current magnitude for 37 bus network using LC method

BRANCH		Phase A		Phase B		Phase C	
Bus_i to Bus_J		Estim.	True	Estim.	True	Estim.	True
799	701	854.329	854.521	666.383	666.434	928.450	928.673
701	702	620.267	635.880	511.350	523.532	629.947	649.269
702	703	456.876	465.553	269.637	276.022	346.547	356.153
703	730	346.275	353.679	197.046	203.016	275.186	285.644
730	709	319.873	324.768	196.751	202.706	228.880	234.919

709	775	0.000	0.000	-0.000	-0.000	-0.000	-0.000
709	708	319.002	323.866	148.552	150.932	201.420	205.153
708	732	15.239	14.697	-0.000	-0.000	28.327	27.302
708	733	303.000	308.375	148.183	150.549	172.892	177.638
733	734	247.441	255.753	115.571	119.963	172.548	177.276
734	737	204.921	209.998	91.467	94.122	83.106	80.931
737	738	121.477	124.368	43.892	45.790	83.052	80.879
738	711	45.313	44.113	0.000	0.000	82.995	80.825
711	741	13.427	13.849	0.000	0.000	25.260	26.045
711	740	31.858	30.238	0.000	0.000	57.705	54.753
734	710	28.533	30.379	23.728	25.435	64.420	68.797
710	735	28.513	30.356	0.000	0.000	51.342	54.638
710	736	0.000	0.000	23.699	25.401	13.029	14.103
709	731	0.000	0.000	47.800	51.358	27.164	29.456
703	727	108.416	109.581	71.613	71.982	70.362	69.434
727	744	92.907	94.749	71.558	71.926	41.852	42.197
744	728	41.541	41.675	42.436	42.144	41.834	42.180
744	729	24.273	26.141	13.755	14.662	-0.000	-0.000
702	713	127.067	131.122	181.452	190.897	201.103	207.092
713	704	94.831	100.194	181.078	190.483	144.133	152.463
704	720	36.349	38.240	134.226	141.118	136.720	144.477
720	706	0.000	0.000	26.555	27.152	14.395	14.865
706	725	0.000	0.000	26.547	27.143	14.387	14.857
720	707	6.894	7.375	107.225	113.467	70.110	74.915
707	722	6.894	7.374	83.428	87.857	57.217	60.904
707	724	0.000	0.000	23.745	25.551	12.836	13.948
704	714	58.388	61.849	46.534	49.014	6.912	7.431
714	718	48.498	51.276	28.391	29.727	-0.000	-0.000
702	705	32.998	35.725	58.675	54.953	80.404	84.018
705	712	27.734	30.769	-0.000	-0.000	48.911	54.231

705	742	5.239	4.925	58.631	54.914	31.429	29.723

Table 6. 20: Estimation of active power flow (kw) for 37 bus network using LC method

Figure 6. 22: Estimated active power flow (kw) comparison for 37 bus network using LC method

BRANCH		Phase A		Phase B		Phase C	
Bus_i to Bus_J		Estim.	True	Estim.	True	Estim.	True
799	701	554.103	554.298	361.938	362.016	285.850	285.863
701	702	354.603	366.643	283.438	289.329	215.160	220.764
702	703	217.884	224.550	241.404	245.833	60.524	63.792
703	730	176.128	183.172	176.565	179.432	40.898	44.285
730	709	137.959	141.380	176.454	179.313	44.781	48.577
709	775	-0.010	-0.010	-0.010	-0.010	-0.010	-0.010
709	708	137.516	140.920	179.620	183.033	5.451	6.495
708	732	23.582	22.721	-0.013	-0.013	-1.793	-1.748
708	733	113.546	117.793	179.489	182.895	7.141	8.132
733	734	118.361	121.942	133.843	139.554	6.938	7.915
734	737	55.435	54.224	134.889	140.816	-6.622	-6.468
737	738	61.738	60.124	64.259	68.017	-6.610	-6.454
738	711	68.063	66.264	-0.077	-0.077	-6.606	-6.449
711	741	20.922	21.562	-0.020	-0.020	-1.588	-1.653
711	740	47.179	44.741	-0.008	-0.008	-4.982	-4.759
734	710	41.974	44.665	-1.155	-1.387	15.086	16.083
710	735	42.097	44.787	-0.008	-0.008	-4.479	-4.807
710	736	-0.051	-0.051	-1.073	-1.307	19.631	20.954
709	731	-0.030	-0.030	-3.351	-3.914	39.139	41.881
703	727	40.717	40.279	64.513	66.052	19.097	18.926
727	744	16.918	17.549	64.509	66.048	20.897	20.665
744	728	20.592	20.987	21.369	21.283	20.937	20.705
744	729	-1.733	-1.690	20.404	22.069	-0.012	-0.012
702	713	93.955	94.759	40.525	42.226	111.486	117.270
713	704	47.193	49.970	40.378	42.058	116.240	121.825
704	720	52.606	55.288	-6.987	-8.247	105.901	110.837

720	706	-0.054	-0.054	-1.374	-1.579	22.068	22.475
706	725	-0.012	-0.012	-1.333	-1.539	22.109	22.515
720	707	9.962	10.648	-5.634	-6.705	88.332	93.092
707	722	10.068	10.754	-4.312	-5.122	68.602	71.935
707	724	-0.031	-0.031	-1.263	-1.526	19.787	21.212
704	714	-5.389	-5.300	47.276	50.200	10.108	10.725
714	718	-4.481	-4.401	40.012	42.478	-0.022	-0.022
702	705	39.991	44.429	0.264	-0.044	41.403	37.840
705	712	40.390	44.772	-0.010	-0.010	-4.287	-4.792
705	742	-0.368	-0.313	0.302	-0.005	45.710	42.650

Table 6. 21: Estimation of reactive power flow (kvar) for 37 bus network using LC method

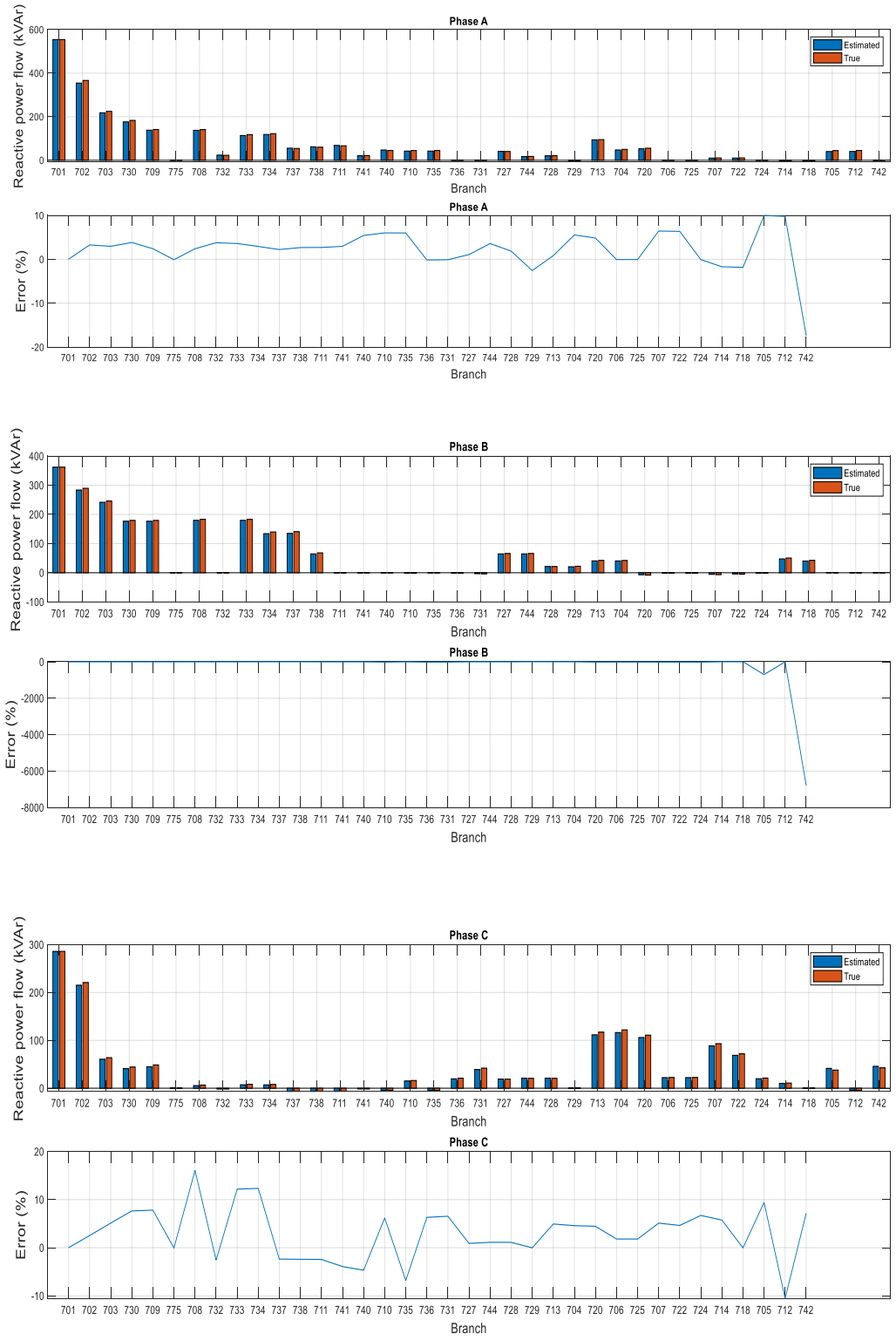

Figure 6. 23: Estimated vs true reactive power flow (kvar) for 37 bus network using LC method

Total estimated active Power (kw)	Total true active power (kw)	Total estim. reactive power (kvar)	Total true reactive power (kvar)
60.548	62.413	53.537	54.947

Table 6. 22: Total estimated vs true active and reactive power loss for 37 bus network using LC

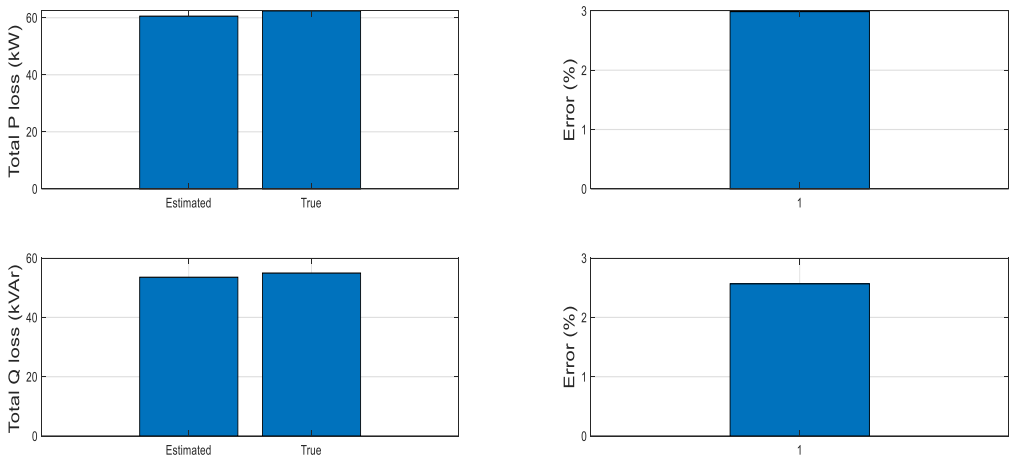

Figure 6. 24: Total active (kw) and reactive (kvar) power loss estimation for 37 bus network based on LC DSSE

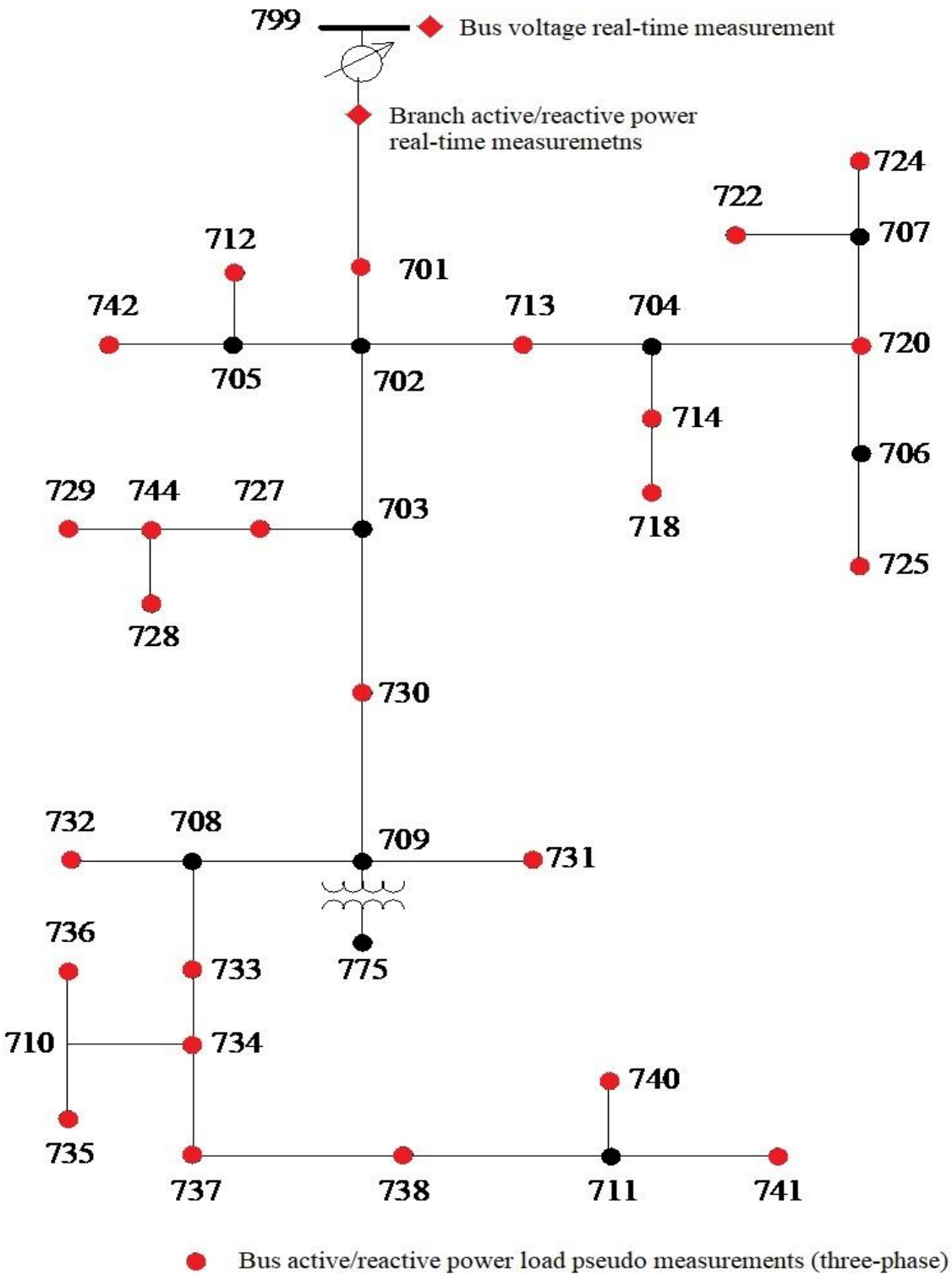

Figure 6. 25: Network Topology for 37 bus feeder network

Chapter 7: Conclusion and Future Scope

This thesis research presents the framework of weighted least squares (WLS) DSSE method and load correction DSSE method for unbalanced radial distribution system. These techniques are suitable for any distribution system containing proper datasheet. The WLS method utilizes the measurement residuals and Jacobian matrices to perform the estimation. Since the measurement is limited, pseudo measurement is introduced in estimation algorithm. Measurement errors are generated as values drawn from a set of numbers with normal PDF having zero mean and the standard deviations are assigned by user. On the other hand, load correction method uses the iterative backward/forward load flow algorithm. The method compares the calculated and measured data to calibrate the quantities until permissible converge criterion is met. Measurements errors are added as normally distributed noise with the load measurements. Minimum number of measurements are required for the proposed method which is a great advantage for the DSSE. Simulation results are analyzed for different percentages of errors to validate the consistency of estimators. It is always challenging to model the three-phase unbalanced distribution network due to distinct characteristics which are addressed in the thesis work. This thesis work also gives an overview of how effectively AMI could be utilized in coming days to solve the problems associated with the distribution network operation. Distribution modeling is never perfect; however, it is possible to get an acceptable amount of accuracy that is demonstrated by the performances of the proposed techniques. There are many challenges that could be addressed using the DSSE analogy in future days including multi-level concept of state estimation that interacts between transmission systems and distribution system, coordination and collection of measurement data more efficiently, fault locating techniques etc.

References

[1] Power Systems Analysis by Hadi Sadat, Second edition, McGraw-Hill series in ECE.

[2] Distribution system modeling and analysis by William H. Kersting, third edition, CRC press.

[3] Power generation, operation and control by Allen J Wood, Bruce F Wollwnberg, and Gerald B Shelbe, third edition, John Wiley and sons.

[4] S. Nanchian, A. Majumdar and B. C. Pal, "Three-Phase State Estimation Using Hybrid Particle Swarm Optimization,"in *IEEE Transactions on Smart Grid*, vol. 8, no. 3, pp.1035-1045, May2017.doi: 10.1109/TSG.2015.2428172.

[5] Kumar M.V., Likith & Prasanna H.A., Maruthi & Ananthapadmanabha, T. (2015). A Literature Review on Distribution System State Estimation. Procedia Technology. 21. 423-429. 10.1016/j.protcy.2015.10.063.

[6] A. Primadianto and C. Lu, "A Review on Distribution System State Estimation," in *IEEE Transactions on Power Systems*, vol. 32, no. 5, pp. 3875-3883, Sept. 2017.
[7] Evaluation and Calculation of Overhead Line Impedance in Distribution Networks R. Ebrahimi, A. Babaee and M. Hoseynpoor Bushehr Branch, Islamic Azad University.

[8] G. W. Chang, S. Y. Chu and H. L. Wang, "A Simplified Forward and Backward Sweep Approach for Distribution System Load Flow Analysis," *2006 International Conference on Power System Technology*, Chongqing, 2006, pp. 1-5.doi: 10.1109/ICPST.2006.321724.

[9] A. Majumdar and B. C. Pal, "A three-phase state estimation in unbalanced distribution networks with switch modelling," *2016 IEEE First International Conference on Control, Measurement and Instrumentation (CMI)*, Kolkata, 2016, pp. 474-478.

[10] F. Shabani, M. Seyedyazdi, M. Vaziri, M. Zarghami and S. Vadhva, "State Estimation of a Distribution System Using WLS and EKF Techniques," *2015 IEEE International Conference on Information Reuse and Integration*, San Francisco, CA, 2015, pp. 609-613.

[11] M. Baran and T. E. McDermott, "Distribution system state estimation using AMI data," *2009 IEEE/PES Power Systems Conference and Exposition*, Seattle, WA, 2009, pp. 1-3. doi: 10.1109/PSCE.2009.4840257.

[12] PhD dissertation of Jian Chen, measurement enhancement for state estimation, Texas A&M University, 2008.

[13] MS thesis of Crome Carx on State estimation in Power distribution systems, University of Waterloo, 2017.

[14] J. Peppanen, M. J. Reno, M. Thakkar, S. Grijalva and R. G. Harley, "Leveraging AMI Data for Distribution System Model Calibration and Situational Awareness," in *IEEE Transactions on Smart Grid*, vol. 6, no. 4, pp. 2050-2059, July 2015.doi: 10.1109/TSG.2014.2385636.

[15] I. Dzafic, D. Ablakovic and S. Henselmeyer, "Real-time three-phase state estimation for radial distribution networks," *2012 IEEE Power and Energy Society General Meeting*, San Diego, CA, 2012, pp. 1-6.doi: 10.1109/PESGM.2012.6345474.

[16] A. Muhamedagić and A. Mujezinović, "State estimation algorithm for radial distribution networks," *2017 XXVI International Conference on Information, Communication and Automation Technologies (ICAT)*, Sarajevo, 2017, pp. 1-6.doi: 10.1109/ICAT.2017.8171646.

[17] K. Dehghanpour, Z. Wang, J. Wang, Y. Yuan and F. Bu, "A Survey on State Estimation Techniques and Challenges in Smart Distribution Systems," in *IEEE Transactions on Smart Grid*. doi: 10.1109/TSG.2018.2870600.

[18] T. Baldwin, D. Kelle, J. Cordova and N. Beneby, "Fault locating in distribution networks with the aid of advanced metering infrastructure," *2014 Clemson University Power Systems Conference*, Clemson, SC, 2014, pp. 1-8.doi: 10.1109/PSC.2014.6808108.

[19] Thesis of Carlos Expedite Bandak on Power systems state estimation, California state University, Sacramento, 2013.

[20] M. Pau, P. Attilio Pegoraro and S. Sulis, "Performance of three-phase WLS Distribution System State Estimation approaches," *2015 IEEE International Workshop on Applied Measurements for Power Systems (AMPS)*, Aachen, 2015, pp. 138-143.doi: 10.1109/AMPS.2015.7312752.

[21] Jie Wan and K. Nan Miu, "A WLS method for load estimation in unbalanced distribution networks," *2002 IEEE Power Engineering Society Winter Meeting. Conference Proceedings (Cat. No.02CH37309)*, New York, NY, USA, 2002, pp. 969-974 vol.2.doi: 10.1109/PESW.2002.985150.

[22] (2017) K. P. Schneider, B. A. Mather, B. C. Pal, C. W. Ten, G. J. Shirek, H. Zhu, J. C. Fuller, J. L. R. Pereira, L. F. Ochoa, L. R. de Araujo, R. C. Dugan, S. Matthias, S. Paudyal, T. E.

McDermott, and W Kersting, “Analytic Considerations and Design Basis for the IEEE Distribution Test Feeders,” IEEE Transactions on Power Systems, vol. PP, no. 99, pp. 1-1, 2017.

[23] IEEE Power engineering society’s Power system analysis computing and economics committee; http://sites.ieee.org/pes-testfeeders/resources/.

[24] P. Samal and S. Ganguly, "A modified forward backward sweep load flow algorithm for unbalanced radial distribution systems," *2015 IEEE Power & Energy Society General Meeting*, Denver, CO, 2015, pp. 1-5.doi: 10.1109/PESGM.2015.7286413.

[25] Y. Gao and N. Yu, "State estimation for unbalanced electric power distribution systems using AMI data," *2017 IEEE Power & Energy Society Innovative Smart Grid Technologies Conference (ISGT)*, Washington, 2017, pp.1-5.doi: 10.1109/ISGT.2017.8085999.

Appendix

Appendix A

Overhead and Underground Conductor Data for Line Modeling Database:

Size	Stranding	Material	Diameter (in.)	GMR (ft)	Resistance (Ω/ mile)	Capacity (A)
1		ACSR	0.355	0.00418	1.38	200
1	7 STRD	Copper	0.328	0.00992	0.765	270
1	CLASS A	AA	0.328	0.00991	1.224	177
2	6/1	ACSR	0.316	0.00418	1.69	180
2	7STRD	COPER	0.292	0.00883	0.964	230
2	7/1	ACSR	0.325	0.00504	1.65	180
2	AWGSLD	Copper	0.258	0.00836	0.945	220
2	CLASS A	AA	0.292	0.00883	1.541	156
2	6-Jan	ACSR	0.281	0.0043	2.07	160
3	AWG SLD	Copper	0.229	0.00745	1.192	190
4	6-Jan	ACSR	0.25	0.00437	2.57	140
4	7-Jan	ACSR	0.257	0.00452	2.55	140
4	AWG SLD	Copper	0.204	0.00663	1.503	170
4	CLASS A	AA	0.232	0.007	2.453	90
5	6-Jan	ACSR	0.223	0.00416	3.18	120
5	AWG SLD	Copper	0.1819	0.0059	1.895	140
6	6-Jan	ACSR	0.198	0.00394	3.98	100
6	AWG SLD	Copper	0.162	0.00526	2.39	120
6	CLASS A	AA	0.184	0.00555	3.903	65
7	AWG SLD	Copper	0.1443	0.00468	3.01	110
8	AWG SLD	Copper	0.1285	0.00416	3.8	90
9	AWG SLD	Copper	0.1144	0.00371	4.6758	80
10	AWG SLD	Copper	0.1019	0.0033	5.9026	75
12	AWG SLD	Copper	0.0808	0.00262	9.3747	40
14	AWG SLD	Copper	0.0641	0.00208	14.8722	20

16	AWG SLD	Copper	0.0508	0.00164	23.7262	10
18	AWG SLD	Copper	0.0403	0.0013	37.6726	5
19	AWG SLD	Copper	0.0359	0.00116	47.5103	4
20	AWG SLD	Copper	0.032	0.00103	59.684	3
22	AWG SLD	Copper	0.0253	0.00082	95.4835	2

Size	**Stranding**	**Material**	**Diameter (in.)**	**GMR (ft)**	**Resistance (Ω/ mile)**	**Capacity (A)**
24	AWG SLD	Copper	0.0201	0.00065	151.616	1
1/0		ACSR	0.398	0.00446	1.12	230
1/0	7STRD	Copper	0.368	0.01113	0.607	310
1/0	CLASS A	AA	0.368	0.0111	0.97	202
2/0		ACSR	0.447	0.0051	0.895	270
2/0	7STRD	Copper	0.414	0.01252	0.481	360
2/0	CLASS A	AA	0.414	0.0125	0.769	230
3/0	12STRD	Copper	0.492	0.01559	0.382	420
3/0	6/1	ACSR	0.502	0.006	0.723	300
3/0	7STRD	Copper	0.464	0.01404	0.382	420
3/0	CLASS A	AA	0.464	0.014	0.611	263
3/8	INCHSTE	Steel	0.375	0.00001	4.3	150
4/0	12STRD	Copper	0.552	0.0175	0.303	490
4/0	19STRD	Copper	0.528	0.01668	0.303	480
4/0	6/1	ACSR	0.563	0.00814	0.592	340
4/0	7STRD	Copper	0.522	0.01579	0.303	480
4/0	CLASS A	AA	0.522	0.0158	0.484	299
250,000	12STRD	Copper	0.6	0.01902	0.257	540
250,000	19STRD	Copper	0.574	0.01813	0.257	540
250,000	CON LAY	AA	0.567	0.0171	0.41	329

266,800	26/7	ACSR	0.642	0.0217	0.385	460
266,800	CLASS A	AA '	0.586	0.0177	0.384	320
300,000	12STRD	Copper	0.657	0.0208	0.215	610
300,000	19STRD	Copper	0.629	0.01987	0.215	610
300,000	26/7	ACSR	0.68	0.023	0.342	490
300,000	30/7	ACSR	0.7	0.0241	0.342	500
300,000	CON LAY	AA	0.629	0.0198	0.342	350
336,400	26/7	ACSR	0.721	0.0244	0.306	530
336,400	30/7	ACSR	0.741	0.0255	0.306	530
336,400	CLASSA	AA	0.666	0.021	0.305	410
350,000	12STRD	Copper	0.71	0.0225	0.1845	670

Size	**Stranding**	**Material**	**Diameter (in.)**	**GMR (ft)**	**Resistance (Ω/ mile)**	**Capacity (A)**
350,000	19STRD	Copper	0.679	0.0214	0.1845	670
350,000	CON LAY	AA	0.679	0.0214	0.294	399
397,500	26/7	ACSR	0.783	0.0265	0.259	590
397,500	30/7	ACSR	0.806	0.0278	0.259	600
397,500	CLASSA	AA	0.724	0.0228	0.258	440
400,000	19STRD	Copper	0.726	0.0229	0.1619	730
450,000	19STRD	Copper	0.77	0.0243	0.1443	780
450,000	CON LAG	AA	0.77	0.0243	0.229	450
477,000	26/7	ACSR	0.858	0.029	0.216	670
477,000	30/7	ACSR	0.883	0.0304	0.216	670
477,000	CLASSA	AA	0.795	0.0254	0.216	510
500,000	19STRD	Copper	0.811	0.0256	0.1303	840
500,000	37STRD	Copper	0.814	0.026	0.1303	840
500,000	CON LAY	AA	0.813	0.026	0.206	483

556,500	26/7	ACSR	0.927	0.0313	0.1859	730
556,500	30/7	ACSR	0.953	0.0328	0.1859	730
556,500	CLASSA	AA	0.858	0.0275	0.186	560
600,000	37STRD	Copper	0.891	0.0285	0.1095	940
600,000	CON LAY	AA	0.891	0.0285	0.172	520
605,000	26/7	ACSR	0.966	0.0327	0.172	760
605,000	54/7	ACSR	0.953	0.0321	0.1775	750
636,000	27/7	ACSR	0.99	0.0335	0.1618	780
636,000	30/19	ACSR	1.019	0.0351	0.1618	780
636,000	54/7	ACSR	0.977	0.0329	0.1688	770
636,000	CLASS A	AA	0.918	0.0294	0.163	620
666,600	54/7	ACSR	1	0.0337	0.1601	800
700,000	37STRD	Copper	0.963	0.0308	0.0947	1,040
700,000	CON LAY	AA	0.963	0.0308	0.148	580
715,500	26/7	ACSR	1.051	0.0355	0.1442	840
715,500	30/19	ACSR	1.081	0.0372	0.1442	840
715,500	54/7	ACSR	1.036	0.0349	0.1482	830
715,500	CLASS A	AA	0.974	0.0312	0.145	680
750,000	37STRD	AA	0.997	0.0319	0.0888	1,090
750,000	CON LAY	AA	0.997	0.0319	0.139	602
795,000	26/7	ACSR	1.108	0.0375	0.1288	900
795,000	30/19	ACSR	1.14	0.0393	0.1288	910
795,000	54/7	ACSR	1.093	0.0368	0.1378	900
795,000	CLASS A	AA	1.026	0.0328	0.131	720

Table A.1: Overhead cable data

Concentric Neutral 15KV Underground Cable data:

Table A.2: Underground concentric 15KV cable data

Conductor Size (AWG or kcmil)	Diameter over Insulation (in.)	Diameter over Screen (in.)	Outside Diameter (in.)	Copper Neutral (No. x AWG)	Ampacity in UG Duct (A)
Full neutral					
2 (7×)	0.78	0.85	0.98	10×14	120
1 (19×)	0.81	0.89	1.02	13×14	135
1/0 (19×)	0.85	0.93	1.06	16×14	155
2/0 (19×)	0.90	0.97	1.13	13×12	175
3/0 (19×)	0.95	1.02	1.18	16×12	200
4/0 (19×)	1.01	1.08	1.28	13 × 10	230
250 (37×)	1.06	1.16	1.37	16×10	255
350 (37×)	1.17	1.27	1.47	20×10	300
One-third neutral					
2(7×)	0.78	0.85	0.98	6×14	135
1 (19×)	0.81	0.89	1.02	6×14	155
1/0 (19×)	0.85	0.93	1.06	6×14	175
2/0 (19×)	0.90	0.97	1.10	7×14	200
3/0 (19×)	0.95	1.02	1.15	9×14	230
4/0 (19×)	1.01	1.08	1.21	11×14	240
250(37×)	1.06	1.16	’ 1.29	13×14	260
350 (37×)	1.17	1.27	1.39	18×14	320
500 (37×)	1.29	1.39	1.56	16×12	385
750 (61×)	1.49	1.59	1.79	15×10	470
1000(61×)	1.64	1.77	1.98	20×10	550

Tape-Shielded (Tap thickness 5 mil) Underground 15 kV Cable:

Conductor Size (AWG or kcmil)	Diameter over Insulation (in.)	Diameter over Screen (in.)	Outside Diameter (in.)	Copper Neutral (No. x AWG)	Ampacity in UG Duct (A)
1/0	0.82	0.88	80	1.06	165
2/0	0.87	0.93	80	1.10	190
3/0	0.91	0.97	80	1.16	215
4/0	0.96	1.02	80	1.21	245
250	1.01	1.08	80	1.27	270
350	1.11	1.18	80	1.37	330
500	1.22	1.30	80	1.49	400
750	1.40	1.48	110	1.73	490
1000	1.56	1.66	110	1.91	565

Table A.3: Underground tape-shielded 15KV cable data

Appendix B

IEEE PES Distribution Test System Data: IEEE 13 and 37 bus systems are used for validating the results for the proposed methods. Conductor data, Overhead line configuration data, underground line configuration data, line segment data, capacitor data, regulator data, transformer data, spot load data, distributed load data, overhead and underground line spacing formation are

used to simulate in MATLAB. All the available data for 13 bus systems are tabled below that has been used for the simulation as reference:

Table A.4: Overhead Line configuration data for IEEE 13 bus-feeder network

Config	Phasing	Phase	Neutral	Spacing
		ACSR	ACSR	ID
601	B A C N	556,500 26/7	4/0 6/1	500
602	C A B N	4/0 6/1	4/0 6/1	500
603	C B N	1/0	1/0	505
604	A C N	1/0	1/0	505
605	C N	1/0	1/0	510

Configur.	Phasing	Cable	Neutral	Space ID
606	A B C N	250,000 AA, CN	None	515
607	A N	1/0 AA, TS	1/0 Cu	520

Table A.5: Underground Line Configuration data for IEEE 13 bus-feeder network.

Node A	Node B	Length(ft.)	Configuration
632	645	500	603
632	633	500	602
633	634	0	XFM-1
645	646	300	603
650	632	2000	601
684	652	800	607
632	671	2000	601

671	684	300	604
671	680	1000	601
671	692	0	Switch
684	611	300	605
692	675	500	606

Table A.6: Line Segment data for IEEE 13 bus-feeder network

	KVA	**kV-high**	**kV-low**	**R - %**	**X - %**
Substation:	5,000	115 - D	4.16 Gr. Y	1	8
XFM -1	500	4.16 – Gr.W	0.48 – Gr.W	1.1	2

Table A.7: Transformer data for IEE 13 bus-feeder network

Node	**Phase-A**	**Phase-B**	**Phase-C**
	KVAR	**KVAR**	**KVAR**
675	200	200	200
611			100
Total	200	200	300

Table A.8: Capacitor data for IEEE 13 bus-feeder network

Regulator ID:	1		
Line Segment:	650 - 632		
Location:	50		
Phases:	A - B -C		

Connection:	3-Phase, LG		
Monitoring Phase:	A-B-C		
Bandwidth:	2.0 volts		
PT Ratio:	20		
Primary CT Rating:	700		
Compensator Settings:	Phase-A	Phase-B	Phase-C
R - Setting:	3	3	3
X - Setting:	9	9	9
Voltage Level:	122	122	122

Table A.9: Regulation data for IEEE 13 bus-feeder network

Node A	**Node B**	**Load**	**Phase 1**	**Phase1**	**Phase2**	**Phase2**	**Phase3**	**Phase3**
		Model	**KW**	**KVAR**	**KW**	**KVAR**	**KW**	**KVAR**
632	671	Y-PQ	17	10	66	38	117	68

Table A.10: Distributed load data for IEEE 13 bus-feeder network

Node	**Load**	**Phase-1**	**Phase-1**	**Phase-2**	**Phase-2**	**Phase-3**	**Phase-3**
	Model	**KW**	**KVAR**	**KW**	**KVAR**	**KW**	**KVAR**
634	Y-PQ	160	110	120	90	120	90
645	Y-PQ	0	0	170	125	0	0
646	D-Z	0	0	230	132	0	0
652	Y-Z	128	86	0	0	0	0
671	D-PQ	385	220	385	220	385	220
675	Y-PQ	485	190	68	60	290	212
692	D-I	0	0	0	0	170	151
611	Y-I	0	0	0	0	170	80

	TOTAL	1158	606	973	627	1135	753

Table A.11: Spot load data for IEEE 13 bus-feeder

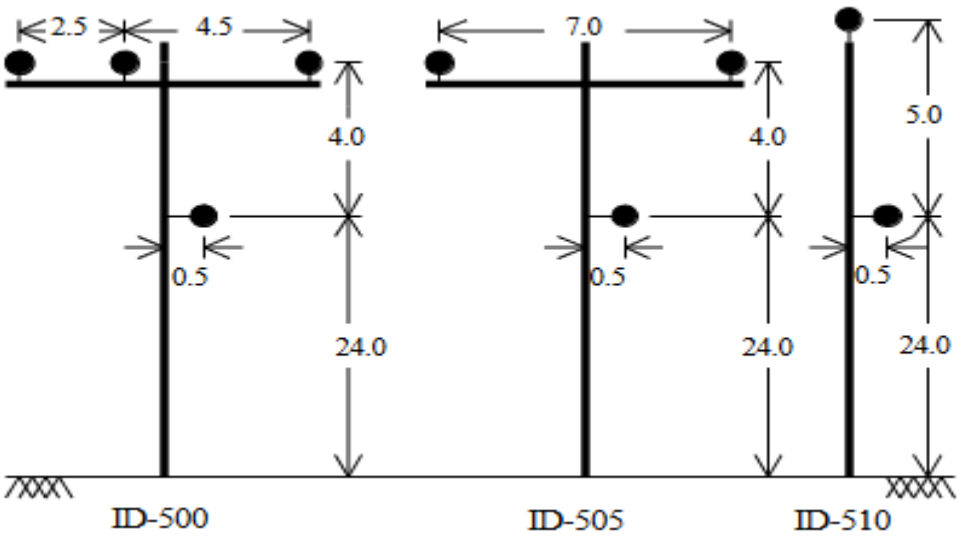

Figure A.1: IEEE 13 bus-feeder overhead line spacing formation

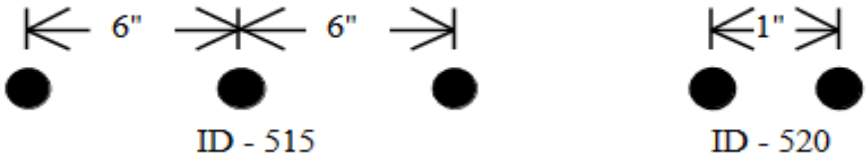

Figure A.2: IEEE 13 bus-feeder underground line spacing formation

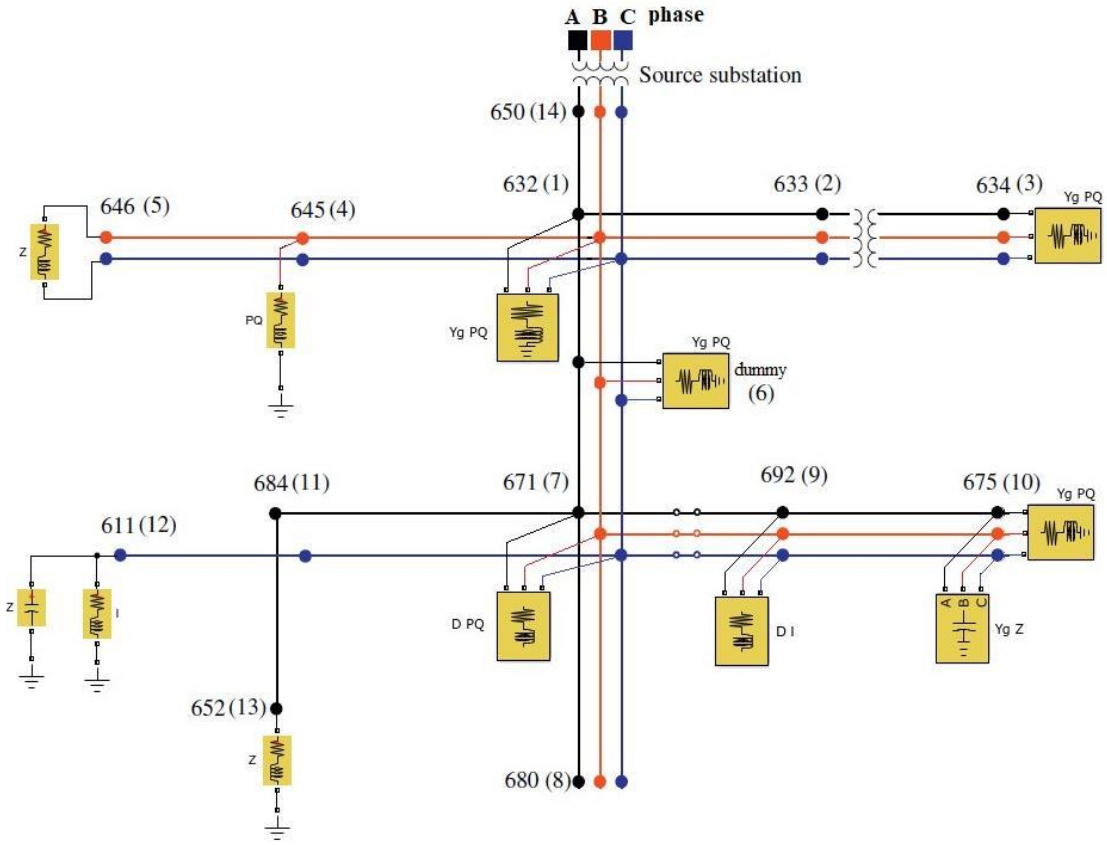

Figure A.3: IEEE 13 bus test systems figure

Appendix C

MATLAB Code for 13 Bus-Feeder Systems: MATLAB coding for the simulation of state estimation including line modeling, forward backward sweep power flow and estimation are presented below:

```
function []=powerflow
% ======================================================================
%Power flow program for unbalanced radial distribution networks
%Backward/Forward power flow method
%Tazwar Muttaqi
%======================================================================
%----------------------------------------------------------------------
[branch,bus,Sbase]=ts_ieee13;
%======================================================================

%branch data
[br_row,~]=size(branch);
bus_i=branch(:,1);
bus_j=branch(:,2);
element=branch(:,3);
typel=branch(:,4);
config=branch(:,5);
lengthLine=branch(:,6)*1.893939393939394*10^(-4);  % (ft)conversion in (mile)
Vbase=branch(:,7);
Zbase=Vbase.^2./Sbase;
%======================================================================

%bus data
busind=bus(:,1);
bustype=bus(:,2);
ppot=bus(:,3:5)'/Sbase;      %phase powers
qpot=bus(:,6:8)'/Sbase;
qc=bus(:,10:12)'/Sbase;
phasing=bus(:,9);

%======================================================================

%Constants and transformation matrices
a=exp(1i*2*pi/3);
Ts=[1 1 1;a^2 a 1;a a^2 1]; % Fortescue's transformation matrix.
av=[1 -1 0;0 1 -1;-1 0 1];  % Transformation matrix for voltages (transformation phase-to-phase in phase-to-neutral, and vice cersa)
ai=[1 0 -1;-1 1 0;0 -1 1];  % Transformation matrix for currents (transformation phase to line, and vice versa)

nbus=length(busind);
%======================================================================

%incidence matrix
inc=zeros(br_row);
typelm=inc;
configm=inc;
lengthLinem=inc;
Zbasem=inc;
for k=1:br_row
    inc(bus_i(k),bus_j(k))=1;
    inc(bus_j(k),bus_i(k))=1;
    typelm(bus_i(k),bus_j(k))=typel(k);
    typelm(bus_j(k),bus_i(k))=typel(k);
    configm(bus_i(k),bus_j(k))=config(k);
    configm(bus_j(k),bus_i(k))=config(k);
    lengthLinem(bus_i(k),bus_j(k))=lengthLine(k);
    lengthLinem(bus_j(k),bus_i(k))=lengthLine(k);
    Zbasem(bus_i(k),bus_j(k))=Zbase(k);
    Zbasem(bus_j(k),bus_i(k))=Zbase(k);
end
%======================================================================

%shunt admitance matrix (yot)
yot=zeros(3,3,nbus);
for k=1:nbus
    for kk=1:nbus
        if typelm(k,kk)==11
            [~,~,Yabc,~]=line_matrices(configm(k,kk));
            Yabc=Yabc*lengthLinem(k,kk)*%basem(k,kk);
            yot(:,:,k)=yot(:,:,k)+Yabc/2;
        elseif typelm(k,kk)==21
            [~,~,~,~,Ymabc]=trafo_matrices(configm(k,kk));
            yot(:,:,k)=yot(:,:,k)+Ymabc; yot(:,:,kk)=yot(:,:,k)-Ymabc;
        end
    end
end
%======================================================================

%INITIALIZATION OF VOLTAGE:
U=zeros(3,nbus);
for k=1:nbus
U(:,k)=[1;1*exp(-1i*2*pi/3);1*exp(1i*2*pi/3)];
end
U(:,14)=[1.0625;1.0500*exp(-1i*2*pi/3);1.0687*exp(1i*2*pi/3)];
U0=U;
%======================================================================
%ITERATIve PROCEDURE
%======================================================================
iter=0; itermax=1000; epsilon=0.0001; maxraz=epsilon+1;
while (iter < itermax) && (maxraz > epsilon)
```

```
iter=iter+1;
Unew=U;
%---------------------------------------------------------------------
%Currents of loads
Ipot=zeros(3,nbus-1);
UnewL=zeros(3,nbus-1);
Ipotf=zeros(3,nbus-1);
UL0=zeros(3,nbus-1);
Icon=zeros(3,nbus-1);
for k=1:nbus-1
if bustype(k)==21 %constant power load model
    if phasing(k)==1   % way-connected load
    Ipot(:,k)=conj(ppot(:,k)+1i*qpot(:,k))./conj(Unew(:,k));
    elseif phasing(k)==2   % delta-connected load
    UnewL(:,k)=av*Unew(:,k);
    Ipotf(:,k)=conj(ppot(:,k)+1i*qpot(:,k))./conj(UnewL(:,k));
    Ipot(:,k)=ai*Ipotf(:,k);
    end
elseif bustype(k)==22 %constant current load model
    if phasing(k)==1  % way-connected load
    Ipot(:,k)=abs(conj(ppot(:,k)+1i*qpot(:,k))./conj(U0(:,k))).*exp(1i*(angle(Unew(:,k))-angle(ppot(:,k)+1i*qpot(:,k))));
    elseif phasing(k)==2  %delta-connected load
    UL0(:,k)=av*U0(:,k);
    UnewL(:,k)=av*Unew(:,k);
    Ipotf(:,k)=abs(conj(ppot(:,k)+1i*qpot(:,k))./conj(UL0(:,k))).*exp(1i*(angle(UnewL(:,k))-angle(ppot(:,k)+1i*qpot(:,k))));
    Ipot(:,k)=ai*Ipotf(:,k);
    end
elseif bustype(k)==23 %constant impedance load model
    if phasing(k)==1  % way-connected load
    Ipot(:,k)=Unew(:,k).*conj(ppot(:,k)+1i*qpot(:,k))./(abs(U0(:,k)).^2);
    elseif phasing(k)==2   %delta-connected load
    UnewL(:,k)=av*Unew(:,k);
    UL0(:,k)=av*U0(:,k);
    Ipotf(:,k)=UnewL(:,k).*conj(ppot(:,k)+1i*qpot(:,k))./(abs(UL0(:,k)).^2);
    Ipot(:,k)=ai*Ipotf(:,k);
    end
end

%Cureents of capacitors
    Icon(:,k)=Unew(:,k).*conj(-1i*qc(:,k))./(abs(U0(:,k)).^2);

end
%=====================================================================

%Backward sweep: branch current
I=zeros(3,nbus-1);
for k=1:nbus-1
    I(:,k)=Ipot(:,k)+Icon(:,k)+yot(:,:,k)*Unew(:,k);
end
J(:,nbus)=[0;0;0];
for k=1:nbus-1
    sumi=[0;0;0];
    for kk=1:k
        if inc(nbus-k,nbus-k+kk)==1
            if typelm(nbus-k,nbus-k+kk)==11   %current through line
                sumi=sumi+J(:,nbus-k+kk);
            elseif typelm(nbus-k,nbus-k+kk)==21   %current through transformer
                [Mj,~,~,~,~]=trafo_matrices(configm(nbus-k,nbus-k+kk));
                sumi=sumi+Ts*Mj/Ts*J(:,nbus-k+kk);
            end
        end
    end
    J(:,nbus-k)=I(:,nbus-k)+sumi;
end
J0=[0;0;0];    % current in the branch connected to the root bus (from supply network)
for k=1:nbus
    if inc(nbus,k)==1
        if typel(k)==11
            J0=J0+J(:,k);
        elseif typel(k)==21
            [Mj,~,~,~,~]=trafo_matrices(config(k));
            J0=J0+Ts*Mj/Ts*J(:,k);
        end
    end
end
J(:,nbus)=J0;
%=====================================================================

%Forward sweep: bus voltages
for k=1:nbus-1
    if inc(k,nbus)==1
        if typelm(k,nbus)==11   % between sending bus and receiving bus is line
            [Zabc,~,~,~]=line_matrices(configm(k,nbus));
            Zabc=Zabc*lengthLinem(k,nbus)./Zbasem(k,nbus);
            U(:,k)=Unew(:,nbus)-Zabc*J(:,k);
        elseif typelm(k,nbus)==21    %between sending bus and receiving bus is transformer
            [~,Mv,Ztdi0,~,~]=trafo_matrices(configm(k,nbus));
            U(:,k)=Ts*Mv/Ts*Unew(:,nbus)-Ts*Ztdi0/Ts*J(:,k);
        end
    end
end
```

```
for k=2:nbus-1
    for kk=1:k-1
        if inc(k,kk)==1
            if typelm(k,kk)==11  % between sending bus and receiving bus is line
                [Zabc,~,~,~]=line_matrices(configm(k,kk));
                Zabc=Zabc*lengthLinem(k,kk)./Zbasem(k,kk);
                U(:,k)=Unew(:,kk)-Zabc*J(:,k);
            elseif typelm(k,kk)==21   %between sending bus and receiving bus is transformer
                [~,Mv,Ztdi0,~,~]=trafo_matrices(configm(k,kk));
                U(:,k)=Ts*Mv/Ts*Unew(:,kk)-Ts*Ztdi0/Ts*J(:,k);
            end
        end
    end
end
      maxraz=max(max(abs(Unew-U)));  % Checking convergence criteria

end    % end of iterative procedure

%=====================================================================

% RESULTS:
%-------------

U(1,4)=eps;U(1,5)=eps;U(2,11)=eps;U(1,12)=eps;U(2,12)=eps;U(2,13)=eps;U(3,13)=eps;  %for no phases at corresponding buses (no phase A at bus 645 (4), 64
6 (5), phases A and B at 611(12), etc)
%=====================================================================
% For power flow calculation the buses are number from 1-14, and here we're going back to original numeration of buses
U650=U(:,14);absU650=abs(U650);angleU650=angle(U650)*180/pi;
U632=U(:,1);absU632=abs(U632);angleU632=angle(U632)*180/pi;
U633=U(:,2);absU633=abs(U633);angleU633=angle(U633)*180/pi;
U634=U(:,3);absU634=abs(U634);angleU634=angle(U634)*180/pi;
U645=U(:,4);absU645=abs(U645);angleU645=angle(U645)*180/pi;
U646=U(:,5);absU646=abs(U646);angleU646=angle(U646)*180/pi;
U671=U(:,7);absU671=abs(U671);angleU671=angle(U671)*180/pi;
U680=U(:,8);absU680=abs(U680);angleU680=angle(U680)*180/pi;
U692=U(:,9);absU692=abs(U692);angleU692=angle(U692)*180/pi;
U675=U(:,10);absU675=abs(U675);angleU675=angle(U675)*180/pi;
U684=U(:,11);absU684=abs(U684);angleU684=angle(U684)*180/pi;
U611=U(:,12);absU611=abs(U611);angleU611=angle(U611)*180/pi;
U652=U(:,13);absU652=abs(U652);angleU652=angle(U652)*180/pi;
Bus=[650;632;633;634;645;646;671;680;684;611;652;692;675];
absUa=[absU650(1);absU632(1);absU633(1);absU634(1);absU645(1);absU646(1);absU671(1);absU680(1);absU684(1);absU611(1);absU652(1);absU692(1);absU675(1)];
angleUa=[angleU650(1);angleU632(1);angleU633(1);angleU634(1);angleU645(1);angleU646(1);angleU671(1);angleU680(1);angleU684(1);angleU611(1);angleU652(1);
angleU692(1);angleU675(1)];
absUb=[absU650(2);absU632(2);absU633(2);absU634(2);absU645(2);absU646(2);absU671(2);absU680(2);absU684(2);absU611(2);absU652(2);absU692(2);absU675(2)];
angleUb=[angleU650(2);angleU632(2);angleU633(2);angleU634(2);angleU645(2);angleU646(2);angleU671(2);angleU680(2);angleU684(2);angleU611(2);angleU652(2);
angleU692(2);angleU675(2)];
absUc=[absU650(3);absU632(3);absU633(3);absU634(3);absU645(3);absU646(3);absU671(3);absU680(3);absU684(3);absU611(3);absU652(3);absU692(3);absU675(3)];
angleUc=[angleU650(3);angleU632(3);angleU633(3);angleU634(3);angleU645(3);angleU646(3);angleU671(3);angleU680(3);angleU684(3);angleU611(3);angleU652(3);
angleU692(3);angleU675(3)];

%-----------------------------------------------------------------------------------------------------------------------------------------------------------
TABLE_V=[Bus absUa angleUa absUb angleUb absUc angleUc];
fprintf('\n                          B U S     V O L T A G E S                    ')
fprintf('\n-------------------------------------------------------------------------')
fprintf('\n     BUS    |       Phase A     |       Phase B      |       Phase C     |')
fprintf('\n==========|==================|==================|==================|')
fprintf('\n     No     |  V (pu)  angle(dg)|  V (pu)  angle(dg)|  V (pu)  angle(dg)|')
fprintf('\n----------|------------------|------------------|------------------|')
for i=1:length(Bus)
fprintf('\n%7d%12.4f%10.3f%10.4f%10.3f%10.4f%10.3f',TABLE_V(i,:));
end

figure(1);  %Voltage profile
absUbar=[absU650';absU632';absU633';absU634';absU645';absU646';absU671';absU680';absU684';absU611';absU652';absU692';absU675'];
bar(absUbar), xlabel('Bus','FontSize',14), xticklabels({'650','632','633','634','645','646','671','680','684','611','652','692','675'}), ylim([0.9,1.1])
, ylabel('Voltage magnitude (pu)','FontSize',14), title('Voltage profile in the IEEE 13-bus feeder','FontSize',14), legend('PhaseA','Phase B','PhaseC'),
 grid on
pause(1);

%BRANCHES
Bus_i=[650;632;633;632;645;632;671;671;692;671;684;684];
Bus_j=[632;633;634;645;646;671;680;692;675;684;611;652];

%BRANCH CURRENTS
absJ=abs(J)*Sbase/Vbase(1)*1000; % A
absJ(:,3)=absJ(:,3)*8.66667;  % secondary zide of XFM-1 (between buses 633-634)
angleJ=angle(J)*180/pi;
absJA=[absJ(1,1:5)';absJ(1,7:13)'];
absJB=[absJ(2,1:5)';absJ(2,7:13)'];
absJC=[absJ(3,1:5)';absJ(3,7:13)'];
angleJA=[angleJ(1,1:5)';angleJ(1,7:13)'];
angleJA(4)=0;angleJA(5)=0;angleJA(7)=0;
angleJB=[angleJ(2,1:5)';angleJ(2,7:13)'];
angleJB(7)=0;angleJB(8)=0;angleJB(10)=0;
angleJC=[angleJ(3,1:5)';angleJ(3,7:13)'];
angleJC(7)=0;angleJC(10)=0;
TABLE_C=[Bus_i Bus_j absJA angleJA absJB angleJB absJC angleJC];
disp(' ')
fprintf('\n                      B R A N C H    C U R R E N T S                    ')
fprintf('\n-------------------------------------------------------------------------')
```

```
fprintf('\n    BRANCH    |       Phase A      |       Phase B     |       Phase C     |')
fprintf('\n=============|====================|===================|===================|')
fprintf('\n Bus_i  Bus_j |    J(A)   angle(dg)|   J(A)   angle(dg)|   J(A)   angle(dg)|')
fprintf('\n-------------|--------------------|-------------------|-------------------|')
for i=1:length(Bus_i)
fprintf('\n%5d%7d%12.3f%10.3f%10.3f%10.3f%10.3f%10.3f',TABLE_C(i,:));
end
fprintf('\n')

figure(2);  %Branch current graph
subplot(3,1,1),bar(absJA), xlabel('Branch','FontSize',12), xticks([1:12]), xticklabels({'650-632','632-633','633-634','632-645','645-646','632-671','671
-680','671-692','692-675','671-684','684-611','684-652'}), ylabel('Current (A)','FontSize',14), title('Phase A','FontSize',14), grid on
subplot(3,1,2),bar(absJB), xlabel('Branch','FontSize',12), xticks([1:12]), xticklabels({'650-632','632-633','633-634','632-645','645-646','632-671','671
-680','671-692','692-675','671-684','684-611','684-652'}), ylabel('Current (A)','FontSize',14), title('Phase B','FontSize',14), grid on
subplot(3,1,3),bar(absJC), xlabel('Branch','FontSize',12), xticks([1:12]), xticklabels({'650-632','632-633','633-634','632-645','645-646','632-671','671
-680','671-692','692-675','671-684','684-611','684-652'}), ylabel('Current (A)','FontSize',14), title('Phase C','FontSize',14), grid on
pause(1);

%BRANCH POWER FLOW
Pbranch=real(U.*conj(J))*Sbase*1000; %kW
Qbranch=imag(U.*conj(J))*Sbase*1000; %kVAr
PbranchA=[Pbranch(1,1:5)';Pbranch(1,7:13)'];
PbranchB=[Pbranch(2,1:5)';Pbranch(2,7:13)'];
PbranchC=[Pbranch(3,1:5)';Pbranch(3,7:13)'];
QbranchA=[Qbranch(1,1:5)';Qbranch(1,7:13)'];
QbranchB=[Qbranch(2,1:5)';Qbranch(2,7:13)'];
QbranchC=[Qbranch(3,1:5)';Qbranch(3,7:13)'];
TABLE_P=[Bus_i Bus_j PbranchA QbranchA PbranchB QbranchB PbranchC QbranchC];
fprintf('\n                  B R A N C H    P O W E R    F L O W                      ')
fprintf('\n-----------------------------------------------------------------------------')
fprintf('\n    BRANCH    |       Phase A      |       Phase B     |       Phase C     |')
fprintf('\n=============|====================|===================|===================|')
fprintf('\n Bus_i  Bus_j |    P(kW)    Q(kVAr)|   P(kW)    Q(kVAr)|   P(kW)    Q(kVAr)|')
fprintf('\n-------------|--------------------|-------------------|-------------------|')
for i=1:length(Bus_i)
fprintf('\n%5d%7d%12.3f%10.3f%10.3f%10.3f%10.3f%10.3f',TABLE_P(i,:));
end
fprintf('\n')

figure(3);  %Power flow graph
PQflowA=[PbranchA,QbranchA];
PQflowB=[PbranchB,QbranchB];
PQflowC=[PbranchC,QbranchC];
subplot(3,1,1),bar(PQflowA), xlabel('Branch','FontSize',12), xticks([1:12]), xticklabels({'650-632','632-633','633-634','632-645','645-646','632-671','6
71-680','671-692','692-675','671-684','684-611','684-652'}), ylabel('Power flows','FontSize',14), title('Phase A','FontSize',14), legend('P (kW)','Q (kV
Ar)'), grid on
subplot(3,1,2),bar(PQflowB), xlabel('Branch','FontSize',12), xticks([1:12]), xticklabels({'650-632','632-633','633-634','632-645','645-646','632-671','6
71-680','671-692','692-675','671-684','684-611','684-652'}), ylabel('Power flows','FontSize',14), title('Phase B','FontSize',14), legend('P (kW)','Q (kV
Ar)'), grid on
subplot(3,1,3),bar(PQflowC), xlabel('Branch','FontSize',12), xticks([1:12]), xticklabels({'650-632','632-633','633-634','632-645','645-646','632-671','6
71-680','671-692','692-675','671-684','684-611','684-652'}), ylabel('Power flows','FontSize',14), title('Phase C','FontSize',14), legend('P (kW)','Q (kV
Ar)'), grid on
pause(1);

%BRANCH LOSSES
Sloss(:,1)=(U(:,14)-U(:,1)).*conj(J(:,1));
Sloss(:,2)=(U(:,1)-U(:,2)).*conj(J(:,2));
Sloss(:,3)=(U(:,2)-U(:,3)).*conj(J(:,3));
Sloss(:,4)=(U(:,1)-U(:,4)).*conj(J(:,4));
Sloss(:,5)=(U(:,4)-U(:,5)).*conj(J(:,5));
Sloss(:,6)=(U(:,1)-U(:,6)).*conj(J(:,6));
Sloss(:,7)=(U(:,6)-U(:,7)).*conj(J(:,7));
Sloss(:,8)=(U(:,7)-U(:,8)).*conj(J(:,8));
Sloss(:,9)=(U(:,7)-U(:,9)).*conj(J(:,9));
Sloss(:,10)=(U(:,9)-U(:,10)).*conj(J(:,10));
Sloss(:,11)=(U(:,7)-U(:,11)).*conj(J(:,11));
Sloss(:,12)=(U(:,11)-U(:,12)).*conj(J(:,12));
Sloss(:,13)=(U(:,11)-U(:,13)).*conj(J(:,13));
Ploss=real(Sloss)*Sbase*1000; %kW
Qloss=imag(Sloss)*Sbase*1000; %kVAr
PlossA=[Ploss(1,1:5)';Ploss(1,7:13)'];
PlossA(6)=Ploss(1,6)+Ploss(1,7);
PlossB=[Ploss(2,1:5)';Ploss(2,7:13)'];
PlossB(6)=Ploss(2,6)+Ploss(2,7);
PlossC=[Ploss(3,1:5)';Ploss(3,7:13)'];
PlossC(6)=Ploss(3,6)+Ploss(3,7);
QlossA=[Qloss(1,1:5)';Qloss(1,7:13)'];
QlossA(6)=Qloss(1,6)+Qloss(1,7);
QlossB=[Qloss(2,1:5)';Qloss(2,7:13)'];
QlossB(6)=Qloss(2,6)+Qloss(2,7);
QlossC=[Qloss(3,1:5)';Qloss(3,7:13)'];
QlossC(6)=Qloss(3,6)+Qloss(3,7);
TABLE_L=[Bus_i Bus_j PlossA QlossA PlossB QlossB PlossC QlossC];

fprintf('\n                        P O W E R    L O S S E S                          ')
fprintf('\n-----------------------------------------------------------------------------')
fprintf('\n    BRANCH     |       Phase A      |       Phase B     |       Phase C     |')
fprintf('\n===============|====================|===================|===================|')
fprintf('\n Bus_i  Bus_j  |   Pls(kW) Qls(kVAr)|  Pls(kW) Qls(kVAr)|  Pls(kW) Qls(kVAr)|')
fprintf('\n---------------|--------------------|-------------------|-------------------|')
for i=1:length(Bus_i)
```

```
fprintf('\n%5d%7d%12.3f%10.3f%10.3f%10.3f%10.3f%10.3f',TABLE_L(i,:));
end
fprintf('\n ')
fprintf('\nTotal active power loss in phase A: %7.3f (kW)\n',sum(sum(PlossA)));
fprintf('Total active power loss in phase B: %7.3f (kW)\n',sum(sum(PlossB)));
fprintf('Total active power loss in phase C: %7.3f (kW)\n',sum(sum(PlossC)));
fprintf('TOTAL ACTIVE POWER LOSS IN THE SYSTEM: %7.3f (kW)\n',sum(sum(Ploss)));
fprintf('\nTotal reactive power loss in phase A: %7.3f (kVAr)\n',sum(sum(QlossA)));
fprintf('Total reactive power loss in phase B: %7.3f (kVAr)\n',sum(sum(QlossB)));
fprintf('Total reactive power loss in phase C: %7.3f (kVAr)\n',sum(sum(QlossC)));
fprintf('TOTAL ACTIVE POWER LOSS IN THE SYSTEM: %7.3f (kVAr)\n',sum(sum(Qloss)));

figure(4);  %Branch power losses graph
PQlossA=[PlossA,QlossA];
PQlossB=[PlossB,QlossB];
PQlossC=[PlossC,QlossC];
subplot(3,1,1),bar(PQlossA), xlabel('Branch','FontSize',12), xticks([1:12]), xticklabels({'650-632','632-633','633-634','632-645','645-646','632-671','6
71-680','671-692','692-675','671-684','684-611','684-652'}), ylabel('Losses','FontSize',14), title('Phase A','FontSize',14), legend('Ploss (kW)','Qloss
(kVAr)'), grid on
subplot(3,1,2),bar(PQlossB), xlabel('Branch','FontSize',12), xticks([1:12]), xticklabels({'650-632','632-633','633-634','632-645','645-646','632-671','6
71-680','671-692','692-675','671-684','684-611','684-652'}), ylabel('Losses','FontSize',14), title('Phase B','FontSize',14), legend('Ploss (kW)','Qloss
(kVAr)'), grid on
subplot(3,1,3),bar(PQlossC), xlabel('Branch','FontSize',12), xticks([1:12]), xticklabels({'650-632','632-633','633-634','632-645','645-646','632-671','6
71-680','671-692','692-675','671-684','684-611','684-652'}), ylabel('Losses','FontSize',14), title('Phase C','FontSize',14), legend('Ploss (kW)','Qloss
(kVAr)'), grid on

open('ieee13Figure.fig')
return
```

B U S V O L T A G E S

BUS	Phase A		Phase B		Phase C	
No	V (pu)	angle(dg)	V (pu)	angle(dg)	V (pu)	angle(dg)
650	1.0625	0.000	1.0500	-120.000	1.0687	120.000
632	1.0211	-2.489	1.0420	-121.720	1.0174	117.829
633	1.0180	-2.554	1.0401	-121.765	1.0148	117.825
634	0.9941	-3.230	1.0218	-122.221	0.9960	117.345
645	0.0000	0.000	1.0328	-121.899	1.0155	117.856
646	0.0000	0.000	1.0311	-121.975	1.0134	117.901
671	0.9901	-5.295	1.0529	-122.342	0.9779	116.025
680	0.9901	-5.295	1.0529	-122.342	0.9779	116.025
684	0.9881	-5.318	0.0000	0.000	0.9759	115.924
611	0.0000	0.000	0.0000	0.000	0.9738	115.777
652	0.9826	-5.242	0.0000	0.000	0.0000	0.000
692	0.9901	-5.295	1.0529	-122.342	0.9779	116.025
675	0.9836	-5.543	1.0553	-122.517	0.9759	116.038

B R A N C H C U R R E N T S

BRANCH		Phase A		Phase B		Phase C	
Bus_i	Bus_j	J(A)	angle(dg)	J(A)	angle(dg)	J(A)	angle(dg)
650	632	558.331	-28.566	414.867	-140.910	586.557	93.590
632	633	81.323	-37.738	61.123	-159.090	62.703	80.476
633	634	704.802	-37.738	529.739	-159.090	543.433	80.475
632	645	0.000	0.000	143.025	-142.662	65.206	57.826
645	646	0.000	0.000	65.207	-122.174	65.207	57.826
632	671	470.132	-26.887	186.409	-131.885	420.610	101.672
671	680	0.002	0.000	0.002	0.000	0.001	0.000
671	692	229.053	-18.152	69.600	0.000	178.360	109.406
692	675	205.292	-5.121	69.589	-55.195	124.059	111.801
671	684	63.074	-39.111	0.000	0.000	71.150	0.000
684	611	0.000	0.000	0.000	0.000	71.150	121.615
684	652	63.083	-39.123	0.000	-167.340	0.000	70.922

B R A N C H P O W E R F L O W

BRANCH		Phase A		Phase B		Phase C	
Bus_i	Bus_j	P(kW)	Q(kVAr)	P(kW)	Q(kVAr)	P(kW)	Q(kVAr)
650	632	1229.846	601.878	980.581	341.295	1306.994	588.438
632	633	162.515	114.573	121.424	92.583	121.495	92.718
633	634	159.998	109.997	120.001	89.998	119.999	89.998
632	645	0.000	0.000	331.753	125.774	79.445	137.766
645	646	0.000	0.000	161.481	0.562	79.175	137.552
632	671	1039.483	411.406	464.877	78.150	957.016	244.887
671	680	-0.000	-0.004	0.001	-0.004	-0.000	-0.004
671	692	531.020	121.206	68.343	-162.196	416.110	48.280
692	675	484.971	-3.572	68.000	-162.741	289.997	21.486
671	684	124.403	83.258	-0.000	0.000	165.939	-16.540
684	611	0.000	0.000	0.000	0.000	165.553	-16.927
684	652	123.595	82.993	-0.000	0.000	0.000	-0.000

P O W E R L O S S E S

BRANCH	Phase A	Phase B	Phase C

Bus_i	Bus_j	Pls(kW)	Qls(kVAr)	Pls(kW)	Qls(kVAr)	Pls(kW)	Qls(kVAr)
650	632	21.507	79.426	-3.247	32.115	41.447	81.213
632	633	0.353	0.524	0.148	0.265	0.306	0.248
633	634	2.517	4.577	1.423	2.586	1.496	2.722
632	645	0.000	0.000	2.547	2.165	0.220	0.231
645	646	0.000	0.000	0.272	0.214	0.269	0.217
632	671	10.497	65.399	-6.173	4.383	31.515	44.609
671	680	0.000	0.000	-0.000	-0.000	0.000	0.000
671	692	-0.008	-0.001	-0.000	-0.001	-0.003	0.003
692	675	3.202	2.095	0.343	0.574	0.580	-0.027
671	684	0.209	0.213	0.000	0.000	0.370	0.261
684	611	0.000	0.000	0.000	0.000	0.386	0.389
684	652	0.808	0.304	-0.000	0.000	0.000	0.000

```
Total active power loss in phase A:  39.084 (kW)
Total active power loss in phase B:  -4.686 (kW)
Total active power loss in phase C:  76.587 (kW)
TOTAL ACTIVE POWER LOSS IN THE SYSTEM: 110.985 (kW)

Total reactive power loss in phase A: 152.537 (kVAr)
Total reactive power loss in phase B:  42.301 (kVAr)
Total reactive power loss in phase C: 129.865 (kVAr)
TOTAL ACTIVE POWER LOSS IN THE SYSTEM: 324.703 (kVAr)
```

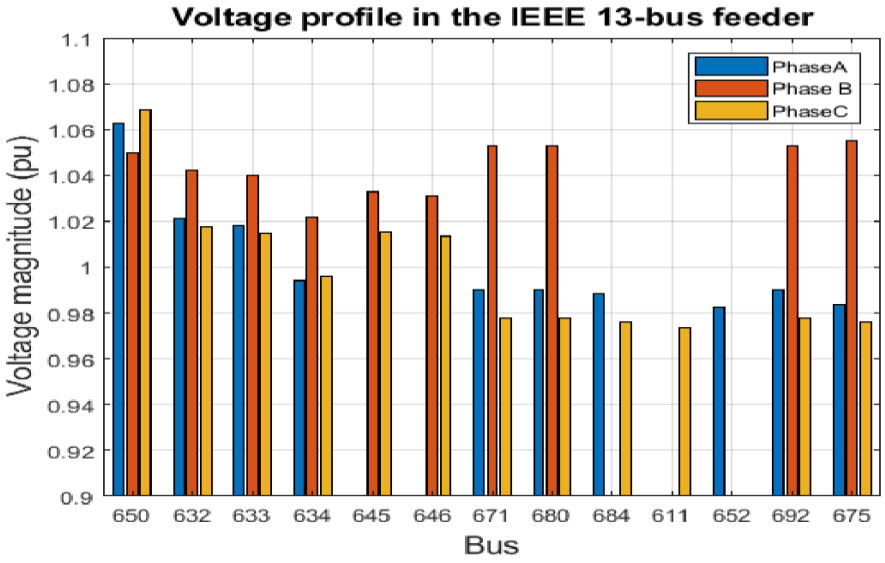

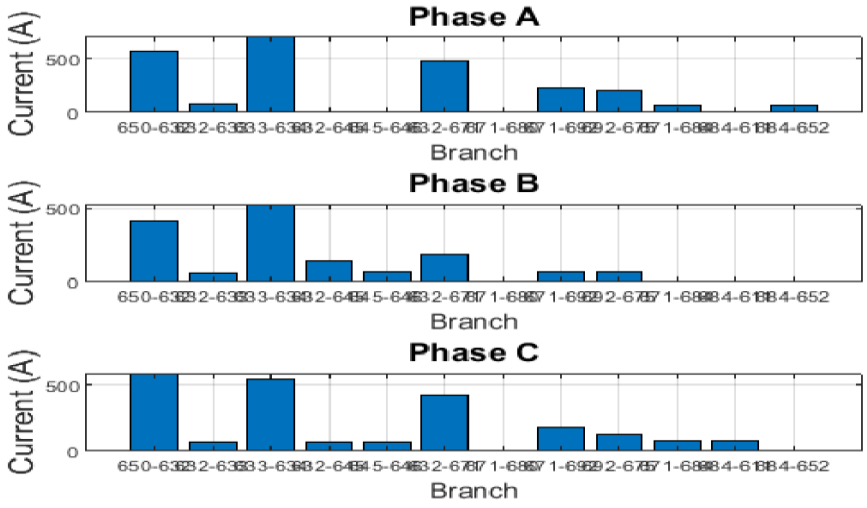

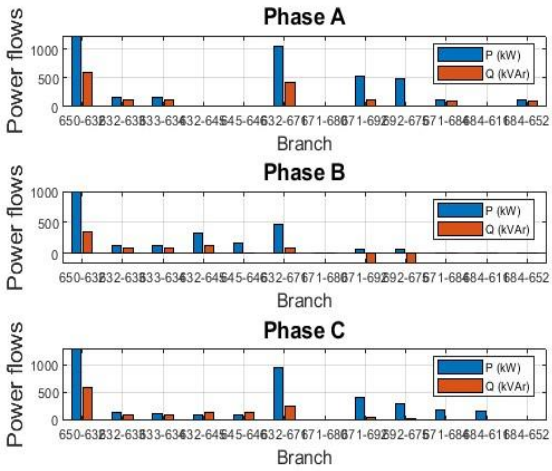
Phase A
Power flows
1000
500
0
P (kW)
Q (kVAr)
650-632 632-633 633-634 632-645 645-646 632-671 671-680 671-692 692-675 671-684 684-611 684-652
Branch
Phase B
Power flows
1000
500
0
P (kW)
Q (kVAr)
650-632 632-633 633-634 632-645 645-646 632-671 671-680 671-692 692-675 671-684 684-611 684-652
Branch
Phase C
Power flows
1000
500
0
P (kW)
Q (kVAr)
650-632 632-633 633-634 632-645 645-646 632-671 671-680 671-692 692-675 671-684 684-611 684-652
Branch

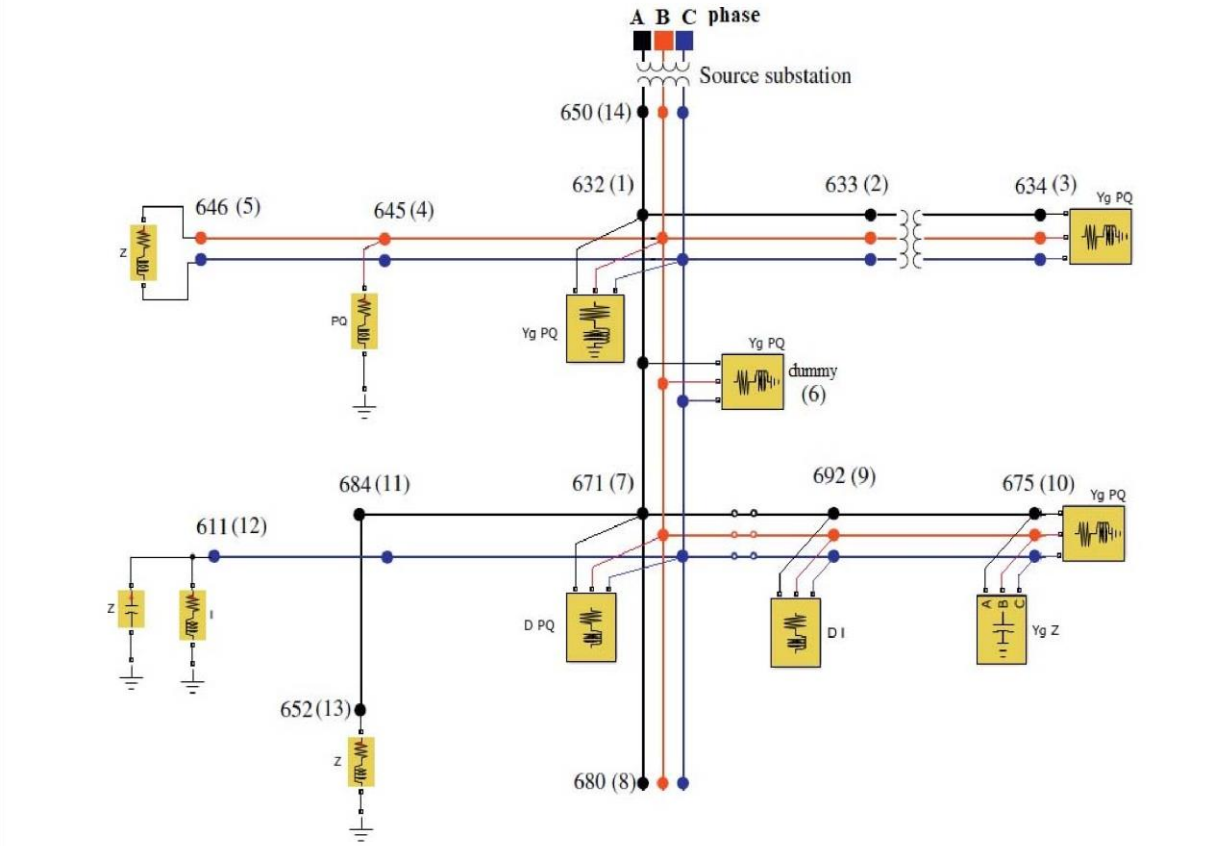
A B C phase
Source substation
650 (14)
632 (1)
633 (2)
634 (3)
Yg PQ
646 (5)
645 (4)
Z
PQ
Yg PQ
Yg PQ
dummy
(6)
684 (11)
671 (7)
692 (9)
675 (10)
Yg PQ
611 (12)
Z
I
D PQ
D I
A B C
Yg Z
652 (13)
Z
680 (8)

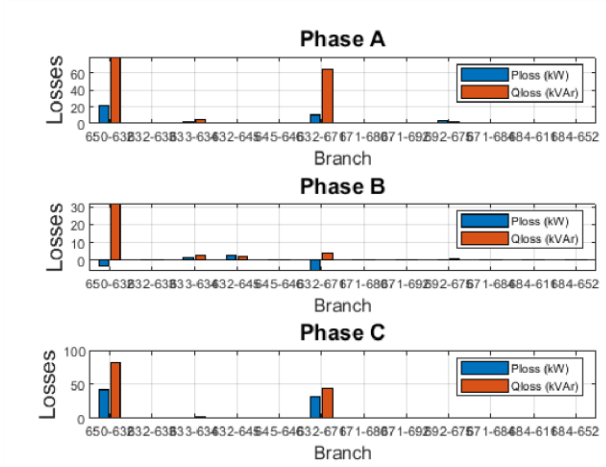

Published with MATLAB® R2018a

```
%State estimation in three-phase unbalanced/unsymetrical rafial distribution szstems
clear all
clc
%  T - time at daily load diagram for which measurement is performed
%  Ep - error associated for  (loads) in (%), usually 10-30 %
%
T=input('Input time T=');
Ep=input('Error in % of pseudo measurement - power of loads, Ep=');
Ert=input('Error in % of real-time measurement - power at substation, Ert=');
ErtV=input('Error in % of real-time measurement - substation voltage, ErtV=');
%U0t=[1.0625;1.0500*exp(-1i*2*pi/3);1.0687*exp(1i*2*pi/3)];
U0t=[1;1*exp(-1i*2*pi/3);1*exp(1i*2*pi/3)];

%GENERATE measurement data as an input to the state estimator.
[ppot0M,qpot0M,Pbranch0M,Qbranch0M,U0M]=measurement(T,Ep,Ert,ErtV,U0t);


%INITIALIZATION:
ppot=ppot0M;
qpot=qpot0M;
%=========================================================================
%STATE ESTIMATION procedure
%=========================================================================
iter=0; itermax=1000;
epsilon=0.0001; %Convergence criterion in state estimation
maxraz=epsilon+1;
while (iter < itermax) && (maxraz > epsilon)
iter=iter+1;

[Pbranch0C,Qbranch0C]=pflow(ppot,qpot,U0M);

deltaP0=abs(Pbranch0M-Pbranch0C);  %The difference between measured and calculated values of
active power at substation (in branch 0-650)
deltaQ0=abs(Qbranch0M-Qbranch0C);  %The difference between measured and calculated values of
reactive power at substation (in branch 0-650)

maxraz=max(max(deltaP0,deltaQ0));  % Checking convergence criteria

kp=Pbranch0M./Pbranch0C;    %coefficients for correction of active power of load
kq=Qbranch0M./Qbranch0C;    %coefficients for correction of reactive power of load

ppot(1,:)=kp(1)*ppot(1,:);  % active power corr. in phase A
ppot(2,:)=kp(2)*ppot(2,:);  % active power corr. in phase B
ppot(3,:)=kp(3)*ppot(3,:);  % active power corr. in phase C
qpot(1,:)=kq(1)*qpot(1,:);  % reactive power corr. in phase A
qpot(2,:)=kq(2)*qpot(2,:);  % reactive power corr. in phase B
qpot(3,:)=kq(3)*qpot(3,:);  % reactive power corr. in phase C
end    % end of state estimation procedure
%=========================================================================
ppot_est=ppot;qpot_est=qpot; iter;

[TABLE_Vest,TABLE_Cest,TABLE_Pest,TABLE_LSest,absUaEstPlot,absUbEstPlot,absUcEstPlot]=pflow_e
st(ppot_est,qpot_est,U0M);      %calculation of estimated values in the system
[TABLE_Vtrue,TABLE_Ctrue,TABLE_Ptrue,TABLE_LStrue,absUaTruPlot,absUbTruPlot,absUcTruPlot]=pfl
ow_true(T,U0t);                 %calculation of true values
```

```
%SHOWING RESULTS
%=========================================================================
% Estimated bus voltages
%-------------------------
TABLE_magnitudeV=[TABLE_Vest(:,1) TABLE_Vest(:,2) TABLE_Vtrue(:,2) TABLE_Vest(:,4) TABLE_Vtru
e(:,4) TABLE_Vest(:,6) TABLE_Vtrue(:,6)];
TABLE_angleV=[TABLE_Vest(:,1) TABLE_Vest(:,3) TABLE_Vtrue(:,3) TABLE_Vest(:,5) TABLE_Vtrue(:,
5) TABLE_Vest(:,7) TABLE_Vtrue(:,7)];

fprintf('\n           B U S     V O L T A G E      M A G N I T U D E S  (pu)       ')
fprintf('\n-------------------------------------------------------------------------')
fprintf('\n     BUS   |       Phase A     |      Phase B      |       Phase C     |')
fprintf('\n===========|===================|===================|===================|')
fprintf('\n     No    |  Estim.     True  |  Estim.     True  |  Estim.     True  |')
fprintf('\n-----------|-------------------|-------------------|-------------------|')
for i=1:length(TABLE_Vest(:,1))
fprintf('\n%7d%12.4f%10.4f%10.4f%10.4f%10.4f%10.4f',TABLE_magnitudeV(i,:));
end
fprintf('\n')
fprintf('\n            B U S     V O L T A G E     A N G L E S   (dg)             ')
fprintf('\n-------------------------------------------------------------------------')
fprintf('\n     BUS   |       Phase A     |      Phase B      |       Phase C     |')
fprintf('\n===========|===================|===================|===================|')
fprintf('\n     No    |  Estim.     True  |  Estim.     True  |  Estim.     True  |')
fprintf('\n-----------|-------------------|-------------------|-------------------|')
for i=1:length(TABLE_Vest(:,1))
fprintf('\n%7d%12.3f%10.3f%10.3f%10.3f%10.3f%10.3f',TABLE_angleV(i,:));
end
fprintf('\n')

figure(1);  %Voltage profile graph
absUa=[absUaEstPlot,absUaTruPlot]; errorUa=abs(absUaTruPlot-absUaEstPlot)./absUaTruPlot*100;
absUb=[absUbEstPlot,absUbTruPlot]; errorUb=abs(absUbTruPlot-absUbEstPlot)./absUbTruPlot*100;
absUc=[absUcEstPlot,absUcTruPlot]; errorUc=abs(absUcTruPlot-absUcEstPlot)./absUcTruPlot*100;
subplot(3,2,1), bar(absUa), xlabel('Bus','FontSize',14), xticks([1:10]), xticklabels({'650','
632','633','634','671','680','684','652','692','675'}), ylim([0.9,1.02]), ylabel('Voltage mag
nitude (pu)','FontSize',14), title('Phase A','FontSize',14), legend('Estimated','True'), grid
 on
subplot(3,2,2), plot(errorUa), xlabel('Bus','FontSize',12), xticks([1:10]), xticklabels({'650
','632','633','634','671','680','684','652','692','675'}), ylabel('Error (%)','FontSize',12),
 title('Phase A','FontSize',12), grid on
subplot(3,2,3), bar(absUb), xlabel('Bus','FontSize',14), xticks([1:10]), xticklabels({'650','
632','633','634','645','646','671','680','692','675'}), ylim([0.94,1.02]), ylabel('Voltage ma
gnitude (pu)','FontSize',14), title('Phase B','FontSize',14), legend('Estimated','True'), gri
d on
subplot(3,2,4), plot(errorUb), xlabel('Bus','FontSize',12), xticks([1:10]), xticklabels({'650
','632','633','634','645','646','671','680','692','675'}), ylabel('Error (%)','FontSize',12),
 title('Phase B','FontSize',12), grid on
subplot(3,2,5), bar(absUc), xlabel('Bus','FontSize',14), xticks([1:12]), xticklabels({'650','
632','633','634','645','646','671','680','684','611','692','675'}), ylim([0.88,1.02]), ylabel
('Voltage magnitude (pu)','FontSize',14), title('Phase C','FontSize',14), legend('Estimated',
'True'), grid on
subplot(3,2,6), plot(errorUc), xlabel('Bus','FontSize',12), xticks([1:12]), xticklabels({'650
','632','633','634','645','646','671','680','684','611','692','675'}), ylabel('Error (%)','Fo
ntSize',12), title('Phase C','FontSize',12), grid on
```

```
% Estimated branch currents
%----------------------------
TABLE_magnitudeC=[TABLE_Cest(:,1) TABLE_Cest(:,2) TABLE_Cest(:,3) TABLE_Ctrue(:,3) TABLE_Cest
(:,5) TABLE_Ctrue(:,5) TABLE_Cest(:,7) TABLE_Ctrue(:,7)];
disp(' ')
fprintf('\n          B R A N C H    C U R R E N T S    M A G N I T U D E S  (A)       ')
fprintf('\n-------------------------------------------------------------------------------')
fprintf('\n    BRANCH    |       Phase A      |       Phase B     |       Phase C     |')
fprintf('\n==============|====================|===================|===================|')
fprintf('\n Bus_i  Bus_j |   Estim.     True  |   Estim.     True |  Estim.     True  |')
fprintf('\n--------------|--------------------|-------------------|-------------------|')
for i=1:length(TABLE_Cest(:,1))
fprintf('\n%5d%7d%12.3f%10.3f%10.3f%10.3f%10.3f%10.3f',TABLE_magnitudeC(i,:));
end
fprintf('\n')
figure(2);  %Branch current graph
absJA=[TABLE_Cest(:,3), TABLE_Ctrue(:,3)];
absJB=[TABLE_Cest(:,5), TABLE_Ctrue(:,5)];
absJC=[TABLE_Cest(:,7), TABLE_Ctrue(:,7)];
subplot(3,1,1),bar(absJA), xlabel('Branch','FontSize',12), xticks([1:12]), xticklabels({'650-
632','632-633','633-634','632-645','645-646','632-671','671-680','671-692','692-675','671-684
','684-611','684-652'}), ylabel('Current (A)','FontSize',14), title('Phase A'), legend('Estim
ated','True'), grid on
subplot(3,1,2),bar(absJB), xlabel('Branch','FontSize',12), xticks([1:12]), xticklabels({'650-
632','632-633','633-634','632-645','645-646','632-671','671-680','671-692','692-675','671-684
','684-611','684-652'}), ylabel('Current (A)','FontSize',14), title('Phase B'), legend('Estim
ated','True'), grid on
subplot(3,1,3),bar(absJC), xlabel('Branch','FontSize',12), xticks([1:12]), xticklabels({'650-
632','632-633','633-634','632-645','645-646','632-671','671-680','671-692','692-675','671-684
','684-611','684-652'}), ylabel('Current (A)','FontSize',14), title('Phase C'), legend('Estim
ated','True'), grid on


% Estimated powers
%------------------
TABLE_activeP=[TABLE_Pest(:,1) TABLE_Pest(:,2) TABLE_Pest(:,3) TABLE_Ptrue(:,3) TABLE_Pest(:,
5) TABLE_Ptrue(:,5) TABLE_Pest(:,7) TABLE_Ptrue(:,7)];
TABLE_reactiveP=[TABLE_Pest(:,1) TABLE_Pest(:,2) TABLE_Pest(:,4) TABLE_Ptrue(:,4) TABLE_Pest(
:,6) TABLE_Ptrue(:,6) TABLE_Pest(:,8) TABLE_Ptrue(:,8)];
fprintf('\n                A C T I V E    P O W E R    F L O W  (kW)                ')
fprintf('\n-------------------------------------------------------------------------------')
fprintf('\n    BRANCH    |       Phase A      |       Phase B     |       Phase C     |')
fprintf('\n==============|====================|===================|===================|')
fprintf('\n Bus_i  Bus_j |   Estim.     True  |    Estim.    True |    Estim.    True |')
fprintf('\n--------------|--------------------|-------------------|-------------------|')
for i=1:length(TABLE_Pest(:,1))
fprintf('\n%5d%7d%12.3f%10.3f%10.3f%10.3f%10.3f%10.3f',TABLE_activeP(i,:));
end
fprintf('\n')
%Active power flows graph
PA=[TABLE_Pest(:,3), TABLE_Ptrue(:,3)]; errorPa=abs(TABLE_Ptrue(:,3)-TABLE_Pest(:,3))./TABLE_
Ptrue(:,3)*100;
PB=[TABLE_Pest(:,5), TABLE_Ptrue(:,5)]; errorPb=abs(TABLE_Ptrue(:,5)-TABLE_Pest(:,5))./TABLE_
Ptrue(:,5)*100;
PC=[TABLE_Pest(:,7), TABLE_Ptrue(:,7)]; errorPc=abs(TABLE_Ptrue(:,7)-TABLE_Pest(:,7))./TABLE_
Ptrue(:,7)*100;
figure(3);
```

```
subplot(2,1,1),bar(PA), xlabel('Branch','FontSize',12), xticks([1:13]), xticklabels({'0-650',
'650-632','632-633','633-634','632-645','645-646','632-671','671-680','671-692','692-675','67
1-684','684-611','684-652'}), ylabel('Active power flow (kW)','FontSize',14), title('Phase A'
), legend('Estimated','True'), grid on
subplot(2,1,2),plot(errorPa), xlabel('Branch','FontSize',12), xticks([1:13]), xticklabels({'0
-650','650-632','632-633','633-634','632-645','645-646','632-671','671-680','671-692','692-67
5','671-684','684-611','684-652'}), ylabel('Error (%)','FontSize',14), title('Phase A'), grid
 on
figure(4);
subplot(2,1,1),bar(PB), xlabel('Branch','FontSize',12), xticks([1:13]), xticklabels({'0-650',
'650-632','632-633','633-634','632-645','645-646','632-671','671-680','671-692','692-675','67
1-684','684-611','684-652'}), ylabel('Active power flow (kW)','FontSize',14), title('Phase B'
), legend('Estimated','True'), grid on
subplot(2,1,2),plot(errorPb), xlabel('Branch','FontSize',12), xticks([1:13]), xticklabels({'0
-650','650-632','632-633','633-634','632-645','645-646','632-671','671-680','671-692','692-67
5','671-684','684-611','684-652'}), ylabel('Error (%)','FontSize',14), title('Phase B'), grid
 on
figure(5);
subplot(2,1,1),bar(PC), xlabel('Branch','FontSize',12), xticks([1:13]), xticklabels({'0-650',
'650-632','632-633','633-634','632-645','645-646','632-671','671-680','671-692','692-675','67
1-684','684-611','684-652'}), ylabel('Active power flow (kW)','FontSize',14), title('Phase C'
), legend('Estimated','True'), grid on
subplot(2,1,2),plot(errorPc), xlabel('Branch','FontSize',12), xticks([1:13]), xticklabels({'0
-650','650-632','632-633','633-634','632-645','645-646','632-671','671-680','671-692','692-67
5','671-684','684-611','684-652'}), ylabel('Error (%)','FontSize',14), title('Phase C'), grid
 on


fprintf('\n                R E A C T I V E    P O W E R    F L O W  (kVAr)             ')
fprintf('\n-------------------------------------------------------------------------------')
fprintf('\n    BRANCH    |       Phase A      |       Phase B     |       Phase C     |')
fprintf('\n==============|====================|===================|===================|')
fprintf('\n Bus_i  Bus_j |   Estim.     True  |   Estim.     True |   Estim.     True |')
fprintf('\n--------------|--------------------|-------------------|-------------------|')
for i=1:length(TABLE_Pest(:,1))
fprintf('\n%5d%7d%12.3f%10.3f%10.3f%10.3f%10.3f%10.3f',TABLE_reactiveP(i,:));
end
fprintf('\n')
%Rective power flows graph
QA=[TABLE_Pest(:,4), TABLE_Ptrue(:,4)]; errorQa=abs(TABLE_Ptrue(:,4)-TABLE_Pest(:,4))./TABLE_
Ptrue(:,4)*100;
QB=[TABLE_Pest(:,6), TABLE_Ptrue(:,6)]; errorQb=abs(TABLE_Ptrue(:,6)-TABLE_Pest(:,6))./TABLE_
Ptrue(:,6)*100;
QC=[TABLE_Pest(:,8), TABLE_Ptrue(:,8)]; errorQc=abs(TABLE_Ptrue(:,8)-TABLE_Pest(:,8))./TABLE_
Ptrue(:,8)*100;
figure(6);
subplot(2,1,1),bar(QA), xlabel('Branch','FontSize',12), xticks([1:13]), xticklabels({'0-650',
'650-632','632-633','633-634','632-645','645-646','632-671','671-680','671-692','692-675','67
1-684','684-611','684-652'}), ylabel('Reactive power flow (kVAr)','FontSize',14), title('Phas
e A'), legend('Estimated','True'), grid on
subplot(2,1,2),plot(errorQa), xlabel('Branch','FontSize',12), xticks([1:13]), xticklabels({'0
-650','650-632','632-633','633-634','632-645','645-646','632-671','671-680','671-692','692-67
5','671-684','684-611','684-652'}), ylabel('Error (%)','FontSize',14), title('Phase A'), grid
 on
figure(7);
subplot(2,1,1),bar(QB), xlabel('Branch','FontSize',12), xticks([1:13]), xticklabels({'0-650',
'650-632','632-633','633-634','632-645','645-646','632-671','671-680','671-692','692-675','67
```

```
1-684','684-611','684-652'}), ylabel('Reactive power flow (kVAr)','FontSize',14), title('Phas
e B'), legend('Estimated','True'), grid on
subplot(2,1,2),plot(errorQb), xlabel('Branch','FontSize',12), xticks([1:13]), xticklabels({'0
-650','650-632','632-633','633-634','632-645','645-646','632-671','671-680','671-692','692-67
5','671-684','684-611','684-652'}), ylabel('Error (%)','FontSize',14), title('Phase B'), grid
 on
figure(8);
subplot(2,1,1),bar(QC), xlabel('Branch','FontSize',12), xticks([1:13]), xticklabels({'0-650',
'650-632','632-633','633-634','632-645','645-646','632-671','671-680','671-692','692-675','67
1-684','684-611','684-652'}), ylabel('Reactive power flow (kVAr)','FontSize',14), title('Phas
e C'), legend('Estimated','True'), grid on
subplot(2,1,2),plot(errorQc), xlabel('Branch','FontSize',12), xticks([1:13]), xticklabels({'0
-650','650-632','632-633','633-634','632-645','645-646','632-671','671-680','671-692','692-67
5','671-684','684-611','684-652'}), ylabel('Error (%)','FontSize',14), title('Phase C'), grid
 on


% Estimated losses
%-------------------
fprintf('\n                P O W E R   L O S S E S                          ')
fprintf('\n---------------------------------------------------------------------')
fprintf('\nESTIMATED TOTAL ACTIVE POWER LOSS: %7.3f (kW)',TABLE_LSest(1));
fprintf('\nTRUE TOTAL ACTIVE POWER LOSS: %7.3f (kW)',TABLE_LStrue(1));
fprintf('\nESTIMATED TOTAL REACTIVE POWER LOSS: %7.3f (kVAr)',TABLE_LSest(2));
fprintf('\nTRUE TOTAL REACTIVE POWER LOSS: %7.3f (kVAr)',TABLE_LStrue(2));
fprintf('\n')

PLOSS=[TABLE_LSest(1),TABLE_LStrue(1)]; errorPLoss=abs(TABLE_LStrue(1)-TABLE_LSest(1))./TABLE
_LStrue(1)*100;
QLOSS=[TABLE_LSest(2),TABLE_LStrue(2)]; errorQLoss=abs(TABLE_LStrue(2)-TABLE_LSest(2))./TABLE
_LStrue(2)*100;

figure(9);
subplot(2,2,1),bar(PLOSS), xticks([1:2]), xticklabels({'Estimated','True'}), ylabel('Total P
loss (kW)','FontSize',14), grid on
subplot(2,2,2),bar(errorPLoss), ylabel('Error (%)','FontSize',14), grid on
subplot(2,2,3),bar(QLOSS), xticks([1:2]), xticklabels({'Estimated','True'}), ylabel('Total Q
loss (kVAr)','FontSize',14), grid on
subplot(2,2,4),bar(errorQLoss), ylabel('Error (%)','FontSize',14), grid on
```

```
Error using input
Cannot call INPUT from EVALC.

Error in ste (line 7)
T=input('Input time T=');
```

Published with MATLAB® R2018a